

**MOLECULAR COMPOSITES OF A CONDUCTING POLYMER:  
SYNTHESES AND CHARACTERIZATION OF  
POLY(1,4-PHENYLENEVINYLENE)-  
CROWN ETHER ROTAXANES**

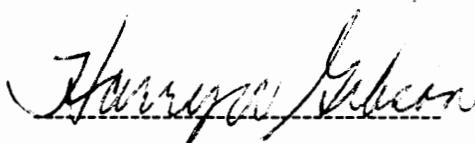
By

Feng Wang

Thesis submitted to the Faculty of the Virginia Polytechnic Institute and State University in  
partial fulfillment of the requirements for the degree of

**MASTER OF SCIENCE  
IN  
CHEMISTRY**

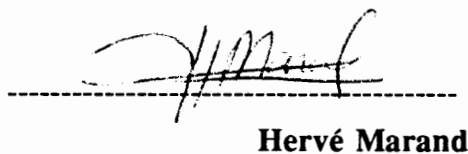
**APPROVED :**



**H. W. Gibson, Chairman**



**James E. McGrath**



**Hervé Marand**

**Dec. 1994  
Blacksburg, Virginia**

# ABSTRACT

## MOLECULAR COMPOSITES OF A CONDUCTING POLYMER: SYNTHESES AND CHARACTERIZATION OF POLY(1,4- PHENYLENEVINYLENE)-CROWN ETHER ROTAXANES

By

Feng Wang

Committee Chairman: Prof. Harry W. Gibson

Department of Chemistry

Polyrotaxanes, a new class of polymer architectures, so called molecular composites, are comprised of macrocycles threaded by linear backbones with no covalent bond between them. By using poly(1,4-phenylenevinylene) (PPV), one of the most promising conductive polymers, as the linear backbone and different sizes of crown ethers (42C14, 60C20) as macrocycles, molecular composites of the conducting polymer were generated. To compare with the PPV rotaxanes, PPV was synthesized and characterized by NMR, IR, UV-vis, photoluminescence spectroscopy, and TGA. The molecular weight of this polymer was measured by low angle laser light scattering. The poly(1,4-phenylenevinylene) rotaxanes were isolated by dialysis and solid-liquid extraction. They were also characterized by TGA, IR, UV-vis, photoluminescence spectroscopy, and solid state  $^{13}\text{C}$  NMR from which the mass contents of the crown ethers were calculated. The conductivities of the PPV rotaxanes were measured by the four-probe method. The conductivities of PPV42C14 rotaxane and PPV60C20 rotaxane were found to be  $1.06 \times 10^{-5}$  S/cm and  $2.0 \times 10^{-9}$  S/cm, respectively, after doping with concentrated sulfuric acid. The photoluminescence spectra of PPV rotaxanes showed different chemical shift and intensity from that of the PPV.

# Acknowledgment

The author wish to express his sincere appreciation and gratitude to many people who contributed greatly to this work. The deepest appreciation goes to Professor Harry W. Gibson, his advisor, whose guidance, patience, encouragement and intellectual challenge brought the author as a metallurgy and material engineer to the wonderful polymer chemistry palace.

The author would like to thank Professor J. E. McGrath and Professor H. Marand for being on his committee and for their valuable suggestions and encouragement throughout his research.

Thanks to Dr. A. R. Schultz and Dr. R. M. Davis for their help in the light scattering experiment.

Thanks to T. Glass for his help in solid NMR characterization.

Appreciation also goes to many friends at Virginia Tech, all of whom have provided support to the author during the years. In particular, the members of his research group: Dr. Devdatt Nagvekar, Ming-Fei Chen, Dong Hang Xie, Jim Yang, Darin Dotson have made the project more pleasurable. Also, the author owes a great gratitude to Shu Liu and San-Hung Lee who not only gave lots of valuable suggestions as labmates but also shared the joyful discussion of many topics as friends.

Finally, a very special thanks to the author's parents: Zheng-Guo Wang and Pei-Fang Zhu, brother and sister, Alex L. Wang and Qing Wang, for their love, support, and inspiration.

# Table of Contents

<b>Abstract</b>	<b>ii</b>
<b>Acknowledgements</b>	<b>iii</b>
<b>List Tables</b>	<b>vii</b>
<b>List of Figures</b>	<b>vii</b>

## CHAPTER I. INTRODUCTION AND LITERATURE REVIEW

I-1	Introduction to polymer classifications	1
I-2	Topology of polymers	2
I-3	Polymer blends	8
I-4	New polymer architectures	8
I-5	Rotaxanes, catenanes and their polymeric analogs	9
I-5.1	Low molecular weight rotaxanes and catenanes	9
I-5.1.1	Definition and early work: statistical threading	9
I-5.1.2	Synthesis about a center core: directed approach	21
I-5.1.3	Template synthese	24
I-5.1.3.1	Metal ion complexes	25
I-5.1.3.2	Cyclodextrin inclusions	29
I-5.1.3.3	Charge transfer and $\pi$ -stacked complexes	37
I-5.2	Oligomeric Rotaxanes & Catenanes	46
I-5.2.1	Statistical threading	46
I-5.2.2	Template threading	52
I-5.3	Polyrotaxanes	56
I-5.3.1	Classes of polyrotaxanes	56
I-5.3.2	Synthetic approaches to the main chain polyrotaxanes 98	57
I-5.3.3	Synthetic approaches to the side chain rotaxanes 100	65
I-6	Conductive polymers	70
I-6.1	Synthesis of poly(1,4-phenylenevinylene)	73
I-6.2	Synthesis of modified PPV	80
I-6.3	Luminescence property of PPV and its application	86
	REFERENCES	88

## **CHAPTER II. BLOCKING GROUP SYNTHESIS AND CHARACTERIZATION**

II-1	Introduction	94
II-2	Results & Discussion	96
II-3	Experimental	99
	REFERENCES	102

## **CHAPTER III. CROWN ETHER SYNTHESSES AND CHARACTERIZATION**

III-1	Introduction	107
III-2	Results & Discussion	111
III-2.1	Linear precursor synthesis	111
III-2.2	Crown ether synthesis and purification	112
III-3	Experimental	115
	REFERENCES	119

## **CHAPTER IV. SYNTHESSES AND CHARACTERIZATION OF POLY(1,4-PHENYLENEVINYLENE) AND POLY-(1,4-PHENYLENEVINYLENE) CROWN ETHER ROTAXANES**

IV-1	Introduction	130
IV-2	Results & Discussion	131
IV-2.1	Synthesis of Poly(1,4-phenylenevinylene)	131
IV-2.1.1	Synthesis of p-xylylene bis(tetrahydrothiophenium) chloride	131
IV-2.1.2	Synthesis of poly(1,4-phenylenevinylene) precursor	131
IV-2.1.3	Molecular weight of poly(1,4-phenylenevinylene)	133
IV-2.2	Synthesis of PPV rotaxane	137
IV-2.2.1	Synthesis of PPV in the presence of 18-crown-6	137
IV-2.2.2	Synthesis of poly(1,4-phenylenevinylene) rotaxane	137
IV-2.3	Photoluminescence of poly(1,4-phenylenevinylene) rotaxanes	142
IV-3	Experimental	144
	REFERENCES	149

## LIST OF TABLES

### CHAPTER I

I-1	Conductivities of conductive polymers	72
I-2	Conditions and products for the polymerization reaction of 1,1'-[1,4-phenylene-bis(methylene)] bis(thiolanylium) dichloride	75

### CHAPTER III

II-2.2	Results of $^{36}\text{C}_{12}$ syntheses by multiple condensation	112
II-2.2	Results of $^{42}\text{C}_{14}$ syntheses by multiple condensations	113

## LIST OF FIGURES

### CHAPTER II

II-1	270 MHz $^1\text{H}$ NMR spectrum of tris-p-t-butylphenyl-methanol in $\text{CDCl}_3$	103
II-2	FTIR spectrum of tris-p-t-butylphenylmethanol in KBr pellet	104
II-3	270 MHz $^1\text{H}$ NMR spectrum of tri-(p-t-butylphenyl)-4-hydroxyphenylmethane in $\text{CDCl}_3$	105
II-4	a) 270 MHz $^1\text{H}$ NMR spectrum of p-[p'-(tris-(p''-t-butylphenyl)methyl)phenoxy]benzylaldehyde in $\text{CDCl}_3$ ; b) FTIR spectrum of p-[p'-(tris-(p''-t-butylphenyl)methyl)phenoxy]benzylaldehyde in KBr pellet	106

### CHAPTER III

III-1	270MHz $^1\text{H}$ NMR spectra of a) di(ethylene glycol) ditosylate; b) tri(ethylene glycol) ditosylate in $\text{CDCl}_3$	120
III-2	270 MHz $^1\text{H}$ NMR spectra of a) 36-crown-12; b) 18-crown-6 in $\text{CDCl}_3$	121
III-3	$^{13}\text{C}$ NMR spectrum of 36-crown-12 in $\text{CDCl}_3$	122
III-4	Thermogravimetric analysis of 36-crown-12 in nitrogen and air	123
III-5	270 MHz $^1\text{H}$ NMR spectrum of 42-crown-14 in $\text{CDCl}_3$	124
III-6	IR spectrum of 42-crown-14 in KBr pellet	125

III-7	Thermogravimetric analysis of 42-crown-14 in nitrogen	126
III-8	270 MHz $^1\text{H}$ NMR spectrum of 60-crown-20 in $\text{CDCl}_3$	127
III-9	Thermogravimetric analysis of 60-crown-20 in nitrogen	128
III-10	Thermogravimetric analysis of 60-crown-20 in air	129

#### CHAPTER IV

IV-1	a) 270 MHz $^1\text{H}$ NMR; b) 100 MHz $^{13}\text{C}$ NMR spectra of p-xylylene bis(tetrahydrothiophenium) chloride in $\text{D}_2\text{O}$	150
IV-2	FTIR spectra of a) poly(1,4-phenylenevinylene) precursor; b) poly(1,4-phenylenevinylene) measured as free standing films	151
IV-3	UV-vis spectrum of poly(1,4-phenylenevinylene) precursor measured in deionized water	152
IV-4	Photoluminescence spectra of poly(1,4-phenylenevinylene) precursor measured in deionized water a) exposed to light; b) kept away from light	153
IV-5	Thermogravimetric analysis of poly(1,4-phenylenevinylene) precursor in $\text{N}_2$	154
IV-6	Molecular weight measurement of the poly(1,4-phenylenevinylene) precursor in deionized water by the low angle laser light scattering : $\text{Kc/R}(\theta)$ vs c	155
IV-7	FTIR spectra of a) poly(1,4-phenylenevinylene) precursor synthesized in the presence of 18-crown-6 measured as a free standing film; b) 18-crown-6 measured in KBr pellet	156
IV-8	a) 400 MHz $^1\text{H}$ NMR spectrum of the extract from poly[(1,4-phenylenevinylene)-rotaxa-(42-crown-14)] in $\text{D}_2\text{O}$ ; b) Quantitative 75 Mhz $^{13}\text{C}$ solid state NMR of poly[(1,4-phenylene-vinylene) rotaxa-(42-crown-14)]	157
IV-9	75 MHz $^{13}\text{C}$ solid state cross-polarization magic-angle spinning (CPMAS) NMR spectra of unstretched poly(1,4-phenylenevinylene) films which had been annealed at: a) 200; b) 250; c) 300 °C (ref. 28)	158
IV-10	75 MHz $^{13}\text{C}$ solid state NMR spectrum of 42-crown-14	159
IV-11	Thermogravimetric analysis of a) poly[(1,4-phenylenevinylene)-	

	rotaxa-(42-crown-14)] in N <sub>2</sub> ; b) poly(1,4-phenylenevinylene) in N <sub>2</sub>	160
	c) Thermogravimetric analysis of 42-crown-14 in N <sub>2</sub>	161
IV-12	Quantitative 75 Mhz <sup>13</sup> C solid state NMR of poly[(1,4-phenylenevinylene)rotaxa-(60-crown-20)]	162
IV-13	Hydrodynamic size of poly(1,4-phenylenevinylene) precursor measured in deionized water at different salt (NaCl) concentrations	163
IV-14	Photoluminescence spectrum of poly(1,4-phenylenevinylene) film measured with 320 nm incident light. film thickness: 40.3±19.6µm	164
IV-15	Photoluminescence spectrum of poly[(1,4-phenylenevinylene)-rotaxa-(42-crown-14)] film measured with 320 nm incident light. film thickness: 73.4±33.8 µm	165
IV-16	Photoluminescence spectrum of poly[(1,4-phenylenevinylene)-rotaxa-(60-crown-20)] film measured with 320 nm incident light. film thickness: 57.0±9.0 µm	166
IV-17	Photoluminescence spectrum of poly(1,4-phenylenevinylene) and 42-crown-14 blend (1.9:1 wt ratio) film measured with 320 nm incident light. film thickness: 91.6±14.1 µm	168
IV-18	Diagram of conductivity measurement via a four-probe method	169
IV-19	Absorption spectra of: a) poly(1,4-phenylenevinylene); b) poly[(1,4-phenylenevinylene)-rotaxa-(42-crown-14)] films	169
IV-20	Absorption spectra of: a) poly[(1,4-phenylenevinylene)-rotaxa-60-crown-20]; b) Physical blend of poly(1,4-phenylenevinylene) and	

	42-crown-14 films	170
IV-21	75 MHz $^{13}\text{C}$ CPMAS spectrum of crown ether and PPV42C14 rotaxane mixture	171

# CHAPTER I. INTRODUCTION AND LITERATURE REVIEW

## 1. Introduction to polymer classifications

Since Staudinger's first proposal of the chain formula in 1920, the structures of polymers have been well understood and tremendous applications have been found for these covalently bonded giant molecules. In addition to the natural polymers, synthetic polymers, which are a kind of lightweight and easily-processible material, have been widely used to replace or supplement those traditional materials in everyday life. Due to different chemical and physical properties, the polymers are used as plastics, rubber, adhesives, fibers and paints.

The term "polymer" is derived from the Greek words "poly" and "meros", meaning "many" and "parts", respectively. The polymers were originally classified by Carothers into condensation and addition polymers on the basis of compositional difference between the monomers and polymers. Examples of condensation polymers include polyesters and polyamides, which are formed from various condensation reactions with the elimination of small molecules. The repeating units of these kinds of polymers are joined by functional groups, e.g. ester, amide, etc... Vinyl monomers are the most widely used monomers in the syntheses of addition polymers which are formed without loss of small molecules. The repeating units of the addition polymers are not linked by functional groups. In addition to this classification, Flory divided the polymers into step growth and chain growth polymers to stress the polymerization mechanism.

## 2. Topology of polymers

Besides the above classifications, the structure or architecture of the polymers is another criteria for polymer distinction. Scheme I shows different polymers that are distinguished by their architectures.

### Scheme I-1

#### Polymers of Different Architectures

##### 1. Linear polymers (two chain ends)

- a. Homopolymer: AAAAAAAAAAAAAAAAAA
- b. Random Copolymer: ABAABBABABABAAABABBABBABA
- c. Alternating Copolymer: ABABABABABABABABAB
- d. Block copolymer: AAAAAAAAAAAAAABBBBBBBBBBBBB

##### 2. Branched polymers (more than two chain ends)

###### a. Random branched polymer



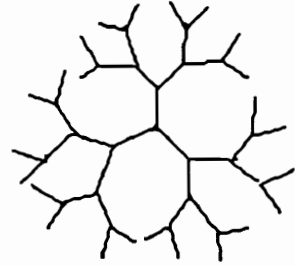
###### b. Star polymer (Homo- or Block-)



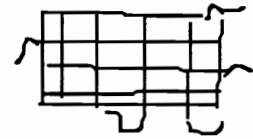
###### c. Graft/Comb polymer (Long chain and short chain branching)



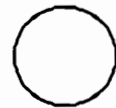
d. Dendrimer



3. Network polymer (one enormous molecule with few chain ends)



4. Cyclic polymer (no chain end)



The different architectures are listed in order by increasing number of chain ends, except for the network polymers, which have few chain ends because of crosslinks, and cyclic polymers, which have no chain end.

The cyclic polymer, which has no chain end, is a very special architecture. This unique architecture provides some special properties, including lower melting viscosity, lower hydrodynamic volume, higher glass transition temperature, and lower frictional coefficient as compared to the linear polymer with similar molecular weight.

Among the four different linear polymers, homopolymers are best understood. Since they are synthesized from identical monomers, the physical properties of these polymers basically depend on the polymer chain interactions. These interactions are determined by the molecular weight, the chain regularity (packing of the chain) and the bonding force between the chains.

When two or more monomers are utilized in the polymerization and incorporated into the polymer chains, copolymers are generated. The copolymers can be subdivided into statistical, alternating, and block copolymers according to the sequence of the

repeating units along the polymer chains. The statistical copolymers, or random copolymers, are characterized by a random distribution of the monomer units along the polymer chains. Because of this structural arrangement, the properties of the statistical copolymers are the average of the constituent homopolymers. In contrast to the random copolymer, the alternating copolymers have a highly ordered alternating sequence of monomer units. The properties of these copolymers are not simply the average of the constituent homopolymers; for example, glass transition temperatures of these copolymers are not the average of the constituent homopolymers. However, because of the high regularity along the chains, the alternating copolymers may exhibit excellent mechanical properties upon stretching.<sup>1</sup>

The block copolymers are comprised of two or more homogeneous long segments of different composition joined end-to-end. Because of chemical heterogeneity, the incompatible compositions have a tendency to segregate. This tendency can result in micelle formation in selective solvents, which is analogous to the aggregation of surface active agent. The segregation may also give rise to microdomain formation in the solid state, which can be utilized in the thermoplastic elastomer design. The glassy (hard) segments can be designed to be incompatible with the rubber segments which are soft at the service temperature. Thus, the hard segments can segregate and form microdomains which act as physical crosslink points to strengthen the mechanical properties of the elastomers. Moreover, these domains can dissociate and flow at elevated temperatures which allows easy processing.<sup>2</sup>

The three copolymers mentioned above may have completely different properties only because of the different structural arrangements even though the total compositions are the same. This suggests that the design of a structural arrangement is an effective tool in obtaining different materials with a variety of properties.

The branched polymers are those main chain polymers having branch points, atoms, or small groups from which more than two chains emanate. The branches or side chains of the branched polymers are constitutionally the same as the main chains. The main chains are usually the longest. The branches are called long-chain or short-chain depending on their length. The branched polymers may have properties similar to those of the linear ones. For example, a branched polymer and its linear analog can both be soluble in the same solvent. However, the branched polymers can also have remarkably different properties from those of linear polymers.<sup>6</sup> According to the shape of the branches, the branched polymers can be classified into randomly branched polymers, star polymers, graft, or comb copolymers and dendrimers.

In the randomly branched polymers, the branches from the main chain can also be branched, which is known as series branching.<sup>5</sup> As branches carry branches, the extensively branched polymers form a shape like a tree. The star polymers with branches radiating from the central core are characterized by their low hydrodynamic volumes which arise from the low radius of gyration. This also gives rise to lower intrinsic viscosities in solutions relative to the linear analogs with the same molecular weight. The star polymers can be homopolymeric or diblock copolymeric, depending on the constitution of the branches. The star diblock copolymers are the best defined groups of the block copolymers so far. The number of their side-arms, compositions, the length of the arms, molecular weight, and molecular weight distribution can be controlled well via anionic polymerization techniques.<sup>3,4</sup>

The graft copolymers are polymers attached with branches having different constitutional or configurational features from those of the main chains, which are also known as graft bases or graft substrates. The constitutional difference is the most distinguishable feature, i.e., the side chain units are composed of different monomers from those of the main chains. The main chains and side chains can be both

homopolymeric or copolymeric; or the main chains may be homopolymeric and side chain may be copolymeric and vice versa. <sup>7</sup> The comb polymers, a special kind of graft copolymers, contain side chains with almost the same length emanating from their main chains at various positions. As a polymer architecture, graft copolymers are common modifying tools on polymer properties. Modification by this architecture also depends on the compatibility of the graft chains and graft bases. Because the graft chains and graft bases are chemically bonded and are usually thermodynamically incompatible, microphase separation can occur similarly to the microphase separation in the block copolymers. The microphase separation in graft copolymers may bring great improvements in thermal and mechanical properties, such as thermoplastic elasticity. For example, the ABS resin is a polymer grafting styrene-acrylonitrile copolymer onto an elastomer, such as polybutadiene, which exhibits excellent toughness and good dimensional stability with sufficient compatibility of graft chains and graft bases. <sup>8</sup>

The dendritic architecture with extensive branches radiating from the central core has attracted substantial attention lately. The dendrimers possess three distinguishing features: 1) a core; 2) interior layers (generations which attach to the center core and are composed of repeating units); and 3) an exterior of terminal functionality possessed by the outermost layer. <sup>9, 10</sup> The divergent construction from center outward and the convergent method which builds the molecules from outward to the center core are the two synthetic ways that lead to the dendrimers. Since the properties and the applications of the dendrimers are still under further investigation, they still remain a challenge to both synthetic polymer chemists and analytical chemists. <sup>11, 12</sup>

The crosslinked polymers are formed when polymer molecules are connected to each other by chemical bonds. The number of crosslinks in a given mass of polymer is called crosslink density. The crosslinks can be made during the polymerization process by using appropriate monomers ( $f > 2$ ). They can also be formed by chemical reactions

after polymerizations, e.g. vulcanization. By forming crosslinked networks, the movements of polymer chains are restrained and the positions of the chain are maintained even at temperatures above  $T_g$ . Therefore, the crosslinked networks impart: 1) increase in  $T_g$ ; 2) good recovery properties; 3) good dimensional stability; 4) good solvent resistance; 5) lower creep rate; and 6) good thermal stability to polymers. <sup>13-15</sup>

Interpenetrating polymer networks (IPN) can be defined as the combination of the two crosslinked polymer networks, at least one of which is synthesized or crosslinked in the immediate presence of the other. According to different synthetic methods, IPN can be classified as: 1) sequential IPN, which is made by mixing swollen polymer network I with monomer II, crosslinking agent, and activators of both network in situ; and 2) simultaneous IPN, which is formed by combining monomers or prepolymers in bulk, solution, or dispersion and polymerizing simultaneously. The individual polymerizations do not interfere with each other due to different polymerization modes. For example, the two polymer networks can be synthesized via step growth and chain growth polymerizations, respectively. <sup>16</sup> Interpenetrating polymer networks are actually blends of two or more polymers, which may generate a less phase separated mixture, especially when two polymers are immiscible. <sup>17</sup> Since the mixing takes place at low molecular weight level and the polymerization is achieved simultaneously with crosslinking, phase separation may be restricted by cross-linking in a kinetic way. However, interpenetrating polymer networks may have less miscibility than crosslinked polymer blends, especially when two polymer networks are miscible. <sup>17</sup> The IPN architecture can be utilized to produce a polymer with synergistic properties. For example, the combination of a glassy polymer with an elastomeric polymer can result in reinforced rubber if the elastomer phase is predominant, or a high impact plastic if the glass phase is continuous. Other mechanical and thermal properties can also be improved by this architecture. <sup>17, 18</sup>

### **3. Polymer blends**

Besides the IPN architecture, polymer blend construction is another way to obtain good polymer properties. It is also less expensive and much easier than chemical modification or new polymer architecture design. Polymer blends are mixtures of two or more polymers or copolymers.<sup>5, 20</sup> Polymer blends can be manufactured by melt blending, solution blending, latex, or dispersion mixing.<sup>21</sup> Depending on the miscibility of the components, the polymer blends may be single phase which exhibit only one glass transition temperature,  $T_g$ , or separated phases which exhibit different glass transition temperatures associated with each phase. When one of the polymers in the blends crystallizes, a separate crystalline phase of this polymer can be formed even though two polymers are miscible and there is still only one  $T_g$  as a result of the remaining mixed amorphous phases.<sup>19</sup> Besides miscibility, the properties of polymer blends also depend on the nature of the components (glassy, rubbery, semicrystalline), means of processing, and interactions between the polymers. Polymer blends with improved mechanical and thermal properties include miscible poly(vinyl chloride)-nitrile rubber blend, and miscible poly(2,6-dimethyl-1,4-phenylene oxide)-polystyrene (Noryl) blend.

### **4. New polymer architectures**

In order to fulfill the increasing demands for polymers with special properties, new polymer architectures have been developed during the past decade. In addition to the dendrimers, hyperbranched polymers, and macromonomers, polyrotaxanes have been one of the novel polymer architectures which have attracted growing interest.

Polyrotaxanes are comprised of linear polymer backbones threaded by macrocycles with no covalent bond between the two components. In other words, the macrocycles and linear polymer backbones are only physically linked. To prevent the

dethreading of the macrocycles from the linear chains, blocking groups are fixed at the chain ends. By careful design, the macrocycles can move laterally and circumferentially with respect to the linear backbone. Because of this unique architecture, the polyrotaxanes are expected to have different physical properties from those of the conventional block copolymers and polymer blends. Compared to the block copolymers, the polyrotaxanes have only physical linkages between the two components instead of chemical bond. However, the polyrotaxanes may have a similar microdomain formation as in the immiscible block copolymer systems because of the immiscibility between the macrocycles and polymer chains. Other than that, the free movement of macrocycles relative to the linear chains can result in aggregation and crystallization. The polyrotaxanes also differentiate from polymer blends in two ways: 1) the rings and the chains may have attractive interactions; and 2) the physical barriers of the chains can hold the rings and restrain their excess movements. Therefore, as one of the novel polymer architectures, polyrotaxanes are expected to have interesting properties in both solid and liquid states and great potential for applications.

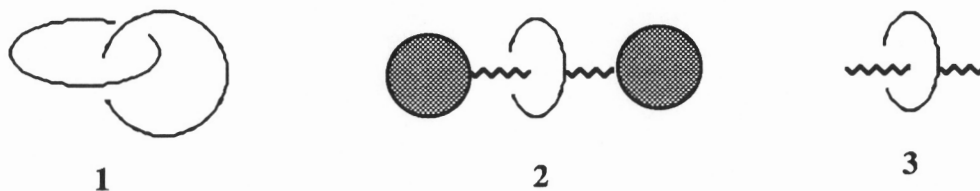
To fully understand polyrotaxanes, it is necessary to begin with their low molecular weight analogies, rotaxanes, and their closely related molecular architectures, catenanes, which can be formed by cyclization of the linear chains of the rotaxanes. Rotaxanes, catenanes and their polymeric analogies are going to be reviewed in the following sections.

## **5. Rotaxanes, catenanes and their polymeric analogs**

### **5.1 Low molecular weight rotaxanes and catenanes**

#### **5.1.1 Definition and early work: statistical threading**

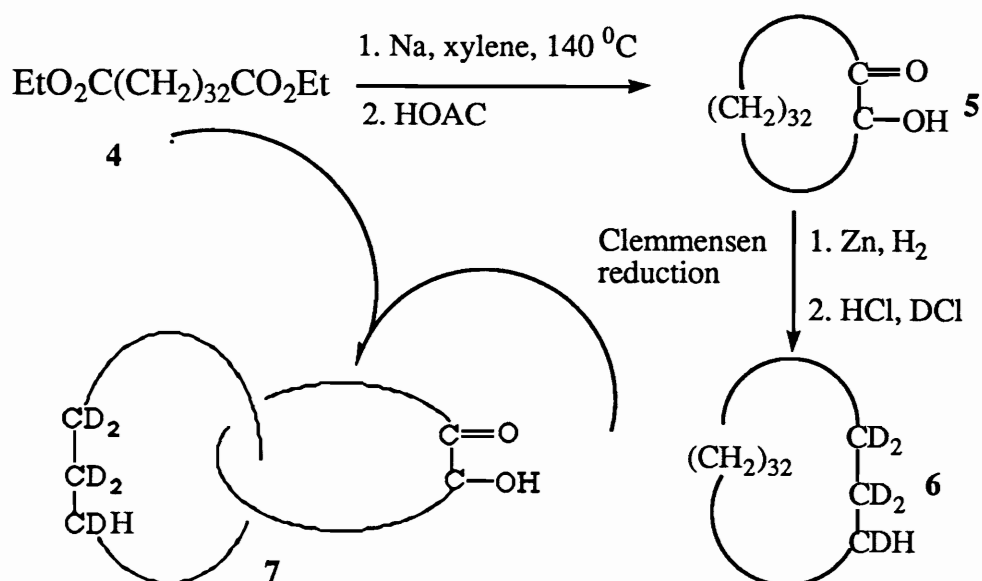
Catenane is a generic name for structure **1**, which consists of mechanically interlocked macrocycles, i.e., no chemical bond between two species. Its name is derived from a Latin word “catena” meaning “the chain”.



The term rotaxane also comes from the Latin “rota”, meaning “wheel” and “axis”, meaning “axle”. It is composed of a linear “rod” that pierces the macrocyclic “ring” with two bulky endgroups, at each end to prevent the dethreading of the macrocycles from the linear rod, **2**. When macrocycles have strong interactions with the linear species or when the linear chains are long and flexible, the blocking groups may not be necessary. The suggested name for this structure is pseudorotaxane, **3**.<sup>22</sup> The rotaxanes fall into several subcategories: homorotaxanes which are composed of chemically equivalent macrocycles and linear chains and heterorotaxanes which consist of macrocycles and linear chains with different chemical constitutions. Homorotaxanes, for example, poly(ethylene oxide) threaded with crown ether, are suitable for studying the architecture effect of the rotaxanes because the two components have no chemical difference. Heterorotaxanes, such as polyurethane threaded with crown ether, offer an opportunity to study interactions between the chemically different components and contributions of the two species to the final properties of the rotaxanes as compared to the copolymers and the polymer blends.

The interlocked ring structure was first mentioned by Willstatter in a seminar in Zurich prior to 1912.<sup>23</sup> In 1953, Frisch et al. proposed the existence of the interlocked rings in polysiloxanes. They postulated the linear chains and chainlike bonded rings consist of 50-100 interlocked monomeric species.<sup>24</sup> Patat and Derst also suggested the

interlocked rings in the polymeric phosphonitrile chloride in 1959.<sup>25</sup> However, no such compounds were isolated and demonstrated by any analytical means. Luttringhaus and Schill were among the first to discuss the principles involved in the synthesis of catenanes and carried out some experimental work.<sup>26</sup> Due to the statistical character of their syntheses, no interlocked chain was isolated.<sup>27, 28</sup> However, the German chemists' work inspired one of the US researchers in the Bell Laboratories, namely, Wasserman, who first synthesized the interlocked macrocycles by acyloin condensation in the presence of the preformed cyclic hydrocarbon.<sup>29</sup>



The cyclic hydrocarbon was generated by a reaction of diethyl tetratriacontanedioate (4) with sodium to yield cyclic acyloin 5 followed by a Clemmensen reduction with deuterated hydrochloric acid to give macrocycle 6. The cyclic hydrocarbon had five atoms of deuterium per molecule. To synthesize the catenane, 4 was mixed 1:1 with 6 and cyclized to give 5 in xylene. Since during the cyclization process, some long chain diesters were threaded statistically into the macrocycle 6, the final ring closure resulted in a small amount of catenane. After the reaction, the deuterated macrocycle 6 was removed from the other products by

chromatography. The product containing acyloin macrocycle **5** was also separated. However, the infrared spectrum of this fraction showed bands at 2105, 2160, 2200  $\text{cm}^{-1}$  which represent the C-D stretch in **6**. To ensure the purity of this fraction, this fraction was rechromatographed and it was demonstrated that the deuterium associated with macrocycle **6** was not due to the contamination of the unthreaded macrocycles **6**. This indicated the formation of the catenane **7**. To further prove the catenane structure, the deuterium containing fraction **5** was oxidized with alkaline hydrogen peroxide. The oxidation cleaved the acyloin macrocycle **5** and gave the diacid related to **5** with  $\text{d}_5$ -macrocycle **6**. The yield of the catenane was first claimed to be 1%, relative to the entire mixture isolated. This claim was later modified to be the chromatographic yield, that is, several powers of ten less than the first reported value.<sup>30</sup> Actually, according to Frisch's calculation,<sup>23</sup> the probability of statistical threading was around  $10^{-2}$ . This also suggests that the formation of the extended interlocked rings has a very small probability. However, the catenane was not proven by mass spectrometry.

After the first synthesis of catenane, Frisch and Wasserman published their famous paper "Chemical Topology".<sup>23</sup> In this paper, the topology of the molecule was asked to be considered as one of the molecular structural characters and topological isomerism was proposed. A simple example of topological isomers is **1** and the two unlocked two components of **1**. Even though **1** is composed of two sets of atoms, each set fulfills the molecule definition and there is no chemical bond between each set. To separate these two sets of atoms chemical bond breaking is necessary. Therefore **3** and its unlocked two components are considered as topological isomers.<sup>23</sup> Frisch and Wasserman also mentioned the stability of the rotaxane system **2** which may be as stable as a catenane when blocking groups are fixed at the ends to prevent the extrusion of a threaded chain from the macrocycle. In fact, this rotaxane structure was synthesized by Harrison & Harrison six years later. They prepared this structure by modifying

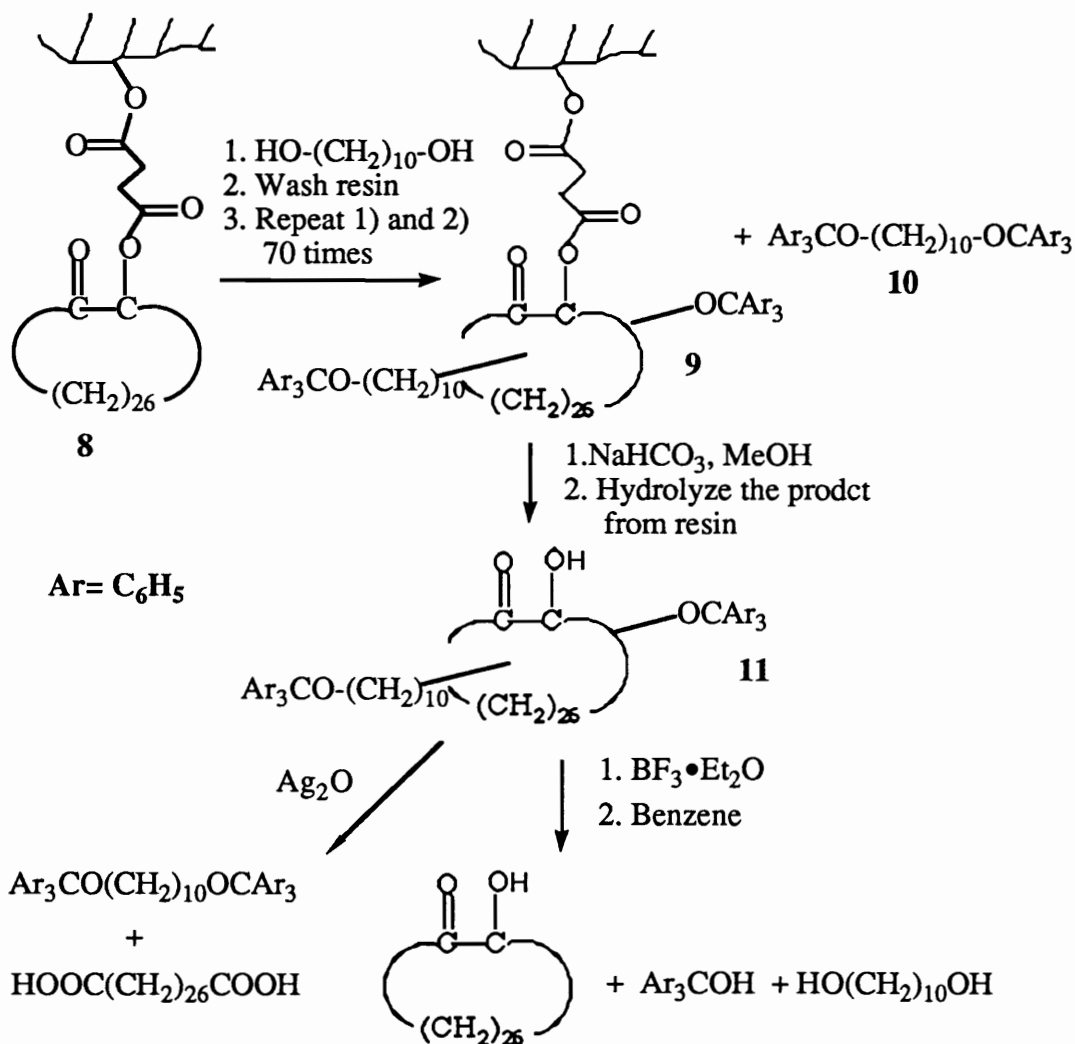
Wasserman's statistical approach. The obtained complex structure was called 'hooplane' which was later changed to rotaxane.<sup>31</sup>

As Wasserman and Frisch discussed in their paper, statistical threading gave very poor yield. To overcome this difficulty, Harrison & Harrison bound the macrocycles onto the resin in a column and washed the column with a solution containing linear chains which increased the possibility of threading.

The resin-bonded macrocycle **8** was formed by reacting 2-hydroxycyclotriacontanone with succinic anhydride to give hemisuccinate ester, followed by coupling with Merrifield's peptide resin. This resin-bonded macrocycle **8** was treated with 1,10-decanediol and triphenylmethyl chloride 70 times to give a complex **9** and a linear "dumbbell" **10**. After extraction of free reagents and soluble materials, the macrocycles were hydrolyzed from the resin by refluxing with sodium bicarbonate in methanol. The product was purified by chromatography and 1% yield was obtained. The purified complex, an oil, was stable up to 200 °C. The IR spectrum of this complex showed similar bands to that of the macrocycle and the linear chain. However, the chromatography demonstrated that the complex was not contaminated by the acyloin macrocycle, or linear dumb bell **10**. The proposed rotaxane structure was also supported by degradation results. Cleavage of complex **11** by oxidation gave octacosane-1,28-dicarboxylic acid, isolated as the dimethyl ester and the linear dumbbell. Another cleavage of complex **10** by boron trifluoride etherate gave 1,10-decanediol, triphenylmethanol and macrocycle which further support the rotaxane structure.

After the synthesis of this rotaxane, Harrison continued studying the effect of macrocycle ring size on the formation and stability of the rotaxane. This was done by reversible cleavage of the blocking groups on the linear dumbbell to provide the statistical threading. The cyclic hydrocarbon mixture **12** was reacted with linear dumb

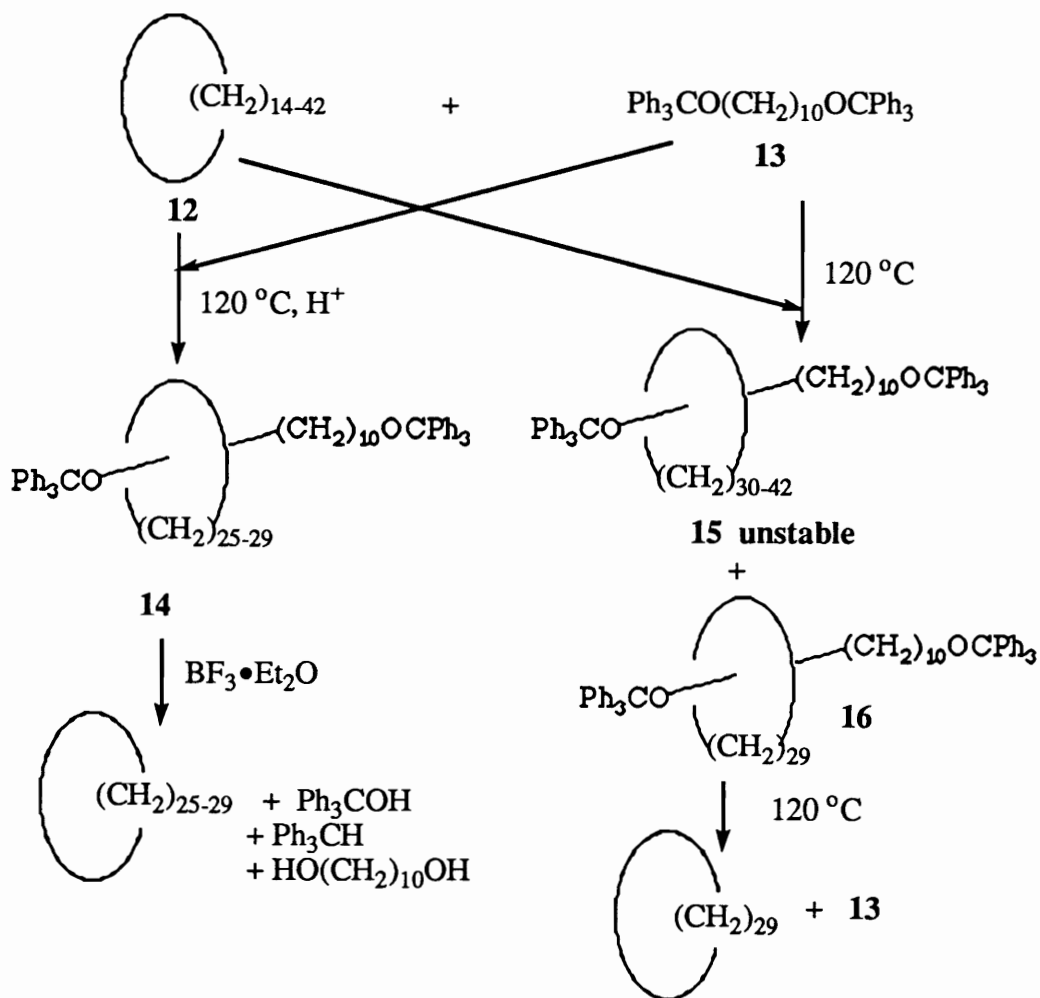
bell **13** and catalyzed by small amounts of trichloroacetic acid which can reversibly cleave the triphenylmethyl groups, thus allowing the statistical threading of cyclic hydrocarbons onto the unblocked linear chains.



The reaction was then quenched with a base and the rotaxanes were separated from unreacted macrocycles and linear dumb bells by chromatography. Acid hydrolysis of purified rotaxanes gave a mixture containing five macrocycles from cyclopentacosane (C<sub>25</sub>) to cyclononacosane (C<sub>29</sub>) and some fractions from linear chains and blocking groups. The very small peaks, possibly corresponding to C<sub>23</sub> and C<sub>24</sub> macrocycles,

were also detected by gas chromatography. However, the C<sub>30</sub> or higher macrocycles were not observed.

The relative yields of macrocycles were 1, 9, 23, 43, and 57 for macrocycles C<sub>25</sub> to C<sub>29</sub>, respectively. This suggested that the threading yields of the rotaxanes increased with the ring size, indicating that the ring size was an important factor in improving the rotaxane yields. Harrison also commented that the reaction results agreed with molecular modeling; this indicated that the ring of 22 methylene units can be threaded by a methylene chain but in close contact, while C<sub>29</sub> or larger macrocycles can slip over a trityl group.

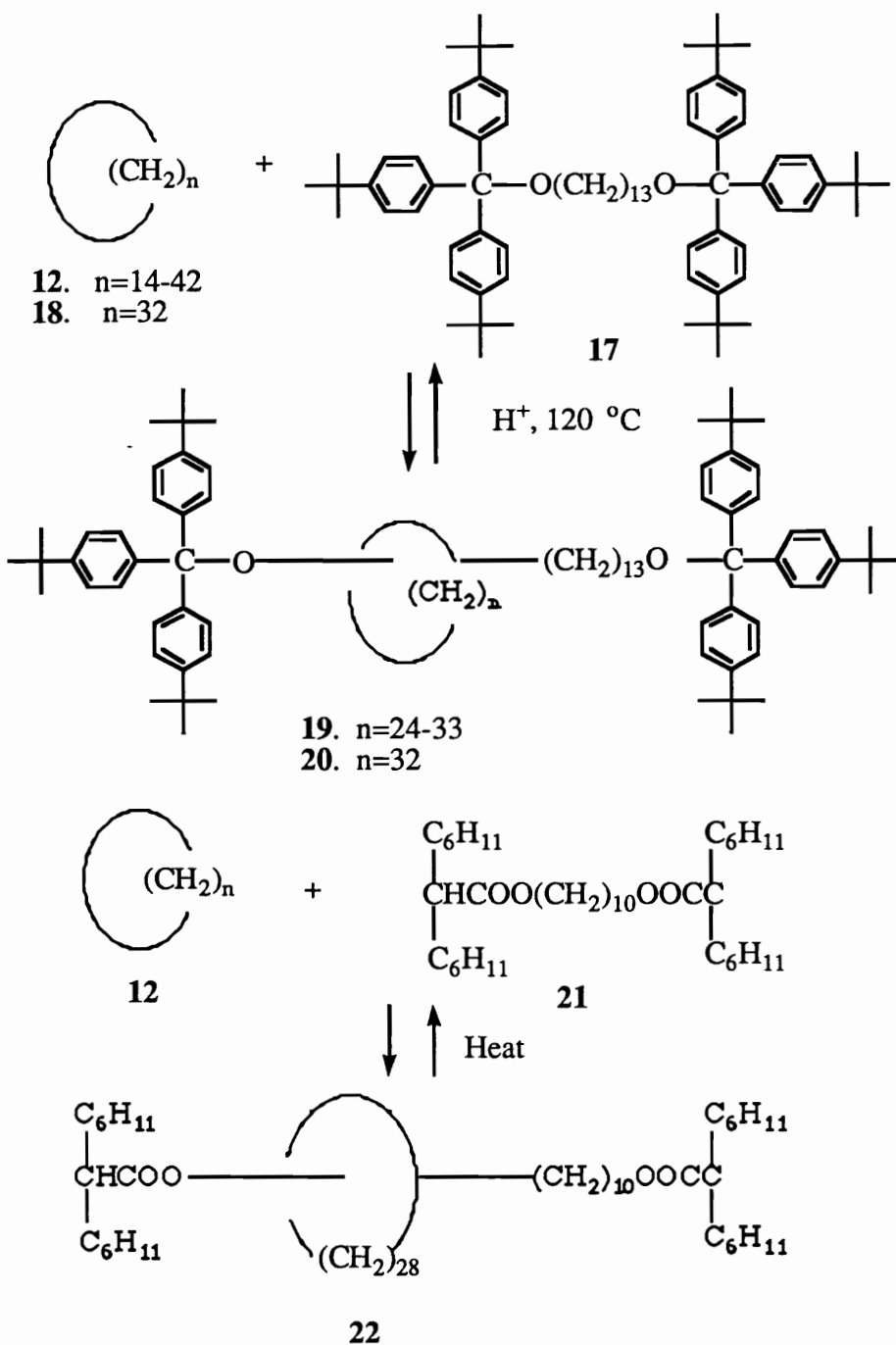


The ring size factor was also studied by thermal analysis. In this test, cyclic hydrocarbon mixture **12** (C<sub>14</sub>-C<sub>42</sub>) was mixed with linear dumbbell **13** and heated to 120 °C. Separation of the reaction mixture gave unreacted **12** and **13**, and the threaded rotaxane **16** formed from C<sub>29</sub> macrocycle only. This rotaxane was purified by chromatography and resubjected to heat at 120 °C. The heat at 120 °C allowed the linear dumbbell to dethread from the C<sub>29</sub> macrocycle and the half life of the rotaxane **16** was about 10 minutes. From this result the author concluded that the macrocycle with a similar cavity (C<sub>29</sub>) to the blocking group size could slip over the blocking group if enough energy was given. The macrocycles having cavities larger than the blocking group size (C<sub>30</sub>-C<sub>42</sub>) can pass over the blocking groups and form only transient rotaxanes at room temperature. The thermal test also demonstrated the stability of the rotaxanes and blocking ability of trityl groups that can block a macrocycle with ring size up to 28.

Having noticed the size of the macrocycles and the bulk of the blocking groups to be the important factors affecting the rotaxane yield and stability, Harrison continued his study by using another linear dumbbell, 1,13-di(tris-4-t-butylphenylmethoxy) tridecane **17**. This linear dumbbell was also heated with macrocycle mixture **12** in the presence of naphthalene-β-sulphonic acid which can reversibly cleave the trityl ether group. The reaction was quenched with a base and the rotaxane **19** was separated by chromatography. The rotaxane **19** was hydrolyzed with acid and different sized macrocycles were released. The yield of the individual rotaxanes was determined by the yields of the individual macrocycles. The results indicated that the yields of rotaxanes increased monotonically with the ring size from C<sub>24</sub> (0.0013%) to C<sub>33</sub> (1.6%) and no rotaxane with a larger ring was detected. However, when chromatography was performed at 0 °C during separation, unstable C<sub>34</sub> rotaxane was detected. This result also agreed with the CPK modeling. The thermal threading of this system gave only

unstable rotaxane when the macrocycle mixture and linear dumb bell **17** were combined and heated to 250 °C.

However, when the bisdicyclohexylacetate of 1,10-decanediol was used as a linear dumbbell, C<sub>28</sub> rotaxane **22** could be prepared by similar thermal means. To prepare rotaxane for sufficient characterization, the mixture of cyclodotriacontane **18** and linear dumb bell **17** was heated in the presence of naphthalene-β-sulfonic acid.



The crystalline rotaxane **20** was isolated in 1% yield by chromatography. The IR spectrum showed no difference between the rotaxane and an equimolar mixture of **17** and **18**. The NMR spectrum showed only a slight difference between the rotaxane and

the mixture in which the proton of macrocycle in rotaxane shifted from 1.25 to 1.21 ppm. The molecular weight of the rotaxane estimated by chromatography was 1300-1600 (the formula weight of rotaxane is 1486). However, the melting point of the rotaxane (150-151 °C) was quite different from that of the macrocycle (64-66 °C) and the linear dumb bell (211-212 °C) components.

From Harrison's results, several conclusions can be drawn:

1. Macrocycles need to have more than 22 methylene units to be threaded.
2. The triphenylmethyl group can block macrocycles with a ring size up to 28 and a macrocycle with 29 methylene units can thermally slip over triphenylmethyl group. Macrocycles with a ring size larger than 29 can form only temporary rotaxanes and easily thread and dethread.
3. The tris(4-t-butylphenyl)methyl group can block a macrocycle with a ring size up to 33.
4. Thermal preparation of rotaxane can be achieved if a macrocycle's cavity is similar to the blocking group.

Harrison's work was later confirmed by the results of Schill and his coworkers when they investigated the ring size, the blocking group effectiveness and the length of linear chain.<sup>34</sup> The experiments were carried out by both thermal and acid catalyzed means, using individual pure macrocycles. The ring size factor was studied by equilibrating the macrocycle **23** (ring size from 21-29) and bis(triphenylmethyl)thio-dodecane (**24**) neat (0.9-1 M in each compound) both thermally and in the presence of p-toluenesulfonic acid (130 °C, 30 minutes). The yields of the rotaxane **25** were found to increase with the ring size in both equilibrations. The yield of rotaxane **28** also increased with length of linear chain from 4.5 to 11.3%, using alkane chain ends blocked with trityl groups **27** and macrocycle **26**. Schill's work confirmed that the threading of the rotaxane strongly depended on the ring size and the length of the chain. However,



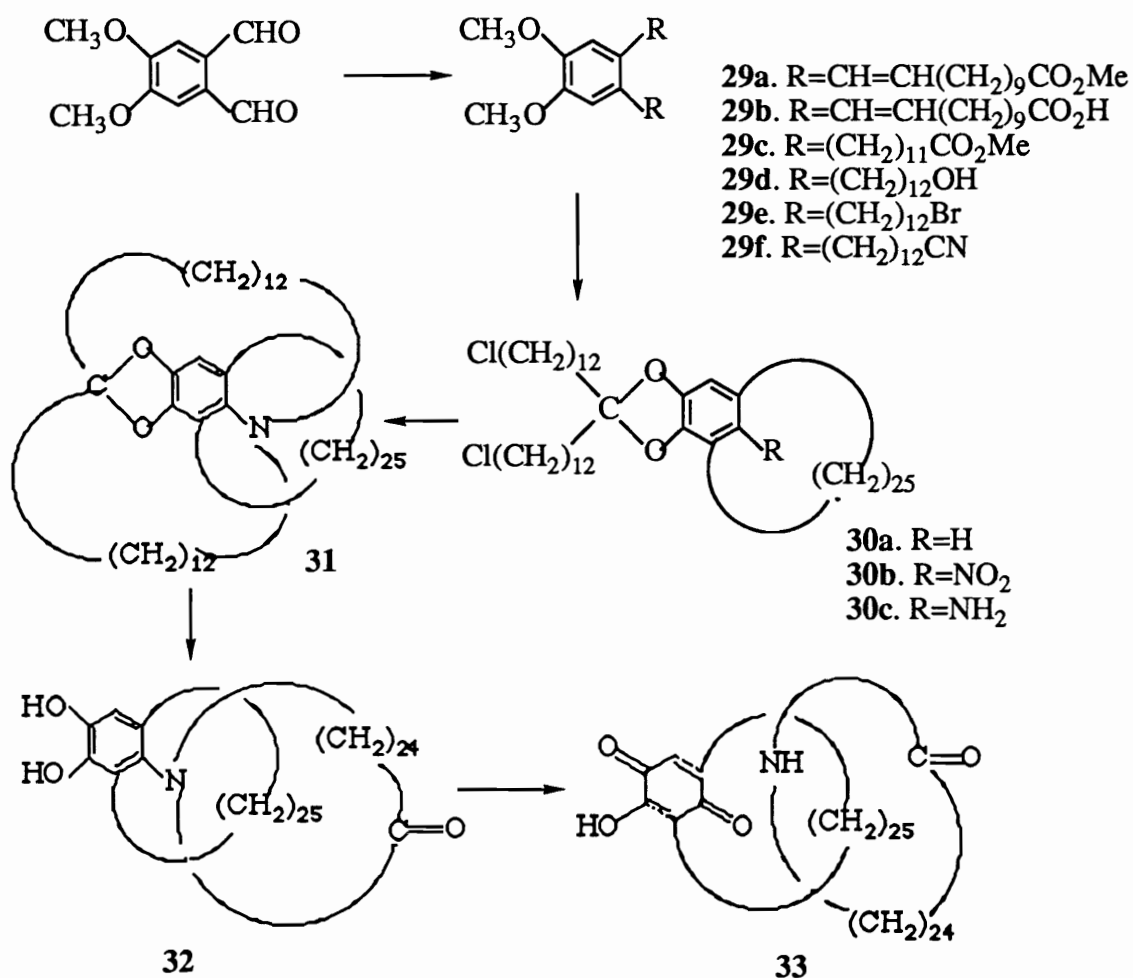
Another question about the blocking groups that arises is: do the blocking groups affect the final threading yield? The answer might be yes because the blocking groups are very bulky. They may “push” some of the threaded macrocycles from the linear chains as they connect to the linear chains.

### 5.1.2 Synthesis about a center core: directed approach

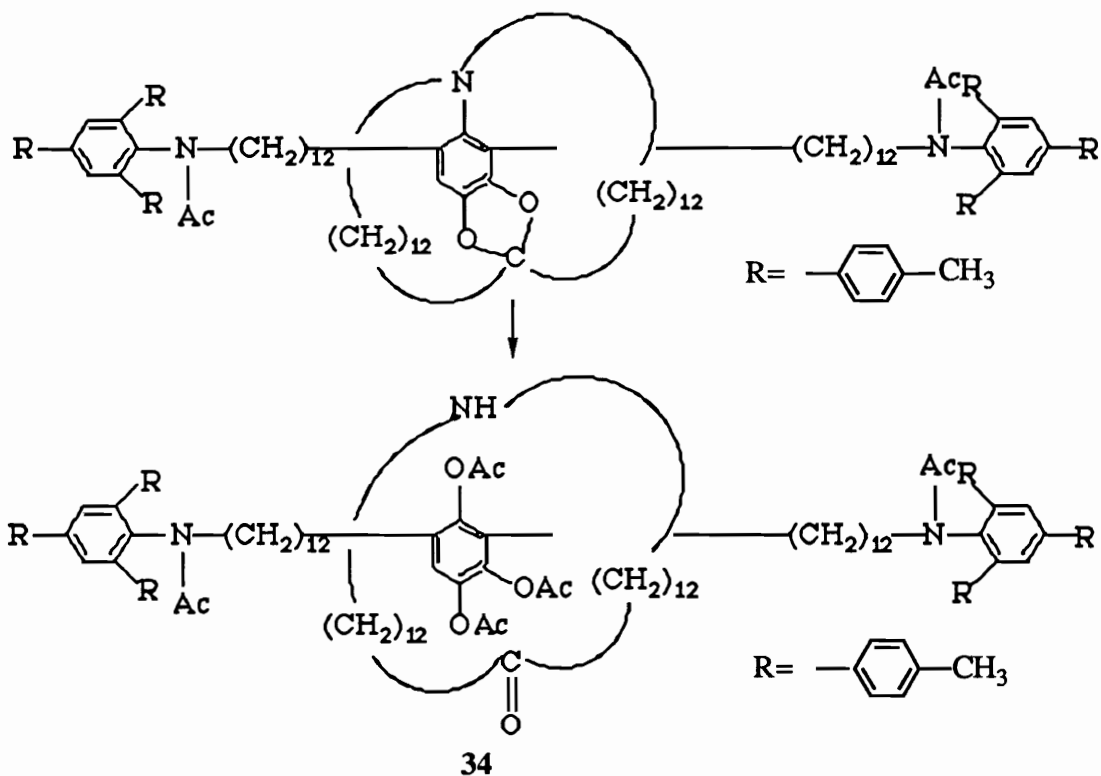
After the disappointing results obtained by statistical method,<sup>27</sup> Schill and Luttringhaus changed their synthetic methodology. They developed a new way to synthesize rotaxane and catenane: directed synthesis. This method involved the formation of a temporary linkage between the macrocycle and the linear chain which resulted in prethreaded and non-threaded isomers existing in conformational equilibrium. To obtain the rotaxane, the isomers can further react with bulky blocking groups to block the two ends followed by the cleavage of the temporary bond. Besides the rotaxane obtained, the linear dumbbell and macrocycle can also be formed from the non-threaded isomer. Catenanes can also be made via this route. Cyclization of the linear chain followed by cleavage of the temporary bond gives a catenane or two macrocycles.<sup>35</sup>

Using this method, Schill started the synthesis of a catenane from 4,5-dimethoxyisophthalaldehyde which was converted to diene ester **29a**. This compound was hydrolyzed to give the dicarboxylic acid which was hydrolyzed and esterified to give ester **29c**. This diester was reduced to diol **29d** with  $\text{LiAlH}_4$ . The diol **29d** was then converted via dibromo **29e** and dinitro **29f** derivatives and demethylation into the cyclic ketone. The cyclic ketone was reduced to 3,5-pentacosamethylenecatechol and converted to cyclic ketal **30a** by reaction with 1,25-dichloropentacosan-13-one. Nitration and hydrogenation of **30a** gave nitro- **30b** and amine **30c** derivatives of the cyclic ketal. Cyclization of **30c** with potassium carbonate gave a precatenane: 2,2-N,N-

bisdodecamethylene-4,6-pentacosamethylene-5-amine-1,3-benzo[d]dioxol (**31**), which was linked intra-annularly; the chain of the double ansa-system was situated on the opposite side of the benzene ring. The extra-annular isomer was avoided. The ketal linkage of **31** was cleaved with HBr in acetic acid to give intra-annularly linked catechol derivative **32** which was dehydrogenated and hydrolyzed to give catenane **33**. In order to analyze catenane **33**, it was acetylated with acetic anhydride to give the O,N-diacetate which was characterized by infrared spectroscopy. Reductive acetylation of O,N-diacetate gave the tetraacetate which was also identified by its infrared spectrum. The molecular weight of this complex was determined by isothermal distillation. The molecular weight (960 and 985) was in agreement with the calculated value of the combined weight of the two interlocked molecules, 1022.5.<sup>7</sup>



Besides the catenane, Schill and Zollenkopf also demonstrated the synthesis of rotaxanes via directed synthesis which was the first report of rotaxane synthesis.<sup>36</sup> The rotaxane was designed around a phenyl ring. The rotaxane **34** was made by cleaving the ketal bond between the macrocycle and the linear chain.



### 5.1.3 Template syntheses

While Harrison and Schill were studying statistical and directed syntheses of the rotaxanes, a new area of chemistry had been developed. This area of chemistry not only had great application potential in the last decade, but also played a very important role in the later rotaxane, catenane and polyrotaxane development. This area is host-guest and supramolecular chemistry, developed by Cram and Lehn. Cram, Lehn and Pederson shared the Nobel prize of chemistry for their contributions in this area. 38, 39 Host-guest and supramolecular chemistry are all based on strong interactions known as template effects between molecules.

By definition, a template effect is a phenomenon by which a guest (a metal ion or neutral molecule) can “coordinate” a ligand of host molecules which is thereby locked into a specific position or in suitable conformation for the formation of a specific

product.<sup>39</sup> The term “template effect” was first defined in the early 60s by Thompson.<sup>40</sup> The template synthesis of rotaxanes and catenanes can be basically divided into three categories: 1. Metal; 2. Cyclodextrin inclusion; and 3. Charge transfer or  $\pi$ -stack complexes.

### 5.1.3.1 Metal ion complexes

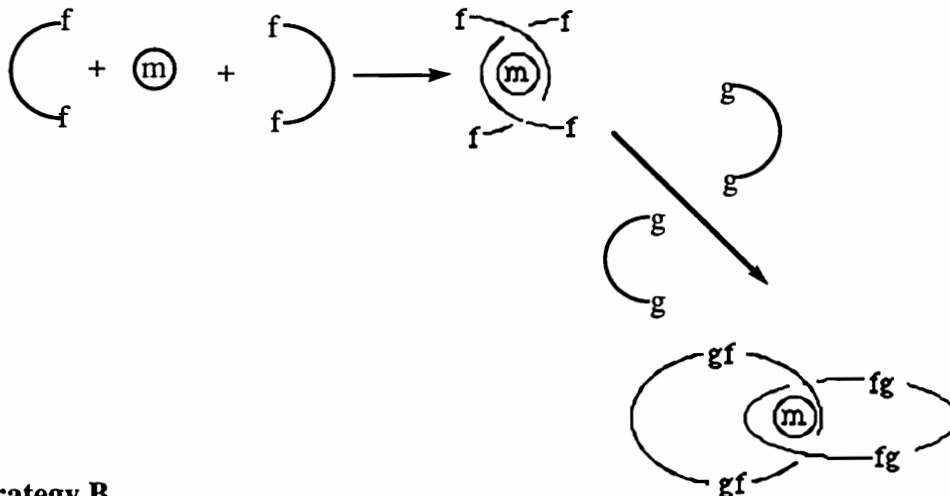
The metal ion complex is the best known and a frequently used method for template syntheses. It acts as a template and ensures a good yield of the reaction. In ring closure reactions, a most frequent reaction in the rotaxane and catenane synthesis, the building blocks wrap themselves around the metal ion which favors the cyclization. This effect was noticed by Sauvage and Dietrich-Buchecker. They took advantage of this effect in building interlocked chains which can be done by setting the ligand around the metal ion followed by ring closure. They proposed two possible strategies for template syntheses of a [2]-catenane.<sup>41</sup>

In strategy A, two ligands were complexed around a metal ion followed by the one step simultaneous connection of eight reacting groups to give a catenane. Compared to strategy A, strategy B was not very straightforward and required the formation of one ring. This ring was then complexed with a metal ion and another ligand which can undergo cyclization in the latter stage. However, the last step required the connection of only four reacting groups instead of eight. To compare the difference between these two strategies, Sauvage carried out reactions using  $\text{Cu}^+$  as a template via both strategy A and strategy B.

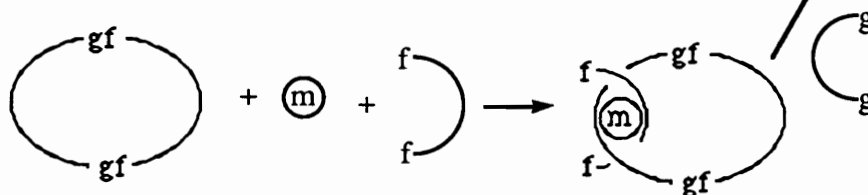
The route B synthesis started from functionalized ligand 2,9-bis(p-hydroxy phenyl)-1,10-phenanthroline (**37**), prepared by the reaction of lithio anisole with 1,10-phenanthroline (**35**), leading to 2,9-dianisyl-1,10-phenanthroline (**36**), which was deprotected with pyridinium chlorohydrate. Reaction of **37** with 1,14-diiodo-3,6,9,12-

tetraoxatetradecane in the presence of a large excess of  $\text{Cs}_2\text{CO}_3$  in the DMF under a high dilution conditions gave macrocycle **38**.

**Strategy A**



**Strategy B**



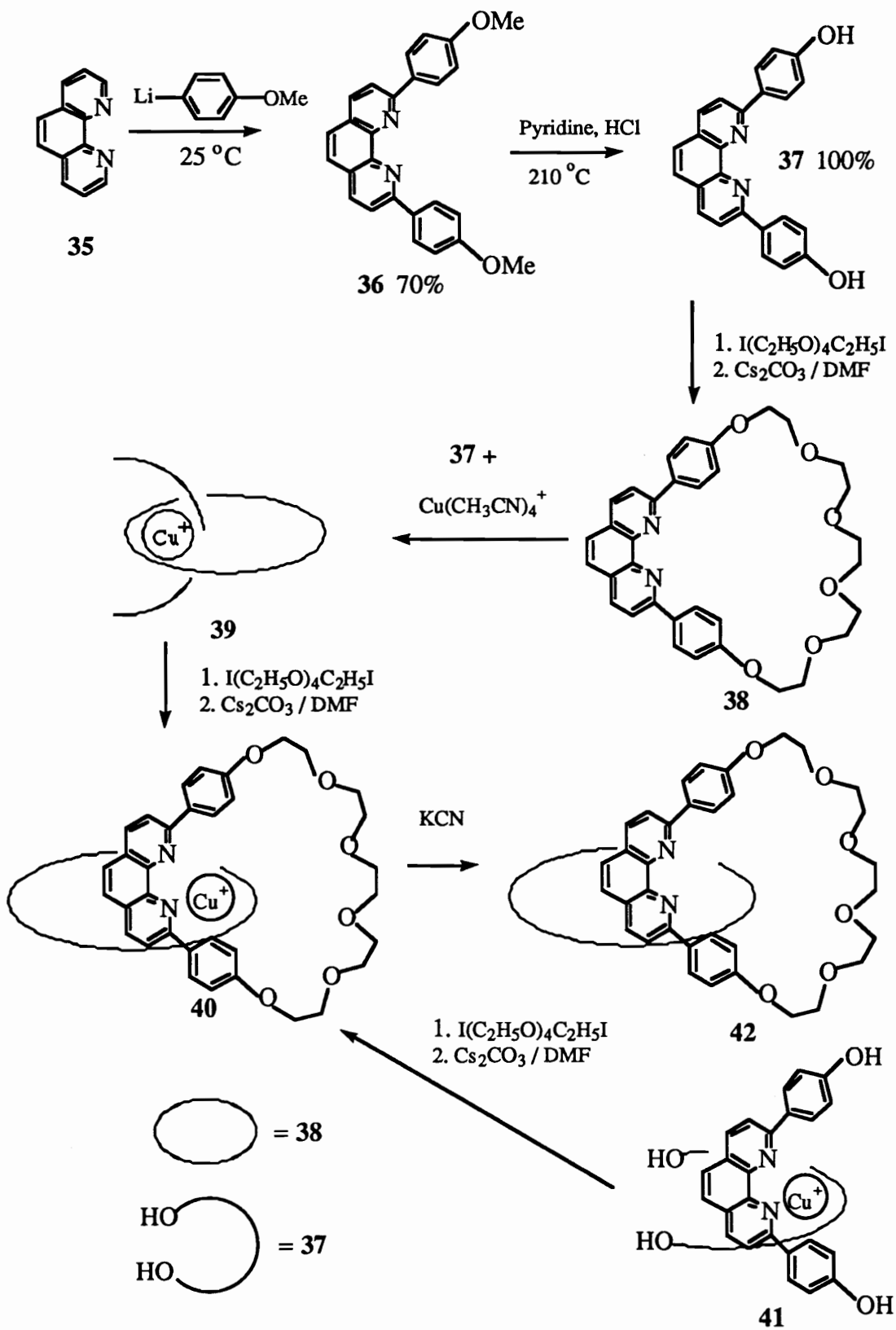
The stoichiometric mixture of macrocycle **38** and **37** in the presence of the  $\text{Cu}(\text{CH}_3\text{CN})_4^+$  gave complex **39** in quantitative yield. The complex **39** can further react with 1,14-diiodo-3,6,9,12-tetraoxatetradecane in DMF to give complexed catenane **40** in 42% yield. Demetallation (100%) of catenane **40** gave catenane **42**.

In route A synthesis, two prepared ligands **37** were complexed with  $\text{Cu}(\text{CH}_3\text{CN})_4^+$  which later reacted with a diiodo derivative to produce complexed catenane **40** in 27% yield.<sup>42</sup> Comparing the yields of strategy A and B, the strategy B seemed to be better (42% yield relative to 27% in route A). However, for the overall yield, strategy A (3 steps, 20% yield) is higher than strategy B (4 steps, 14% yield).

The complexed catenane **40** and decomplexed catenane **42** were characterized by  $^1\text{H}$  NMR and mass spectroscopy. In the NMR spectra, the chemical shifts of the protons

in **40** and **42** were different which might be due to the locked tetrahedral conformation of the two diphenylphenanthroline in **40** but not in **42**. The spectrum of **42** was rather like that of the single macrocycle **38**. The mass spectroscopy further demonstrated the **42** structure. The molecular peak of **42** was observed at 1132. No peak was observed between 566 and 1132, indicating the two macrocycles were only mechanically linked. The molecular structures of **40** and **42** were later proved by X-ray crystallography.<sup>43, 44</sup> Multiring catenanes have also recently been made by Sauvage and Vogtle et al. and the structures were demonstrated by NMR and mass spectroscopy.<sup>45</sup>

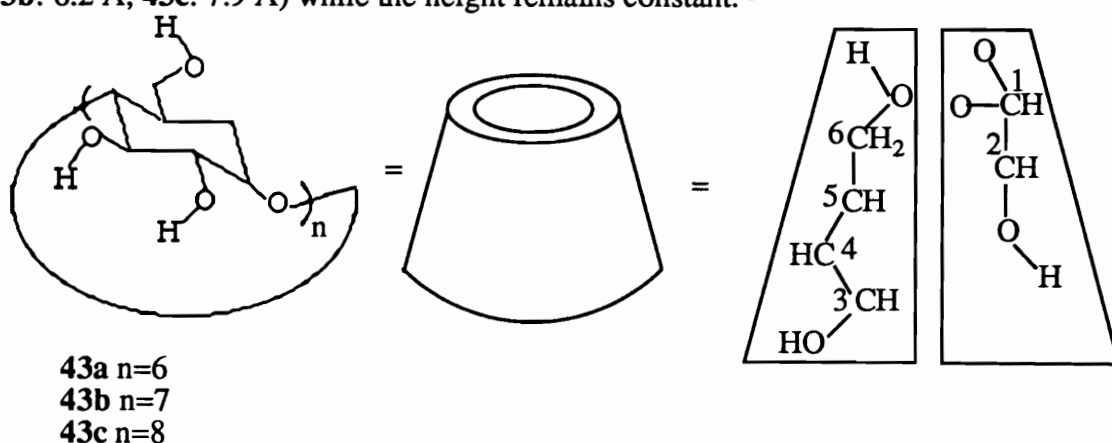
In light of the template synthesis of Sauvage, Wu carried out the synthesis of a rotaxane via a similar route.<sup>55</sup> The final rotaxane structure was confirmed by NMR and mass spectroscopy. The molecular ion peak at 1725 was observed with the linear fragment peak at 1159 when a macrocycle was cleaved and macrocycle peak at 568 when the linear portion fragmented. Sauvage also carried out the rotaxane synthesis by using porphyrin as a stopper to study the electron transfer between the two porphyrins. The porphyrin stopper was characterized by proton NMR, UV-vis and mass spectroscopies.<sup>56</sup>



### 5.1.3.2 Cyclodextrin inclusions

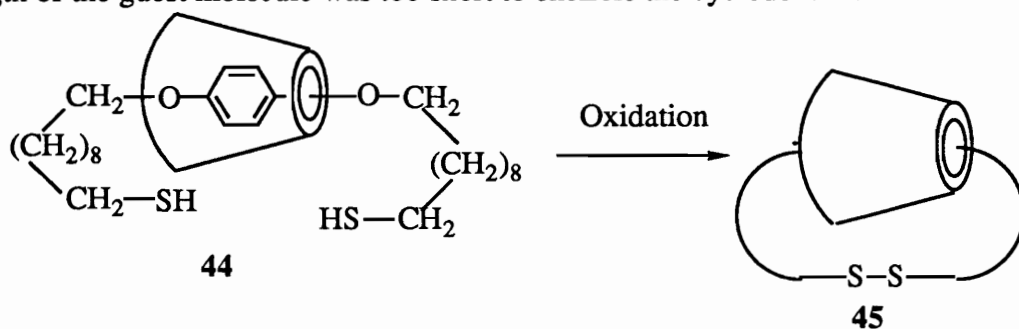
During the rapid development of supramolecular chemistry, a lot of attention had been devoted to finding and utilizing the simple building blocks to form supramolecules by self-assembly instead of the conventionally stepwise construction of structure by covalent bond formation. Cyclodextrins, called “off the shelf components” by Prof. Stoddart,<sup>46</sup> are indeed the active building blocks which fit the role. They demonstrated their applications in nanostructure syntheses, such as catenanes,<sup>47</sup> rotaxanes,<sup>48-51</sup> and polyrotaxanes.<sup>52</sup>

Cyclodextrins are cyclic oligomers of amylose consisting of six, seven, or eight glucose units ( $\alpha$ -,  $\beta$ -,  $\gamma$ -cyclodextrin, **43a**, **b**, **c**, respectively). They were first isolated in 1891 by Villiers as degradation products of starch and they were characterized by Schardinger as cyclic oligosaccharides in 1904. The structure of the cyclodextrins resembles a torus. The primary hydroxyl groups are located towards the inside of the torus and secondary hydroxyl groups are located towards the outside. The internal diameter of the cyclodextrin increases with the number of glucose units (**43a**: 4.9 Å; **43b**: 6.2 Å; **43c**: 7.9 Å) while the height remains constant.<sup>54</sup>

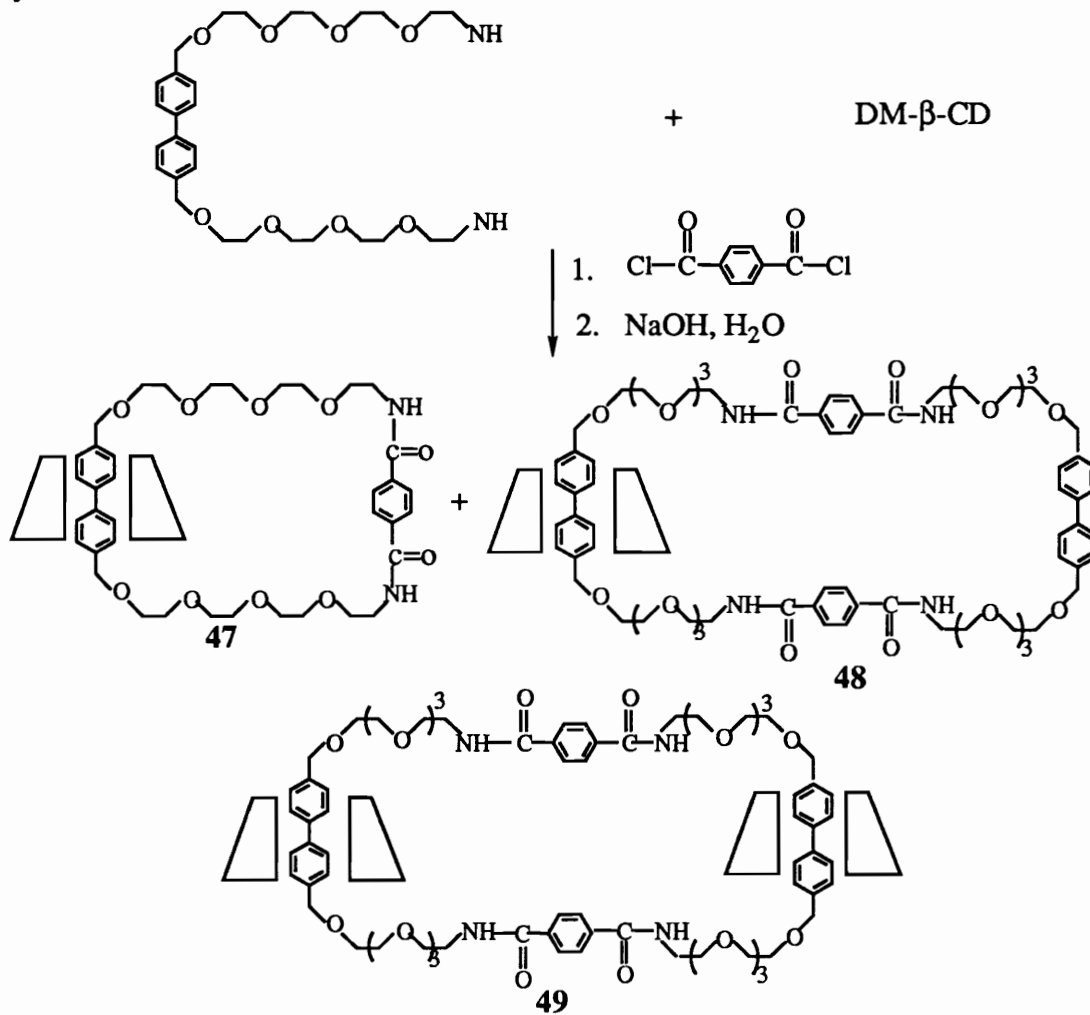


The first attempt to use a cyclodextrin in a catenane synthesis was done by Luttringhaus et al. They tried to link the two ends of a dithiol threaded into  $\alpha$ -cyclodextrin **44** by air oxidation. However, the attempt was not successful and they just

recovered the starting materials instead of catenane **45**. The reason might be that the length of the guest molecule was too short to encircle the cyclodextrin.



Thirty-five years later, Stoddart et al. finally successfully made a catenated cyclodextrin.<sup>47</sup>

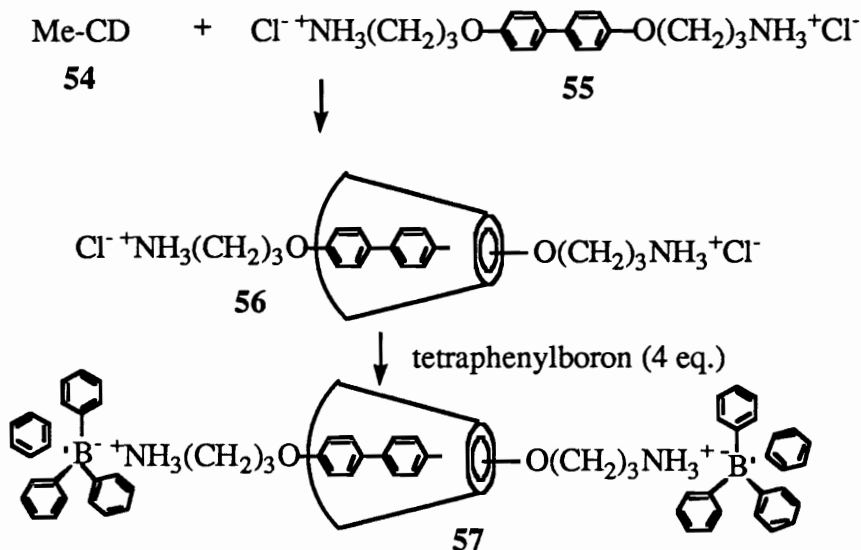


They made two [2]catenanes, **47**, **48** and two [3]catenanes, **49**, **50** from inclusion of ditoyl diamine derivatives into heptakis(2,6-di-O-methyl- $\beta$ -cyclodextrin (DM- $\beta$ -CD). The cyclization step was completed by the reaction of diamine with 1:1 equivalent of terephthaloyl chloride in an NaOH aqueous solution. However, the yields of **47** and **48** were only 3% and 0.8%, respectively. Catenanes **49** and **50** were also isolated as an equimolar mixture in 1.1% yield. The low yield of **47** indicated that the reactivity of diamine might be diminished. The catenanes were characterized by NMR and FAB-MS which showed the molecular peaks of **47** and **48**. X-ray crystallography was also carried out on **47**.

In addition to the cyclodextrin inclusion catenanes, inclusion of cyclodextrins in rotaxane syntheses was also studied by several other research groups. In 1981 Ogino reported the synthesis of a rotaxane consisting of inclusion of **43a** and **43b** onto the  $\alpha$ ,  $\omega$ -diaminoalkanes with Co (III) complex fixed at the ends. <sup>48</sup>



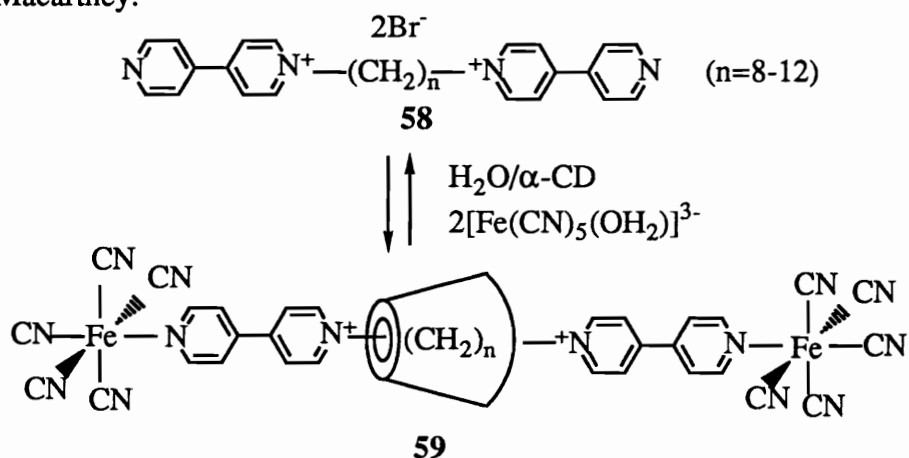
In 1990, Rao and Lawrence reported self-assembly of a rotaxane in 71% yield by the inclusion complex of heptakis (2,6-O-methyl)- $\beta$ -cyclodextrin (**54**) (Me-CD) with diammonium salt **55**.<sup>58</sup>



The inclusion complex **56** was formed by combining the diammonium salt with 1.5 equivalents of Me-CD in aqueous solution. Although bearing double charge, the diammonium salt was sparingly soluble in water. However, it was freely water soluble upon the addition of Me-CD, which indicated that the inclusion complex might be formed. The structure of the inclusion complex **56** was confirmed by the  $^1\text{H}$  NMR spectrum in which Me-CD  $\text{C}_3$  and  $\text{C}_5$  protons were shifted upfield, which is generally recognized as the result of the formation of the cyclodextrin inclusion complex. Complex **56** precipitated from the aqueous solution upon the addition of 4 equivalents of tetraphenylboron, forming rotaxane **57**. The rotaxane **57** was confirmed by  $^1\text{H}$  and  $^{13}\text{C}$  NMR, FAB-MS which gave reasonably high molecular fragments of rotaxane **57** and thin layer chromatography which showed a single spot, in contrast of different migration aptitudes of Me-CD, diammonium salt and tetraphenylboron. The NOE study also confirmed that the diammonium salt was closely associated with Me-CD. Another

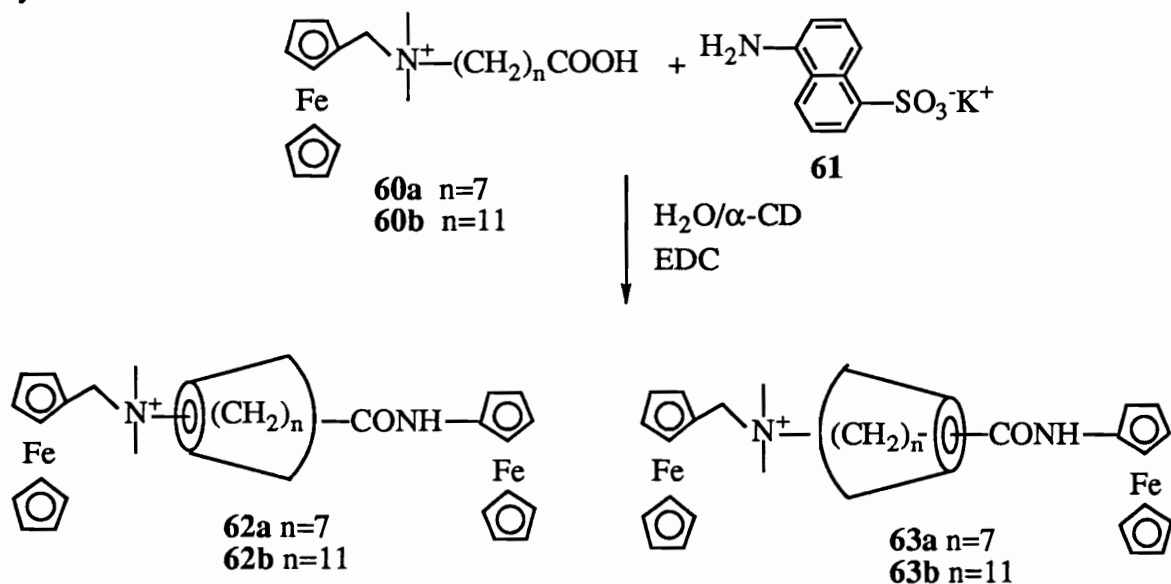
interesting issue is that the ammonium tetraphenylboron salt was known to be a primary solvent-separated ion pair in polar aprotic solvent. This was demonstrated by the dissociation of Me-CD in refluxing acetone. However, no dissociation was observed in acetone by thin layer chromatography, suggesting the positively charged ammonium salt was solvated and acted as a blocking group to preclude the dethreading.

Selfassembly synthesis of a rotaxane using the cyclodextrin was also reported by Wylie and Macartney.<sup>50</sup>



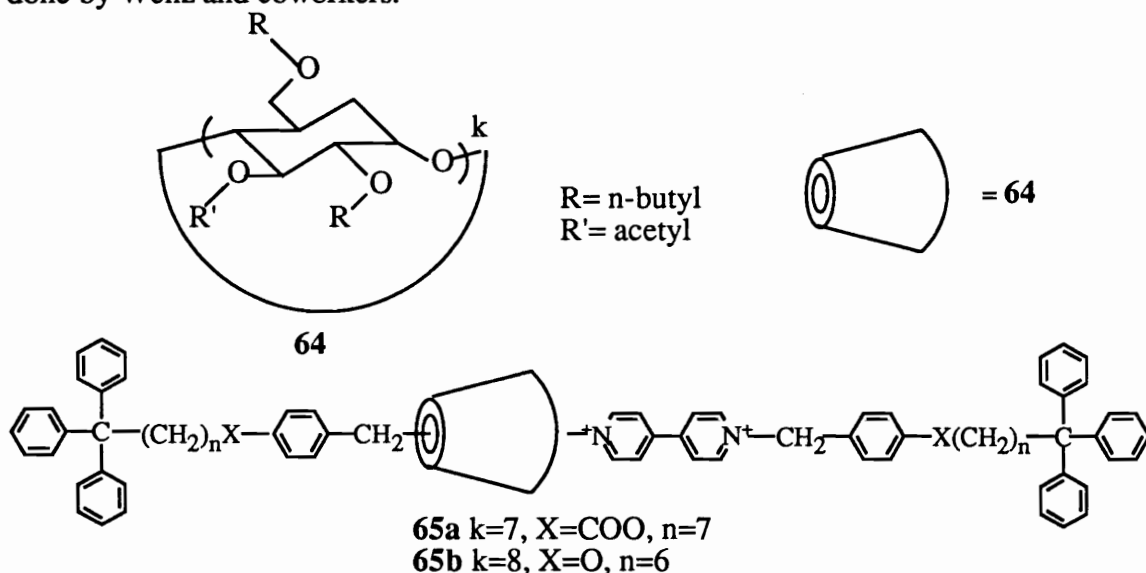
A series of  $\alpha$ -cyclodextrin rotaxanes was produced quantitatively by the reactions of  $[\text{Fe}(\text{CN})_5\text{OH}_2]^{3-}$  ions with prethreaded 1,1''-( $\alpha,\omega$ -alkanediyl) bis (4,4'-bipyridinium) bromide ( $\text{bpy}(\text{CH}_2)_n\text{bpy}^{2+}$ ,  $n=8-12$ ). The rotaxanes can be formed irrespective of the addition order of  $\alpha$ -CD, linear ligand **58**, and  $[\text{Fe}(\text{CN})_5]^{3-}$  which resulted from the slow dissociation of  $[\text{Fe}(\text{CN})_5]^{3-}$ . This dissociation resulted in the formation of a semirotaxane which was followed by rapid recomplexation by  $[\text{Fe}(\text{CN})_5\text{OH}]^{3-}$ . This suggested that even if  $\alpha$ -CD was combined with a linear dumbbell ligand, the rotaxanes could still be generated. The rotaxane structure was demonstrated by  $^1\text{H}$  NMR spectra in which the signals of the symmetry-related protons of  $[\text{bpy}(\text{CH}_2)_n\text{bpy}^{2+}]$  were split by the end-to-end asymmetry of a trapped  $\alpha$ -CD ring.

Isnin and Kaifer reported the formation of an asymmetric zwitterionic rotaxane by inclusion of  $\alpha$ -CD. <sup>49</sup>



The rotaxane was formed by the prethreading of  $\alpha$ -CD onto alkyldimethyl-(ferrocenylmethyl)ammonium unit **60** followed by end capping with potassium 5-amino-2-naphthalenesulfonate (**61**) in the presence of a catalyst, 1-[3-(dimethylamino)propyl]-3-ethylcarbodiimide hydrochloride (EDC). The reaction was based on  $\alpha$ -CD bound selectively to the alkyl chain. The COOH group at the chain end was reported as an ionizable gate for  $\alpha$ -CD threading, and deprotonation resulted in 6-fold decrease of the binding constant with  $\alpha$ -CD. The resulting rotaxanes were reported as isomeric rotaxane mixture **62**, **63** in 15% yield in both n=7 and n=11 cases. The structures of the rotaxanes were assigned based on <sup>1</sup>H NMR spectra. Moreover, the NOSEY 2D NMR showed the correlation between the resonance of amidic protons and secondary hydroxyl and primary hydroxyl protons on the  $\alpha$ -CD. Another observation of these rotaxanes was that the isomers **63a**, **63b** were completely stable while **62a**, **62b** underwent slow dethreading.

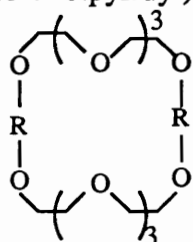
In most inclusion cyclodextrin syntheses of rotaxanes, water was used as the reaction medium; it is the best solvent for the formation of inclusion compounds. However, this limited the preparation possibility since the blocking groups are poorly soluble in water in general. Therefore, the development of lipophilic cyclodextrins is important; this can lead to rotaxane syntheses in an inert organic solvent. This work was done by Wenz and coworkers.<sup>51</sup>



The modified cyclodextrin was heptakis(3-O-acetyl-2,6-di-O-butyl)-β-cyclodextrin (64). This cyclodextrin could complex with a substituted bipyridinium ion monitored by <sup>1</sup>H NMR. The rotaxane was obtained by end capping the complex with triphenylmethyl bromide in 20% yield. The rotaxane structure was demonstrated by the mass spectrum which gave the molecular ion peak at 3293, <sup>1</sup>H NMR shifts, NOE effect and induced circular dichroism in the aromatic absorption. This work also demonstrated that the rotaxane yield was affected by the length of the linear chains and the ring size. When 30-membered α-CD and 40-membered γ-CD were used, zero and 15% yield were obtained, respectively. When n=1, no rotaxane was isolated.

### 5.1.3.3 Charge transfer and $\pi$ -stacked complexes

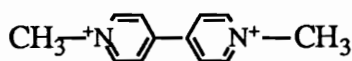
In addition to the metal complex and cyclodextrin inclusion complex, another important complex among the template effect family is charge transfer between the electron rich and electron poor species. This area was pioneered by Stoddart and coworkers. Their research started from the complexes of a variety of dibenzo crown ethers **66a**, **66b**, **66c** with [diquat]<sup>2+</sup> (N,N'-dimethyl-2,2'-bipyridyl) and [paraquat]<sup>2+</sup> (N,N'-dimethyl-4'-bipyridyl) (**67**) in the 1980's. 59-64



**66a** R= p-C<sub>6</sub>H<sub>4</sub>

**66b** R= m-C<sub>6</sub>H<sub>4</sub>

**66c** R=

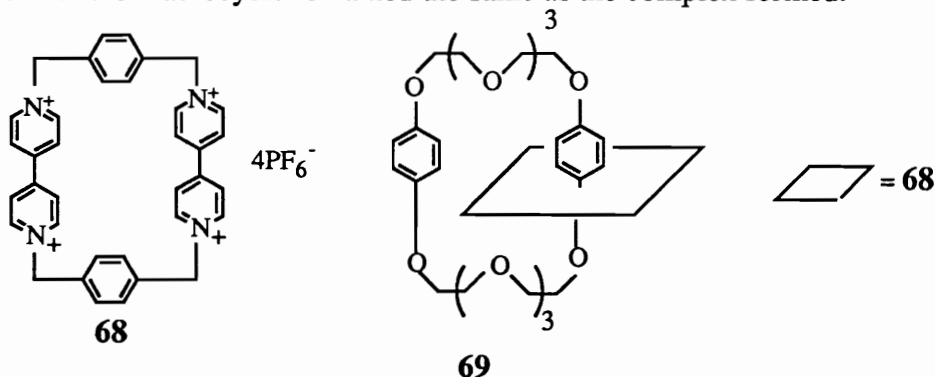


**67**

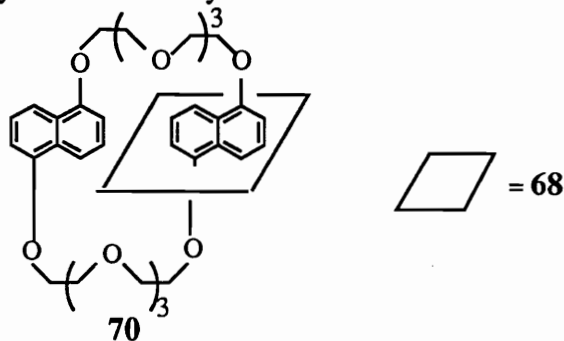
The complexes of the crown ethers and [diquat]<sup>2+</sup> and [paraquat]<sup>2+</sup> were believed to result from electrostatic and charge transfer between the  $\pi$ -electron deficient pyridium rings of [diquat]<sup>2+</sup> and [paraquat]<sup>2+</sup> and the  $\pi$ -electron rich hydroquinone units in the crown ethers. The 1:1 complexes provided the formation of the rotaxanes with guest molecules threaded through the host molecules, demonstrated by X-ray crystal structural analysis. 65

To reverse the constitutional role of the receptor and the substrate, Stoddart et al. proposed to incorporate two  $\pi$ -electron deficient [paraquat]<sup>2+</sup> moieties into a macrocycles. The tetracationic molecules were connected by two para-phenyl units to form cyclobis(paraquat-p-phenylene) (**68**). This macrocycle can be studied in both aqueous and organic media by simply changing the counterions of the receptor. <sup>1</sup>H

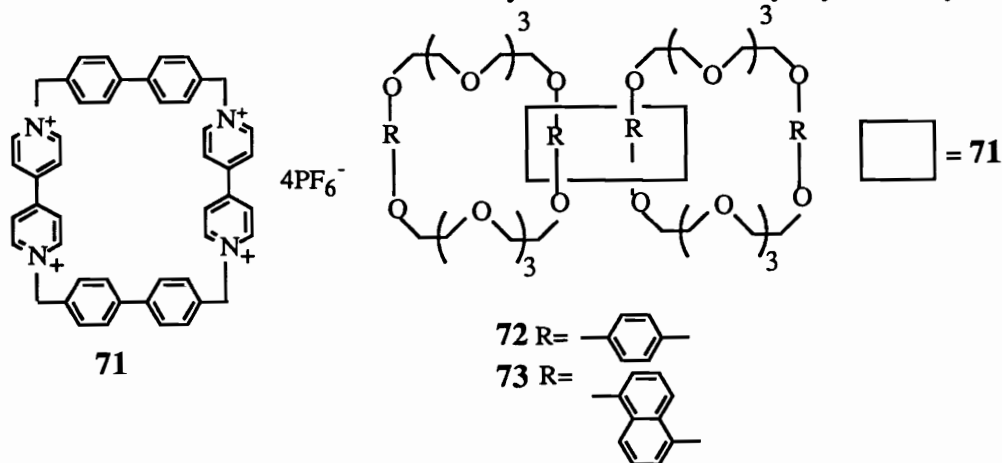
NMR and UV spectra showed evidence for the complex formation between **68** and 1,2-; 1,3-; 1,4-dimethoxybenzenes in acetonitrile and 1,4-dihydroxybenzene in water. X-ray analysis demonstrated the formation of a stable complex between **68** and hydroquinone dimethyl ether. The hydroquinone dimethyl ether molecule was inserted through the center of tetracationic macrocycle receptor **68** with the methyl group protruding above and below the plane of **68**. The formation of this stable complex was due to  $\pi$ - $\pi$  stacking, the charge transfer between the  $\pi$ -electron rich aromatic ring of the hydroquinone derivative and the  $\pi$ -electron deficient [paraquat]<sup>2+</sup> macrocycle and the electrostatic interactions between the ether linkage and the cationic sites. The dimensions of the macrocycle remained the same as the complex formed.



With different donors and receptors in hand, the stable complexes were used in a series of selfassembly syntheses of rotaxanes and catenanes. [2]Catenanes **69** and **70** were reported in 70% and 51% yield, respectively. The structures of both catenanes were supported by X-ray structural analysis. <sup>68, 69</sup>

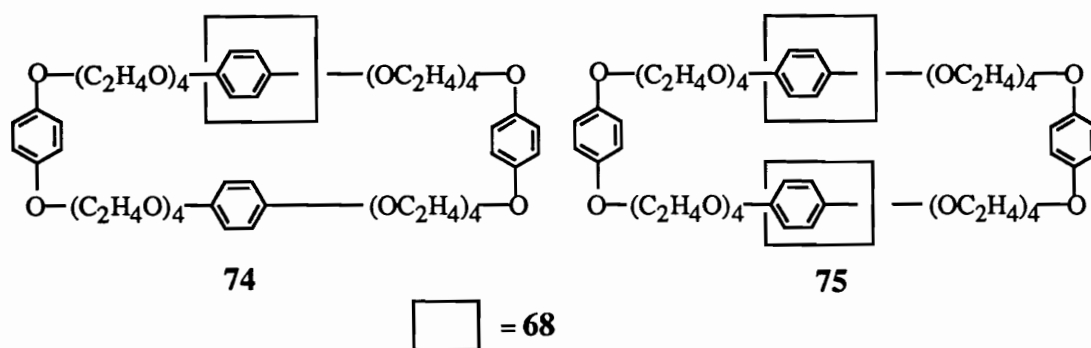


[3]Catenanes (three interlocked rings) **72** and **73** consisting of macrocycle **71** and two benzo-crown ethers have been reported in 20% and 30% yield, respectively. Both structures **72** and **73** were confirmed by FAB/MS and X-ray crystal analyses.



[2]Catenane **74** and [3]catenane **75** synthesized from macrocycle **68** and a tetrabenzo-crown ether have been reported in 11-12% yield.<sup>70</sup>

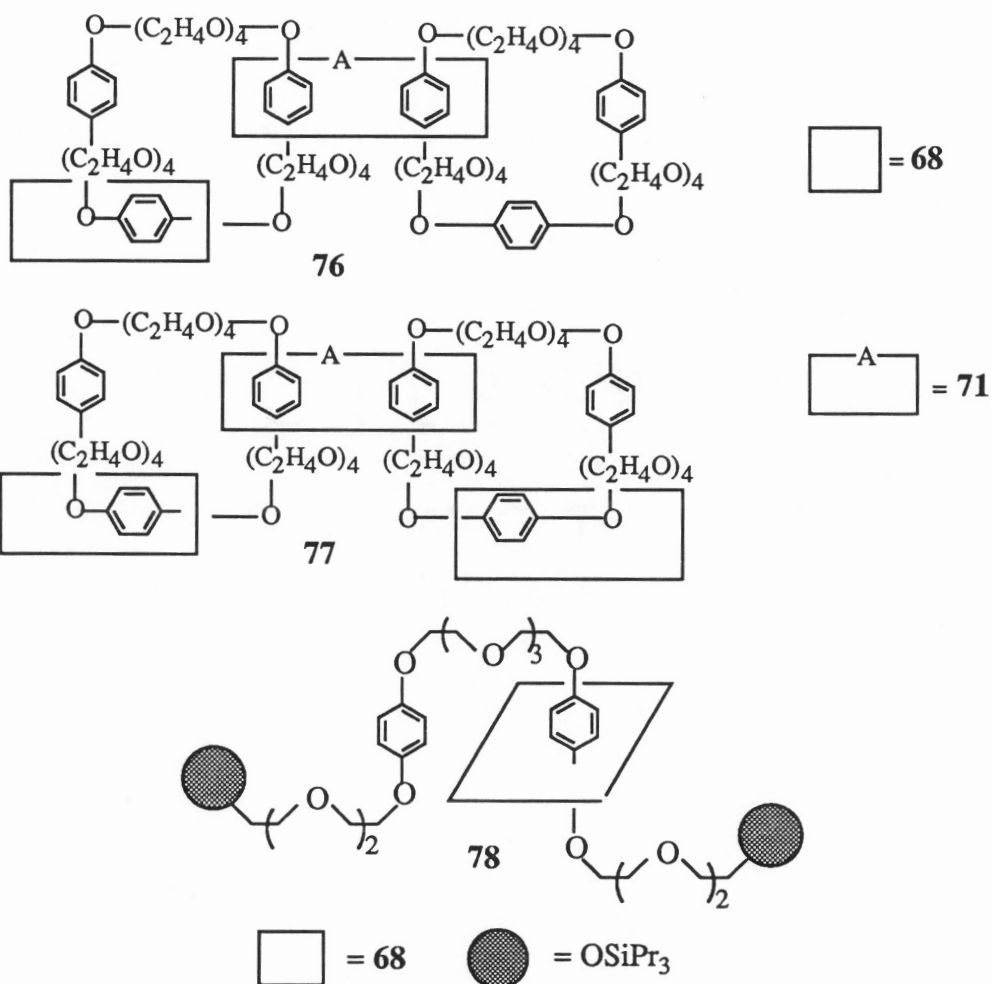
Recently, [4]catenane **76** and [5]catenane **77** made from macrocycles **68**, **71** and tribenzo-crown ether have also been reported by Stoddart in 22% yield and trace amounts, respectively.<sup>72</sup>



Applying the complex concept to rotaxane syntheses, Stoddart prepared the rotaxane **78** in 32% yield by cyclization of macrocycle **68** in the presence of  $AgPF_6$  and the polyether was terminated by large triisopropyl silyl groups that acted as stoppers.<sup>73,74</sup> Since hydroquinone units in the linear chains can complex with

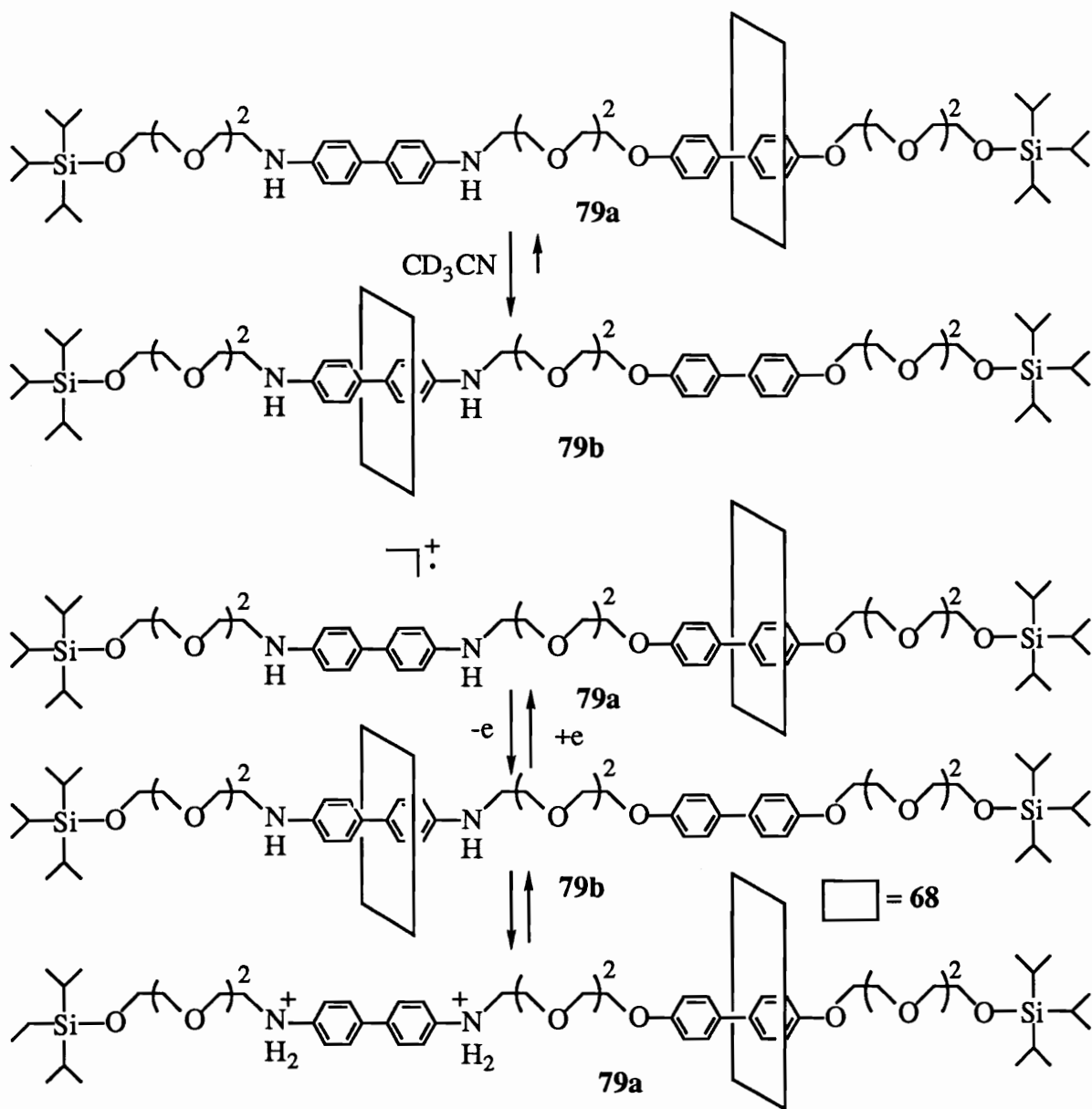
tetracationic macrocycles, an interesting phenomenon was observed by  $^1\text{H}$  NMR spectroscopy. The macrocycle “bead” moved back and forth like a shuttle, approximately 500 times a second between the two identical stations, hydroquinone units at room temperature. <sup>74</sup> A similar phenomenon was also observed in rotaxane **74**.

70

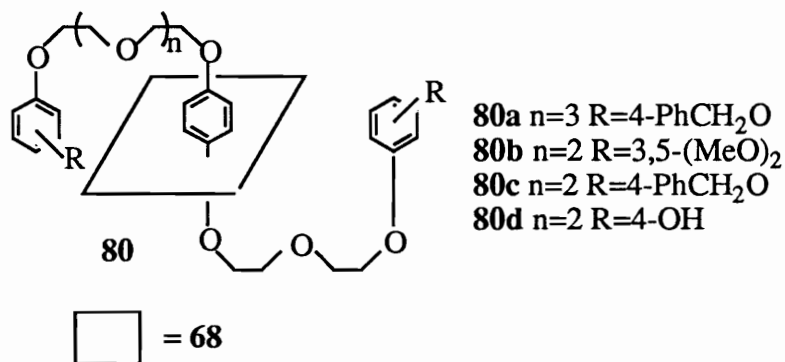


Another molecular shuttle containing two different ‘stations’ has been reported by Kaifer and Stoddart. <sup>71</sup> The rotaxane **79** contained a  $\pi$ -electron accepting tetracationic macrocycle **68** and a linear dumb bell which consisted of a triisopropylsilyl terminated polyether chain with a biphenol and a benzidine unit ( $\pi$ -electron donor). The [2]rotaxane **79** was synthesized via a route similar to [2]rotaxane **78** in 19% yield in the

last step. At room temperature, the macrocycle moved back and forth along the thread. However, when the temperature was decreased to 229K, an equilibrium transition of the macrocycle between the two stations was established. Both stations were occupied at equilibrium with 84% occupation of the benzidine station and 16% occupation of the biphenol station. The preferential occupation of the benzidine station was about 5 times greater than that of the biphenol. The switch of macrocycle from benzidine station **79b** to the biphenol station **79a** can be controlled by protonation of the basic nitrogen atoms of the benzidine moieties or by electrochemical oxidation of this station which generates a positive charge on the benzidine. The repulsive electrostatic interactions between the positively charged benzidine and the macrocycle constrained the movement of the macrocycle.



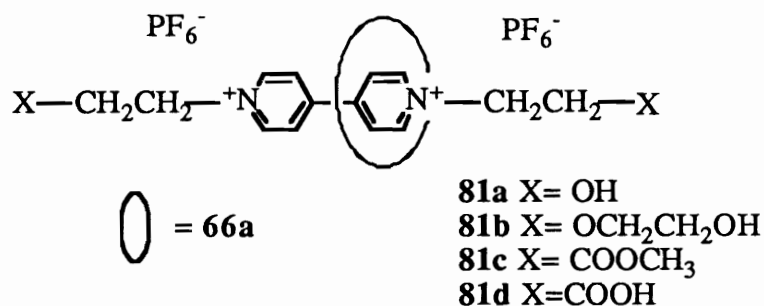
Stoddart also prepared the linear chains without blocking groups to complex with macrocycles which he called pseudorotaxanes.<sup>74</sup> The pseudorotaxanes **80a-80d** were synthesized by mixing equimolar amounts of macrocycle **68** and linear chains in MeCN. The solution immediately turned red in color, indicating the occurrence of electron transfer interactions.



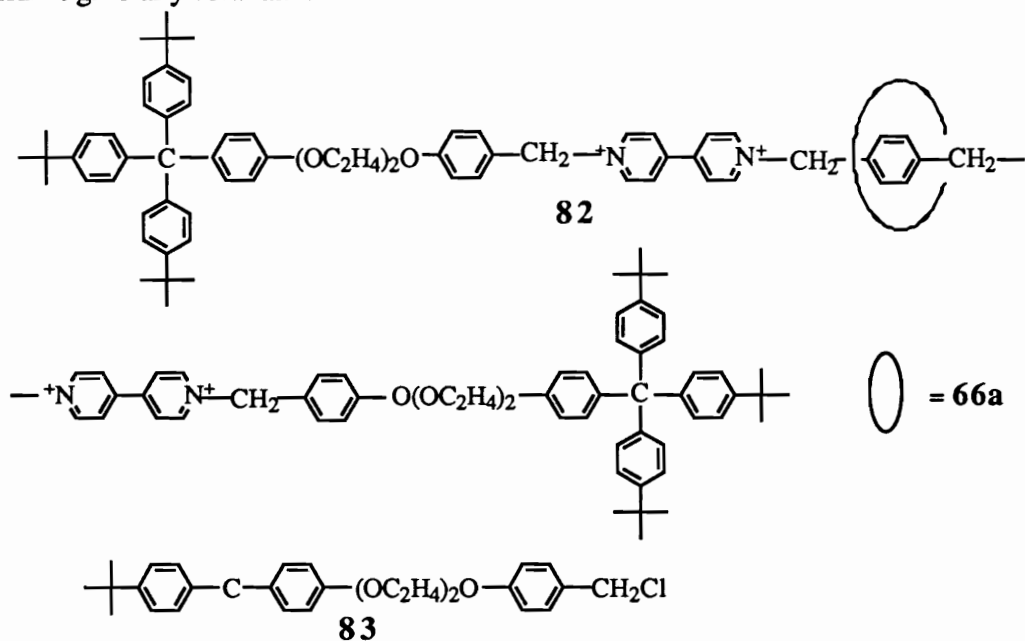
The structures of the pseudorotaxanes were demonstrated by X-ray crystallography which showed that the polyether chains were not only threaded through the center of the tetracationic macrocycles as the middle hydroquinone rings were enriched, but also the polyether chains curled back on themselves around the macrocycles allowing the aromatic donors at both ends to stack against the side of the  $\pi$ -electron accepting bipyridinium units of the macrocycles. The chain linkage between hydroquinone units in **80a** provided an optimum length and geometry allowing  $\pi/\pi$  stacking interactions to occur between the donors and the acceptors, whereas in **80b** there was no formation of continuous stacks.

Returning to the original complexes between the benzocrown ethers and the [paraquat]<sup>2+</sup>, Stoddart reported the syntheses of the pseudorotaxanes **81a** and **81b** with functional groups at the ends.<sup>77</sup> The structures of the complexes were supported by NMR, FAB-MS and X-ray crystallography. The stability constants were found to be 700 dm/mol and 810 dm/mol, respectively.

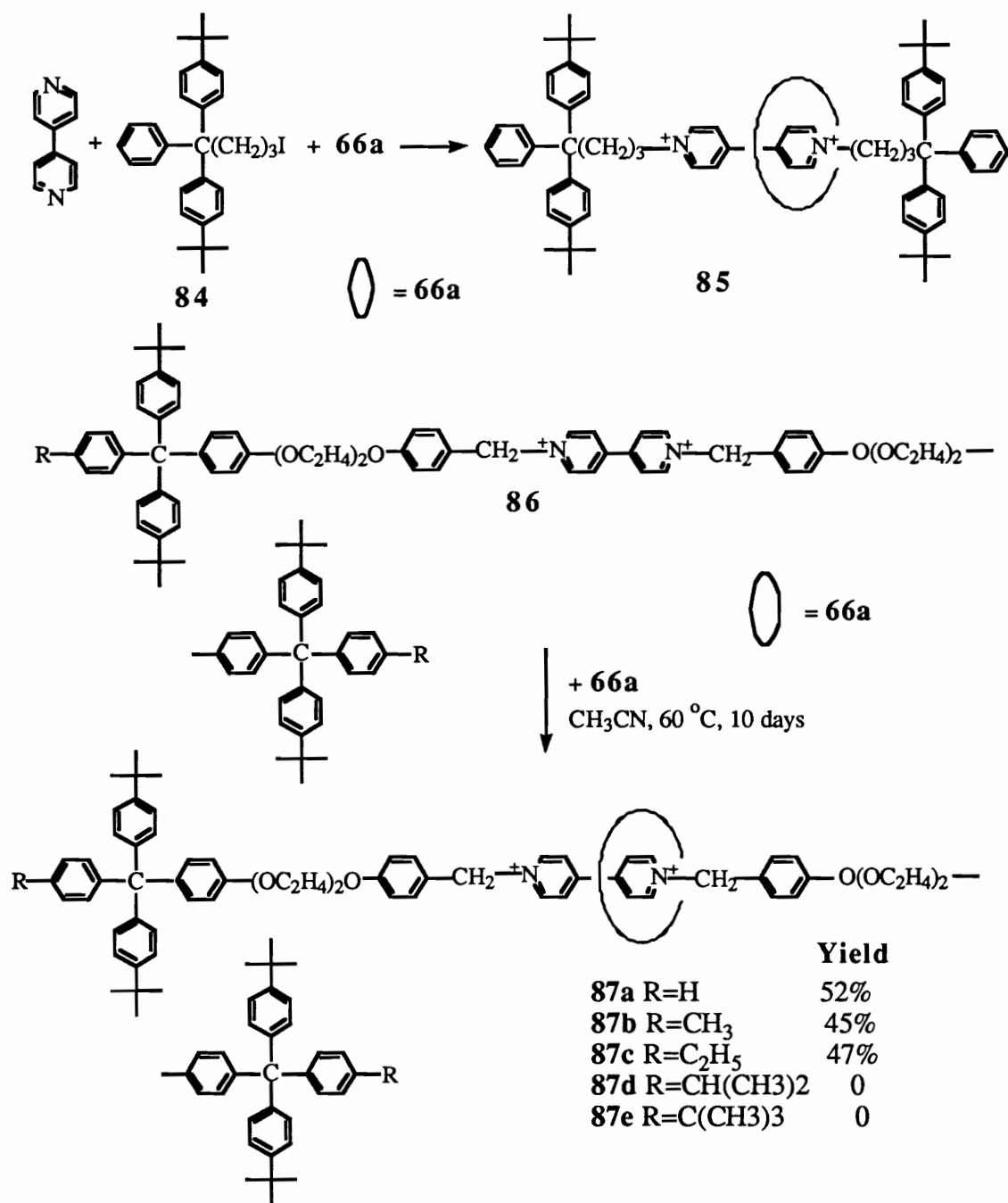
Gibson et al. were also involved in the syntheses of **81a**, **81c** and **81d** at the same time.<sup>78</sup> Their essentially quantitative yields were confirmed by NMR, MS and crystal structural analysis.



Besides the complex **81**, Stoddart and coworkers also prepared rotaxane **82** end blocked by the bulky tris(4-*t*-butylphenyl)methyl group **83** in 23% yield.<sup>79</sup> However, the reaction of the blocking group **83** and 4,4'-bipyridine in the presence of macrocycle **66a** didn't give any rotaxane.



Nevertheless, this rotaxane **85** was successfully synthesized later on by Gibson et al. in 94% yield from functional blocking group **84**, 4,4'-bipyridine and crown ether **66a**.<sup>80</sup>



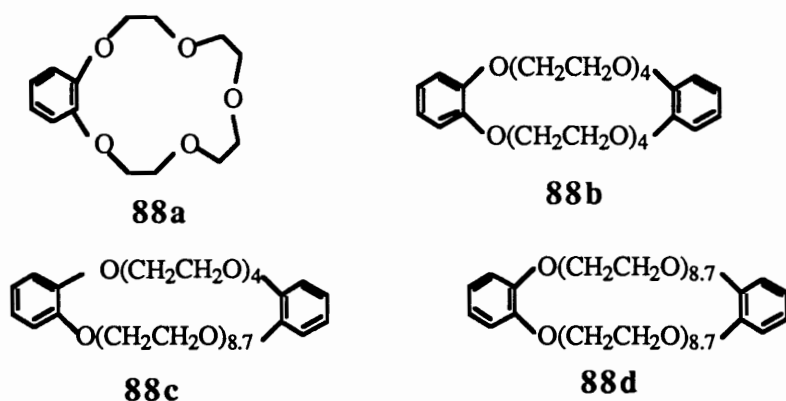
This rotaxane was also demonstrated by Stoddart in his "slippage synthesis".<sup>81,82</sup> Similar to Harrison's thermal preparation of rotaxanes, slippage synthesis of rotaxane **87** involved mixing the crown ether **66a** with dumbbell shaped compound **86** and allowing the crown ether **66a** to pass over the stoppers at elevated temperatures. The

slippageformed rotaxane should be stable at room temperature because once the rotaxane was formed, the complex between the crown ether **66a** and 4,4'-bipyridine salt would provide a thermodynamic trap for the crown ether to prevent the extrusion process. However, if the blocking groups were too bulky, as in **87d** and **87e**, no rotaxane could be formed even at elevated temperatures.

## 5.2 Oligomeric Rotaxanes & Catenanes

### 5.2.1 Statistical threading

To fully understand the statistical threading, Zilkha and coworkers initiated a thorough study of the factors that affected the statistical threading efficiency in the rotaxane syntheses. They chose poly(ethylene glycol)s as linear molecules having molecular weights 150, 194, 400, 600, 1000. The ring molecules chosen were dibenzo crown ethers: dibenzo-30-crown-10 (**88b**) (mixed with half molar amount of dibenzo-15-crown-5 (**88a**)), dibenzo-44.1-crown-14.7 (**88c**) and dibenzo-58.2-crown-19.4 (**88d**). The fractional number indicate that the crown ethers were a mixture of different sizes of rings.



The threading was established by mixing the two components and heating to 120 °C for 30 minutes to reach the threading equilibrium. The threaded rings were “frozen” onto the linear chains by polymerizing linear polyethylene glycols with naphthalene-1,5-

diisocyanate to yield high molecular weight polyurethanes. Though the naphthalene group was not bulky enough to prevent the dethreading, the author assumed that the falling off of the macrocycles only happened at the chain ends due to the polymer coiling. To determine the amount of threaded macrocycles, the reaction mixture was adsorbed on the silica gel and the unthreaded free macrocycles were extracted by alcohol. Therefore, the threaded macrocycles can be determined from the difference between the amount of the initial macrocycles and the macrocycles extracted out. This method proved to be valid by controlled experiment.

Through a series of such experiments, Zilkha demonstrated that the following factors have effects on the extent of threading:

- a. The ratio of chain to ring molecules
- b. The length of the chain molecule
- c. The size of the ring molecule
- d. The volume of the reaction system (or concentration)
- e. Temperature

The results of different ring to chain molar ratios showed that the total amount of threaded rings increased with the molar ratio of rings to chains up to 1:1 for all three different sizes of rings. The experimental results also demonstrated that poly(ethylene glycol) (PEO) with a 400-600 molecular weight gave maximum threading. Shorter or longer chains were less threaded. This can be explained as the increasing length of the chain reducing the number of chain ends (from which the threading begins), thus decreasing the threading. The low threading of short chains can be explained by rapid dethreading. The study of the ring size effect showed that for the same ring to chain ratio and the same chain length, the extent of threading increased with the ring size. The volume effect of the system was studied by diluting the reaction mixture with a neutral component, hexachloroethane. The result was what we expected: the threading

decreased 50% as the volume of the system doubled. The temperature factor was investigated by carrying out the threading reactions at various temperatures ranging from 100 to 207 °C. No obvious change of threading was observed at different temperatures. This result suggested that the energy factor in this system seemed to be insignificant which may be due to the similarity of the macrocycles and the linear chain ends resulting in no preferred interaction. That is  $\Delta H=0$ ; hence the equilibrium constants K for the formation of the rotaxanes are independent of temperature.

$$\Delta G = -RT \ln K$$

$$\ln K = -\Delta G/RT = -(\Delta H/RT) + \Delta S/R$$

To correlate the factors that influence the extent of threading, Zilkha et al. derived a mathematical expression which can estimate the number of crown ethers threaded in the poly(ethylene glycol) system:

$$N = K [M_c M_g (1 - e^{-n_c / \pi n_g}) n_c n_g^{\beta \theta}] / V$$

Where N= number of penetrations

$M_c, M_g$  = number of moles of rings and chains, respectively

$n_c, n_g$  = number of atoms in a ring and a chain, respectively

$\beta$  = constant characterizing the degree of curling up of the chain molecules which affects the threading and the dethreading of the rings ( $1 < \beta < 2$ )

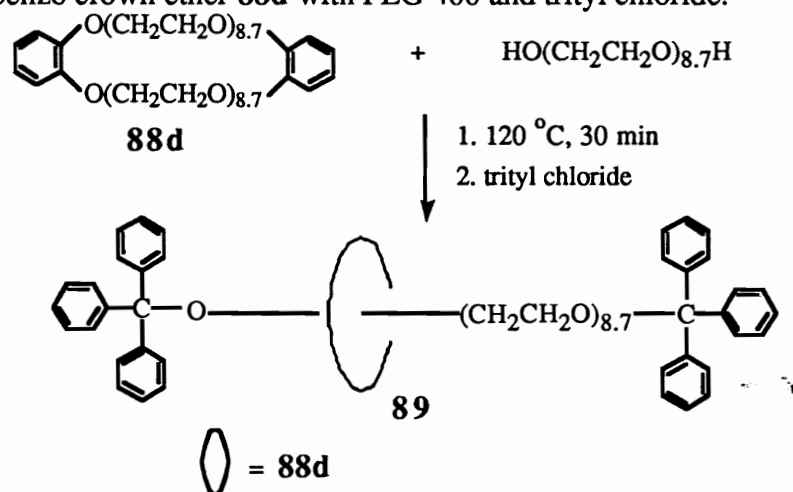
$\theta$  = penetration angle, depending on the ring radius (r) and chain diameter (d) and determined as  $\cos \theta = d/2r$

V = total volume

All the variables in the equation are measurable except for  $\theta$  which can be calculated from bond distances in the molecule and an assumption of an extended zig-zag structure for the ring. By choosing  $K=0.195$  and  $\beta=1.3$  a good agreement was found between the mathematical modeling and the experimental data.

From the experimental results and mathematical modeling, the authors concluded that the size of the rings affects the threading more than any other parameter which was demonstrated by a large increase in threading yield, compared to Harrison who used the mixture of macrocycles with ring size from 14-42. Moreover, each ring size had an optional chain length for the maximum threading. It was also calculated from the equation that this length, for a molar ratio of 1:1, is 2.5-3 times of the ring diameter. If the chain was very long and the molar ratio of the ring to the chain was 1:1, the extent of the threading decreased with the increase of the chain length. This was rationalized as the overall volume was increased without a parallel increase in the number of the chains. For very large rings, increased chain length and the number of chains can increase the amount of threading.

Zilkha and coworkers got a 15% yield of rotaxane **89** after optimizing the reaction of dibenzo crown ether **88d** with PEG 400 and trityl chloride.

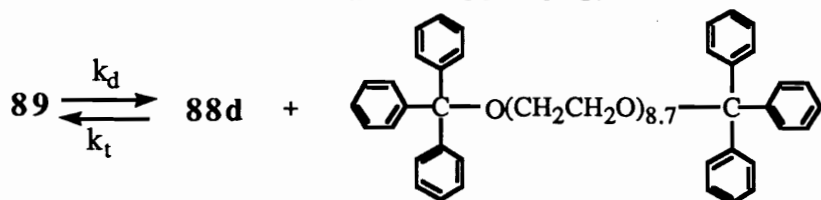


The rotaxane was separated from the reaction mixture by column chromatography. The IR, UV, NMR and elemental analysis showed no difference from the equimolar mixture of linear PEG 400 and crown ether **88d**. The mass spectrum didn't give a molecular ion peak which might be due to the high molecular weight of the compound and the instability of the blocking groups. However, thin layer

chromatography showed the different migration characteristics between rotaxane **89** and the equimolar mixture of PEG and **88d**. The interesting aspect of the rotaxane was that its colligative property, molecular weight, was close to the mean of the molecular weight of the components instead of their sum. This was explained as the large ring size of the crown ether allows the independent movement of the two components in the rotaxane.

Zikha et al. were the first to attempt the syntheses of the polyrotaxanes by chain growth polymerization in the presence of macrocycles under neat condition. The polymerization was initiated by the dipotassium derivative of tetra(ethylene glycol). The ethylene oxide was polymerized in the crown ethers which served as a solvent. The reaction was terminated after 7 days by the addition of triphenylchloromethane which terminated and blocked the chain ends. The yield of the reaction was 11.2% and the rotaxane was isolated by column chromatography. Like rotaxane **89**, UV, IR, NMR spectra showed no difference between the rotaxane and the mixture of components. The molecular weight of the rotaxane, measured by gel permeation chromatography, was higher than that of the components.

The last aspect Zikha investigated was the thermal stability of the rotaxanes, with respect to dethreading. The extent of dethreading of rotaxane **89** was measured by TLC and quantitative UV in different solvents from 130-190 °C.

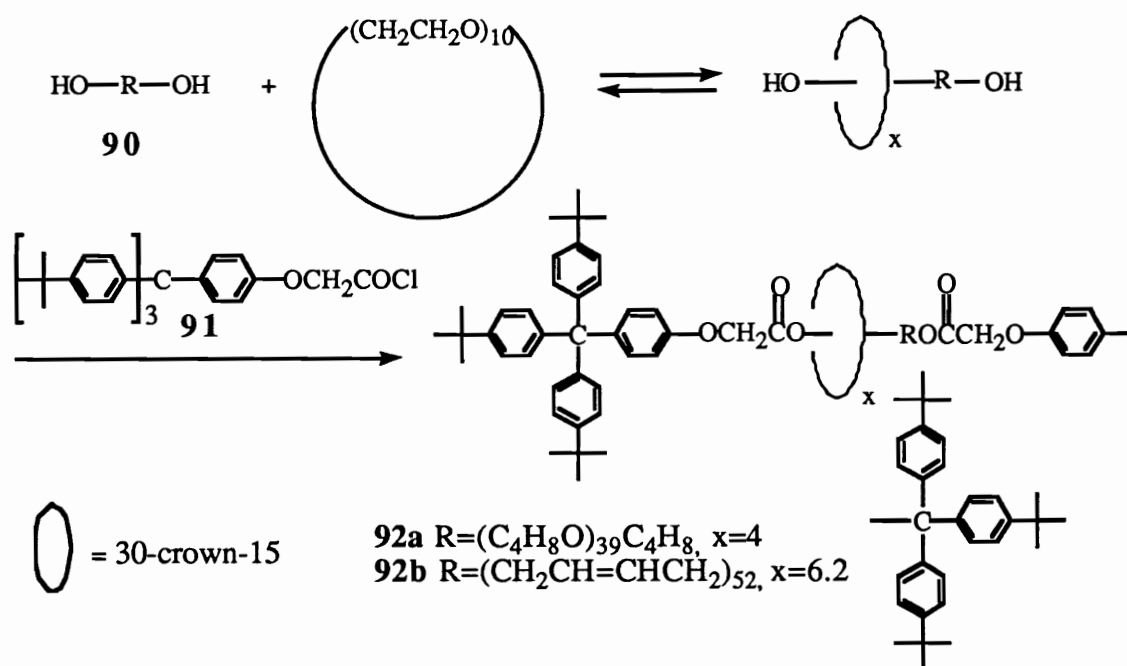


The dethreading rate constant  $k_d$  was determined from the initial slope of the measurements. The equilibration constant for dethreading  $K_d$  ( $K_d = k_d/k_t$ ) was determined from the equilibrium composition at long times. The dethreading rate constant  $k_d$  was found to be almost the same for the rotaxanes in diglyme and neat. This

was rationalized by the solvent, the linear chain and the crown ether having similar structures. Thus the diglyme only diluted the system without interfering with the chain-ring interactions. The  $k_d$  in xylene, a nonpolar solvent, however, decreased by a factor of two, presumably due to the dipole-dipole interactions in rotaxane **89** which were stronger than those between the linear and cyclic components and xylene. The hydrogen bonding between the rotaxane and the solvent was investigated by using 2-octanol as a solvent in which  $K_d$  increased 2-3 times, suggesting the strong H-bonding interactions between the solvent and the crown ether **88d** and the PEG which drove the macrocycles to fall off the linear chains.

The activation energies ( $E_a$ ) for threading and dethreading were 3.4 and 15.9 kcal/mol, calculated from the Arrhenius equation. The low activation energy of the threading process was explained as the process is dominated by geometrical and statistical factors, not energetical. The high  $E_a$  for dethreading was interpreted as the requirement for breaking the dipole-dipole interactions between the two components.

Bheda and Gibson carried out rotaxane syntheses using diol species and simple crown ether, 30-crown-10.

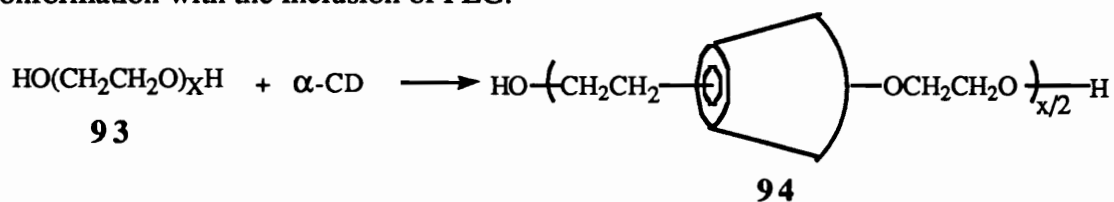


The diols **90**, poly(tetramethylene oxide) of molecular weight around 2900 and poly(1,3-butadiene) of MW around 2800, were stirred with 32 equivalents of crown ether at 60-70 °C for 3.5 months. The pseudorotaxanes formed were blocked with **91** to give rotaxanes **92a** and **92b**. The results of threading are surprising: **92a** contained 38% macrocycle by mass and **92b** 48%.<sup>101</sup> These results suggested that a high threading yield can be achieved even in the absence of strong attractive interactions between the two components.

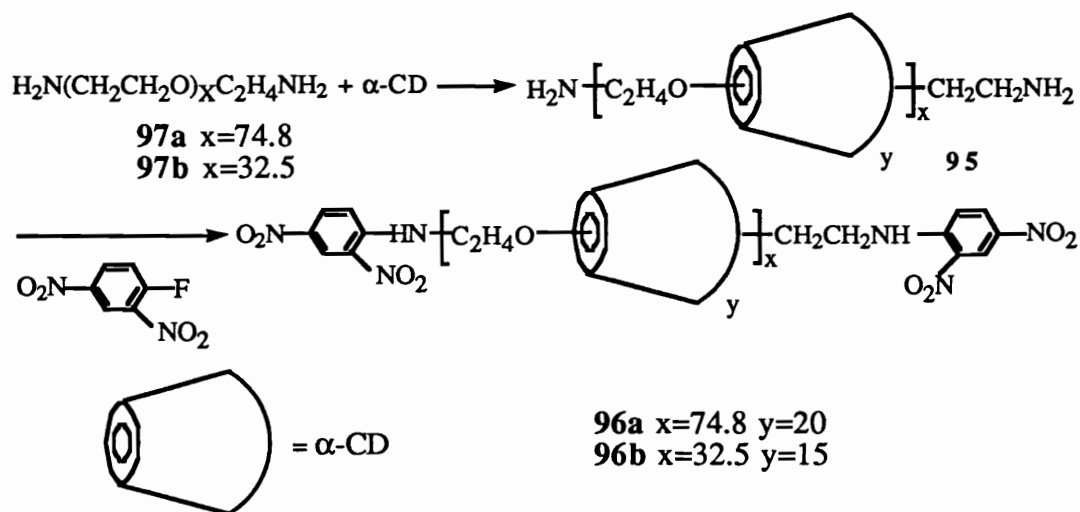
### 5.2.2 Template threading

Harada and Kamachi reported that  $\alpha$ -CD can complex with poly(ethylene glycol) (**93**), but not its low molecular weight analog (MW < 200).<sup>85, 86</sup> The  $\alpha$ -CD was found not to complex with polypropylene glycol as well because of the hindrance of the pendant methyl group. The rate of complexation between the  $\alpha$ -CD and the poly(ethylene glycol) was found to depend on the molecular weight of the polyethylene glycol. The rate increased from nearly zero for PEG (MW=200) to the maximum for

PEG (MW=1000) and then decreased as the molecular weight increased. The complex formed as a precipitate in aqueous solution when the two components were combined. The precipitate was isolated by filtration or centrifugation. The yields of complexes increased from 20% (**93**, x=200) to 91-95% (**93**, x>1000) as the molecular weight of **93** increased. The  $\alpha$ -CD inclusion complex structure **94** was supported by  $^1\text{H}$  NMR which showed both  $\alpha$ -CD and PEG peaks; the X-ray powder pattern, which indicated the complex in a “channel type” rather than the “cage type” structure;  $^{13}\text{C}$  CD/MAS NMR, which showed the less symmetrical conformation of  $\alpha$ -CD, changed to a symmetrical conformation with the inclusion of PEG.

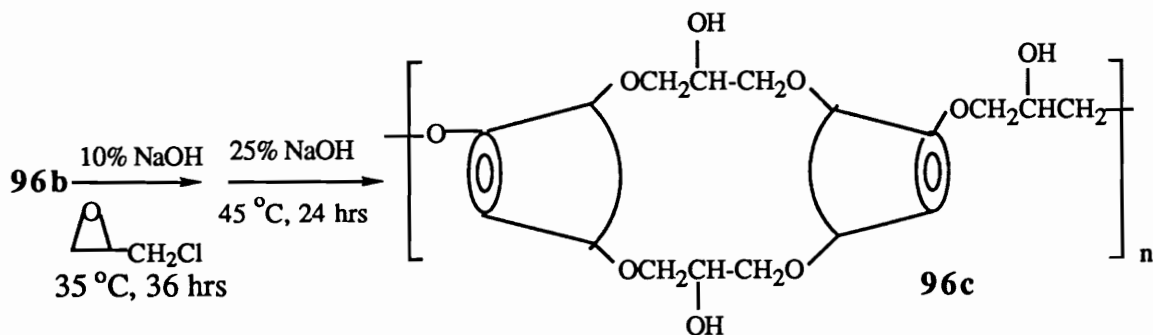


The number of  $\alpha$ -CD units on the PEG was calculated based on continuous variation which gave a 2:1 (2 PEG:1  $\alpha$ -CD) stoichiometry of the complexes. This was confirmed by the  $^1\text{H}$  NMR spectrum. Complex formations were also observed in nearly quantitative yield when the end groups of PEG were modified to amine and methoxide. This modification of the end groups allowed the end capping of the complex to make polyrotaxanes.<sup>86</sup> The polyrotaxane **96** was synthesized by blocking the amine ended PEG **97** and  $\alpha$ -CD complex **95** with excess (46 equivalents) 2, 4-dinitrofluorobenzene in DMF.



The yields of polyrotaxanes ranged from 19% to 60%. The polyrotaxanes were characterized by UV-vis,  $^1\text{H}$  NMR,  $^{13}\text{C}$  NMR,  $^{13}\text{C}$  CP/MAS NMR or 2D-NOESY NMR, X-ray powder patterns and elemental analysis. The number of CD units on the polyrotaxanes increased with an increase in molecular weight of PEG, ranging from 15-20 ( $x/y=2.3$  to  $3.9$ ). Polyrotaxane **97a** gave the highest molecular weight, 23.5 kg/mole, with 20 CDs on the rotaxane. Harada also assumed that the CD on the PEG were closely packed in a head-to-head and tail-to-tail arrangement according to the possible H-bonding between the cyclodextrines.

With polyrotaxanes in hand, Harada further synthesized molecular tube **96c**.<sup>85</sup> Polyrotaxane **96b** was reacted with epichlorohydrin in a basic solution. The product of the reaction was treated with a strong base to remove the end blockers from the linear PEG. The molecular tube **96c**, formed by linking all 3 hydroxy groups, was demonstrated by the GPC which showed only one peak;  $^1\text{H}$  NMR;  $^{13}\text{C}$  NMR which showed the CDs and the bridge; and the UV spectrum. The yield of the reaction was 92% and the molecular weight of the tube was about 20 kg/mole. One thing that should be addressed is that all assignments were based on a head-to-head, tail-to-tail CD arrangement assumption which was not fully demonstrated.



Harada and Kamachi also reported that  $\beta$ -cyclodextrin and  $\gamma$ -cyclodextrin would complex with poly(propylene glycol), but not with poly(ethylene glycol) (PPG).<sup>84</sup> The yields of the complex between poly(propylene glycol) and  $\beta$ -CD increased as the molecular weight of the PPG increased from 400 to 1000 and then decreased as the molecular weight went higher.  $\gamma$ -CD also formed a complex with PPG in high yield even when the molecular weight of PPG was low. The complex structures were characterized by  $^1\text{H}$  NMR and X-ray powder patterns. The stoichiometry of the complex was found to be 2:1 (two PPG units per  $\beta$ -CD) by continuous variation and it was confirmed by  $^1\text{H}$  NMR and a molecular modeling study. The isolated complexes were thermally stable. They decomposed  $> 320\text{ }^\circ\text{C}$ , although  $\beta$ -CD melts and decomposes  $< 310\text{ }^\circ\text{C}$ .

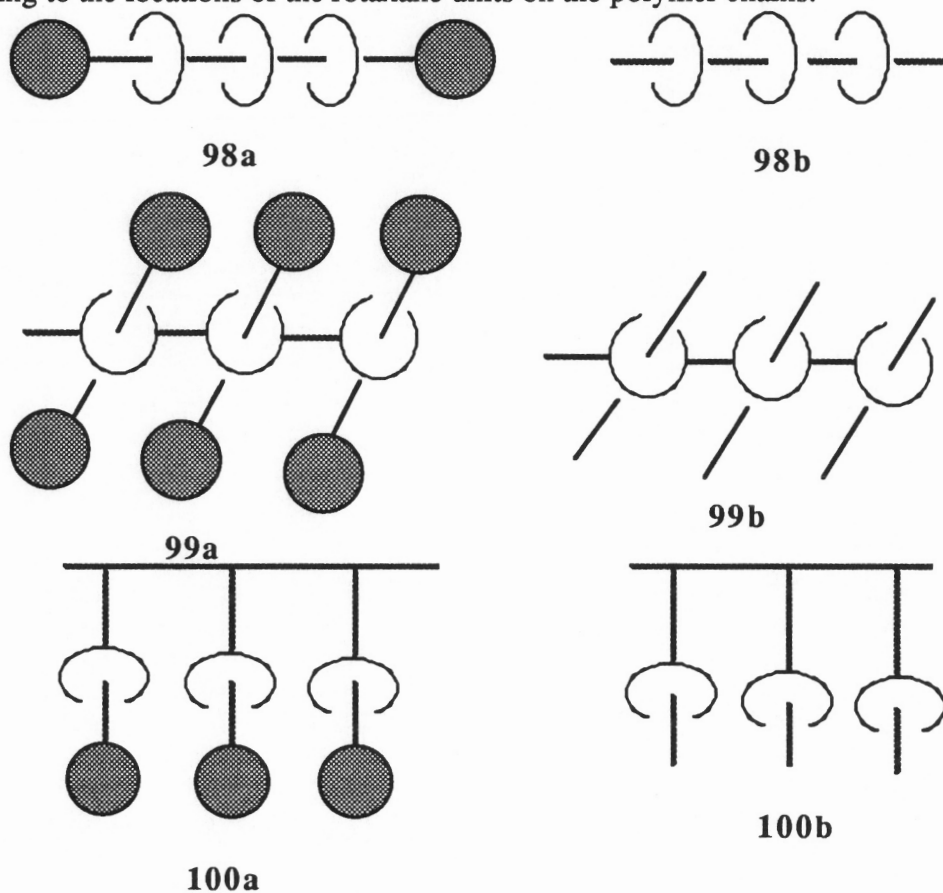
Polyisobutylene (PIB) was also reported to complex with  $\beta$ -CD and  $\gamma$ -CD, but not  $\alpha$ -CD.<sup>88</sup> This is the first observation that the cyclodextrins can form a complex with water insoluble polymers.  $\beta$ -CD and  $\gamma$ -CD showed different selectivities toward the length of the polyisobutylene in forming complexes.  $\beta$ -CD can form a complex with 2,2,4-trimethylpentane in high yield but the yield of the complex decreased as the molecular weight of PIB increased. However, the yield of the complex between  $\gamma$ -CD and poly(propylene glycol) increased as the molecular weight of PIB increased. The continuous variation plot for the formation of the complex between the  $\gamma$ -CD and the PIB showed 3:1 stoichiometry of the complex (3 PIB units per  $\gamma$ -CD) and it was

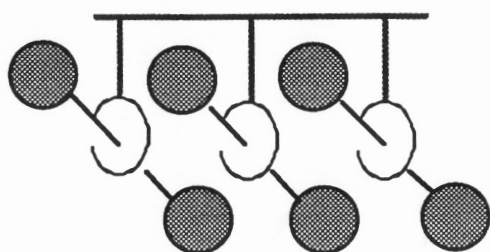
confirmed by  $^1\text{H}$  NMR. The complex structure was supported by X-ray diffraction patterns and  $^{13}\text{C}$  PST/MAS NMR.

### 5.3 Polyrotaxanes

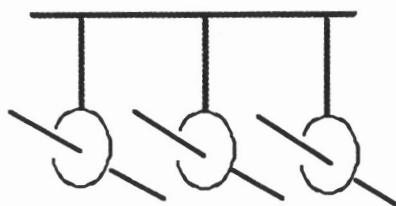
#### 5.3.1 Class of polyrotaxanes

Polyrotaxanes can be classified as homorotaxanes and heterorotaxanes, as discussed previously, based on the chemical structure of the cyclics and the linear components. Polyrotaxanes can also be divided into two other subgroups: main chain polyrotaxanes **98a**, **98b**, **99a**, **99b**, and side chain polyrotaxanes **100a**, **100b**, **101a**, **101b**, according to the locations of the rotaxane units on the polymer chains.





101a



101b

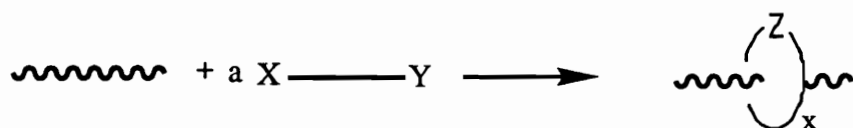
From the results of the rotaxanes and the oligomeric rotaxanes, some promising potential has been shown by this molecular architecture, such as molecular shuttles. Similar characteristics are expected for the polyrotaxanes, which have the same distinguishing potential of free movement, both lateral and translational, of the macrocycles relative to the linear backbones. Moreover, the non-chemical linkage between the two components allows the properties of each component to be independent of each other, such as high thermal stability, and good solvent resistance. On the other hand, the mechanical barriers which prevent the two components from separating force the characteristics of the one component to affect that of the other, such as solubility. These interactions within the structures give chemists great opportunities to tailor polymeric materials.

### 5.3.2 Synthetic approaches to the main chain polyrotaxanes 98

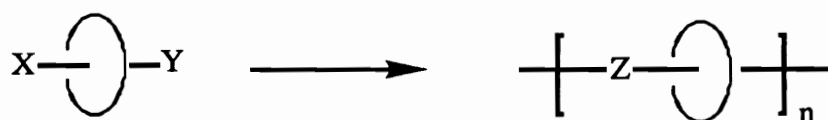
For the main chain polyrotaxanes **98a** and **98b** at least five routes can lead to such structures. The first one is to form the macrocycles in the presence of the linear polymer backbones. However, the cyclization requires a high dilution condition which conflicts with the requirement of high concentration of the macrocycles in the polyrotaxanes syntheses. The dilemma of this synthetic route unavoidably results in a low yield of polyrotaxanes except when the template effect exists during cyclization.

The second route is to obtain a preformed monomeric rotaxane first, formed by a template effect, inclusion complex, or even statistical threading.

1. Cyclization in the presence of linear macromolecules



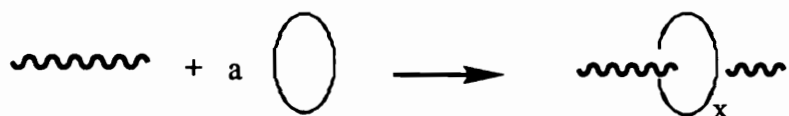
2. Polymerization of monomeric rotaxanes



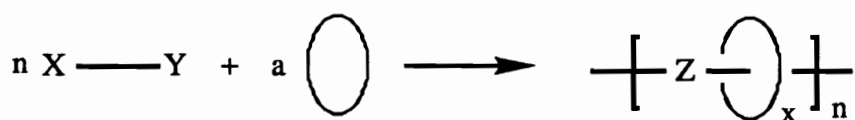
3. Chemical Conversion



4. Threading of preformed linear macromolecules through preformed macrocycles



5. Production of linear macromolecule in the presence of preformed macrocycle



The monomeric rotaxanes can then be polymerized to give the polyrotaxanes. The macrocycles threaded on the monomeric rotaxanes will presumably remain on the polymer chains due to the ring-chain interactions. Moreover, more macrocycles can be threaded during the growth of the linear backbones. Therefore, this route is practically applicable, especially when the rings and the chains have specific interactions.

The third method is to design a chemical structure resembling the monomeric rotaxanes but with covalent bonds between the macrocycles and linear monomeric units. These monomeric molecules can be polymerized, followed by breaking the chemical bonds between the macrocycles and the linear backbones to give polyrotaxanes. However, this method requires very careful design and the isolation of polyrotaxanes is very complicated. The yields of the final polyrotaxanes are very low.

The fourth way is to synthesize the linear macromolecules and macrocycles at the first step. The two obtained components are then combined to allow statistical threading. In this case, a large excess of macrocycles must be used to obtain polyrotaxanes; mostly the macrocycles are used as solvents for threading processes.

The last possible route is to combine the monomers of the linear backbones and macrocycles and polymerize the linear backbones in the presence of the macrocycles. The threading is thought to be accomplished while the linear chains grow. Similar to route 4, to make the threading happen, large amount of the macrocycles are needed. The macrocycles might be used as a solvent or cosolvent.

The threading processes of these five synthetic approaches consist of either statistical threading or template threading. In statistical threading, the macrocycles and the linear chains don't have to be complementary. There may be some weak attractions, negligible or even repulsive interactions between the two components. However, the reaction equilibria are forced to the right by using a large excess of macrocycle. The template threading requires the attractive interactions between the linear chains and the macrocycles. The equilibrium is enthalpy driven. Therefore, the threading yields are high and the stoichiometry of the linear backbones and macrocycles can be well controlled.

The syntheses of polyrotaxanes were first conducted by Agam et al. in 1976 in their study of statistical threading of poly(ethylene glycol) with dibenzo crown ethers.

The threaded PEGs were reacted with naphthalene-1,5-diisocyanate to give polyurethane rotaxanes. However, the polyurethane rotaxanes were not isolated. It was just a means to lock the threaded rings and the polyrotaxanes were just an intermediate of the separation.

In 1975, Ogata reported the syntheses of polyamide rotaxanes with  $\beta$ -CD inclusion via solution and interfacial polymerizations.<sup>91</sup> The polyrotaxane structures were characterized by IR, elemental analysis and differential thermal analysis (DTA). The molecular weights of the polyrotaxanes seemed low, with inherent viscosity (0.1/mL, m-cresol, 30 °C) less than 0.18 with one exception. The polyamide rotaxanes were claimed to differentiate greatly from the linear chains in terms of water adsorption.

In 1977, Harrison reported that the macrocycles could be threaded onto the polymer chains.<sup>92</sup> In gas chromatography, the threading of the macrocycles onto the polymer chains of the stationary phase would decrease the macrocycles' vapor pressure, resulting in increased retention time. This phenomenon was observed for cycloalkanes with more than 25 methylene units when the experiments were performed on the polar poly(ethylene glycol) stationary phase. However, this was not observed when linear alkanes,  $n\text{-C}_{16}\text{H}_{34}$  to  $n\text{-C}_{34}\text{H}_{70}$ , were used. Moreover, neither cycloalkanes, from  $\text{C}_{14}\text{H}_{28}$  to  $\text{C}_{33}\text{H}_{66}$ , nor n-alkanes, from  $n\text{-C}_{16}\text{H}_{34}$  to  $n\text{-C}_{34}\text{H}_{70}$ , had increased retention time in the gas chromatography when a non-polar silicone stationary phase was used. The author explained this as a conformational effect. Cycloalkanes with more than 25 methylene units had open conformations which allow the threading to take place while the macrocycles pass through the column, resulting in a delay of the retention time.

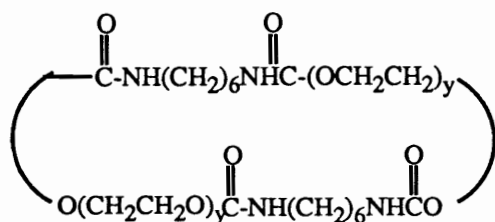
Maciejewski reported syntheses of polyrotaxanes from the crystalline monomeric adducts of vinylidene chloride (VDC) and  $\beta$ -CD, which had 20,000 g/mole molecular weight. This corresponded to one macrocycle for every 2.9 repeating units of the vinylidene chloride. The author also investigated the possible chain transfer reactions

between the  $\beta$ -CD and the VDC during the polymerization of VDC by substituting the VDC with several other vinyl monomers (e.g., methyl methacrylate, styrene) in the radiation polymerizations. The products of these test reactions, unlike those of the  $\beta$ -CD and the VDC product, were unstable and dissociated when they were purified in hot water. The author suggested these results indicated there were no chemical bond formations between the  $\beta$ -CD and the vinyl monomers, namely no chain transfer reaction between the  $\beta$ -CD and the VDC because of the chemical similarity of the VDC and other vinyl monomers. The lack of a chemical bond between the VDC and the  $\beta$ -CD was also confirmed by copolymerization of the VDC with allyl chloride and the VDC with methyl methacrylate (MM) in the presence of the  $\beta$ -CD. In both cases polyrotaxanes were formed. However, when the VDC copolymerized with the allyl chloride, more  $\beta$ -CDs were included (87 wt%) on the copolymer than homopolymer of the VDC. Since allyl chloride monomer may compete with  $\beta$ -CD if chain transfer happens, which may result in less  $\beta$ -CD inclusion, the high inclusion content indicated that  $\beta$ -CD was not bonded to the polymer chain by the chain transfer. The  $\beta$ -CD inclusion decreased in the copolymer of VDC and MM. In an extreme case, when MM and VDC were copolymerized in a 90:10 ratio, no  $\beta$ -CD was included after purification of the product, which suggested chemical bonding was not the force for  $\beta$ -CD inclusion. The inclusion force was suggested by the author to be the high tendency of the chlorine derivative to form adducts with the cyclodextrin, in general. The same X-ray pattern of the  $\beta$ -CD-VDC adduct and the polymerization products also demonstrated no chemical bond formation between the  $\beta$ -CD and the VDC during the polymerization.

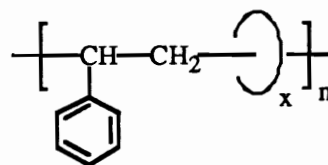
Maciejewski was also the first one to synthesize polyrotaxanes via radical polymerization.<sup>94</sup> The polyrotaxane syntheses were carried out in two ways: 1. the free monomer was added to the DMF solution of  $\beta$ -CD; and 2. the monomer was added to

DMF as an inclusion complex with  $\beta$ -CD. Azobisisobutyronitrile (AIBN) was used as an initiator. The polymerization method 1 gave only pure linear polymer when methyl methacrylate (MM), methacrylonitrile (MAN) and styrene (St) were used as monomers. Method 2 gave pure polymer for MAN, but polymers containing considerable amounts of cyclodextrins were obtained for MM and St. However, these polymer adducts dissociated into the pure polymers and free  $\beta$ -CD when heated with water. Moreover, when polymerization of the VDC was carried out in the temperature range between 50 and 140 °C via route 1, considerable amounts of  $\beta$ -CDs were included on the linear polymer chains (35 to 72 wt%). The ratio of PVDC containing  $\beta$ -CD to the pure linear polymers increased with temperature and the maximum  $\beta$ -CD content was reached at 90-100 °C. The  $\beta$ -CD inclusion polymers were soluble in DMF, but not soluble in other organic solvents, such as acetone, alcohol. The polymerization product of VDC from method 2 contained only  $\beta$ -CD including PVDC with a high  $\beta$ -CD content (85% by weight); no free PVDC was observed. The X-ray study of the  $\beta$ -CD and the VDC showed nearly the same specific volume which can only be possible when the polymer chains are threaded through the  $\beta$ -CDs.

Lipatova reported the syntheses of polyrotaxanes by radical polymerization of neat styrene in the presence of swollen cyclic urethane, both complexed and uncomplexed with  $ZnCl_2$  (**102a** and **102b**).<sup>95</sup> The polymerizations were carried out heterogeneously at room temperature without addition of initiator over 3-5 months. The cyclic urethanes were swollen by the penetration of styrene which can be polymerized and 'pierce' the cyclic urethanes to form polyrotaxanes. The product was extracted with ethanol, benzene and DMSO to remove  $ZnCl_2$ , free polystyrene and free CD.



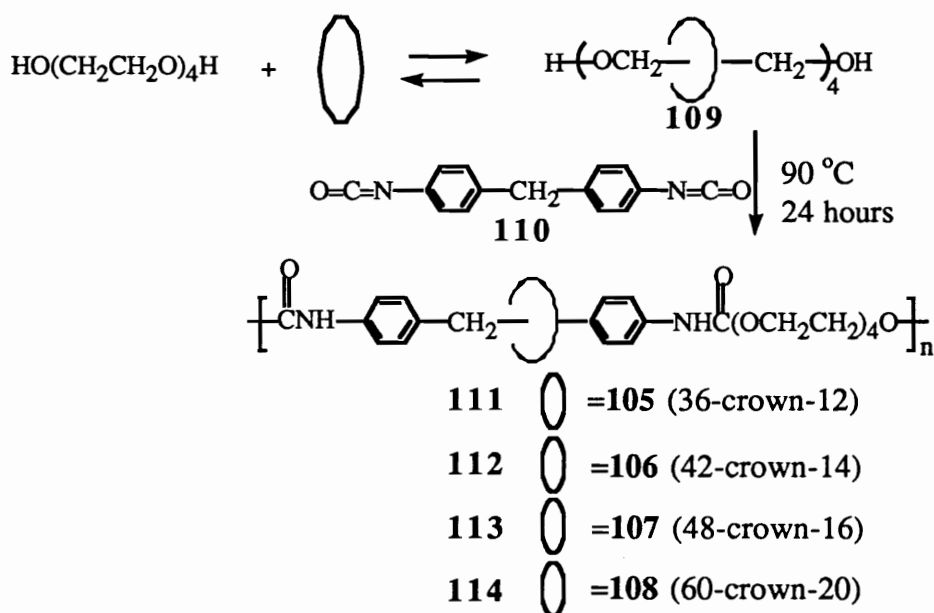
**102a**  $y=2$   
**102b**  $y=3$



**103a**  $\text{O} = \text{102a}$   $x=0.053$   
**103b**  $\text{O} = \text{102a}$   $x=0.14$   
**104a**  $\text{O} = \text{102b}$   $x=0.05$   
**104b**  $\text{O} = \text{102b}$   $x=0.083$

The polyrotaxane **103 a** was found to have a higher threading yield than analog **104a** in which macrocycle **102b** was larger than **102a**. This was interpreted as follows: **102a** had a larger magnitude of swelling (150%) than **102b** (50%) and **102b** had some unthreadable conformations which **102a** didn't have. The increase in threading both in final polyrotaxane **103b** and **104b** relative to **103a** and **104a** by using complexed CDs was explained by hypothesizing that the complexed CDs were present as a more ordered system, called "swarm", than the uncomplexed CDs. The author concluded the degree of "piercing" was dependent on the size of the complex aggregate and the possibility of opening the ring cavities which they believed can be done by DMSO. No blocking was used in this system since the author thought long polymer chains can prevent the slippage of the rings. The polyrotaxanes were also found to be insoluble in benzene and DMSO, which are good solvents for polystyrene. <sup>96</sup>

Shen and Gibson reported the syntheses of polyurethane rotaxanes. <sup>97</sup> The linear polyurethane was formed by the reaction of tetra(ethylene glycol) and bis(p-isocyanatophenyl)methane (MDI) (**110**). Various sizes of crown ethers (**105-108**) were used as macrocycles and also served as reaction solvents.



The melted crown ethers were first stirred one hour with tetra(ethylene glycol) to achieve the rotaxane structures **109**. The monomeric rotaxane units were polymerized by the addition of bis(p-isocyanatophenyl)methane (**110**). The polyrotaxanes were purified by reprecipitating into a solvent which is good for crown ethers but poor for polyrotaxanes. Since the polyrotaxanes had different crown ether contents, the solubilities of the polyrotaxanes were different. Therefore, the polyrotaxane mixtures were purified in different solvents. The polyrotaxanes were not clean until a constant composition (x/n value) was reached as measured by  $^1\text{H}$  NMR after each reprecipitation. The isolated polyrotaxanes, **111-114**, were also characterized by GPC which confirmed that the polyrotaxanes were free of unthreaded macrocycles. No blocking group was used in this system because of random coiling of the chains. The statistical threading in the polyrotaxane syntheses was also studied as a function of ring size and the ratio of the crown ethers to the glycols in neat reaction condition under the assumption that threading can only occur prior to the addition of diisocyanate and the polymerization. The threading efficiency (x/n) was found to be a linear function of ring size at constant

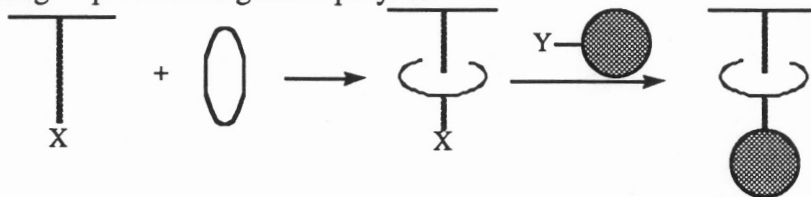
crown ether to glycol ratio. The amount of threading ( $x/n$ ) increased with the feed ratio of the macrocycles to the glycols under neat condition. These observations were similar to Zilkha's results. All the polyrotaxanes were found to be soluble in acetone; **113** and **114** were even soluble in water, while the simple polyurethane was insoluble in acetone and water. These polyrotaxanes had a single weighted average  $T_g$  and the crown ethers could be crystallized if enough large size rings were present in the polyrotaxanes.

The polyrotaxane architecture was reported by Sze and Gibson to improve the solubility of mesomorphic polyazomethine backbones.<sup>98</sup> A bisphenol was equilibrated with 8 equivalents of the crown ether in DMAc at 80 °C for 12 hours, followed by the addition of diacid chloride to give the polyrotaxane. A monofunctional blocking group was used to control the molecular weight. The polyrotaxane was isolated by reprecipitation from THF into methanol. The polyrotaxane was soluble until the degree of polymerization reached 10, which is much higher than that of simple polyazomethine, soluble only when the degree of polymerization is below 5. This polyrotaxane also exhibited a greatly decreased melting point, transition temperature and smectic behavior.

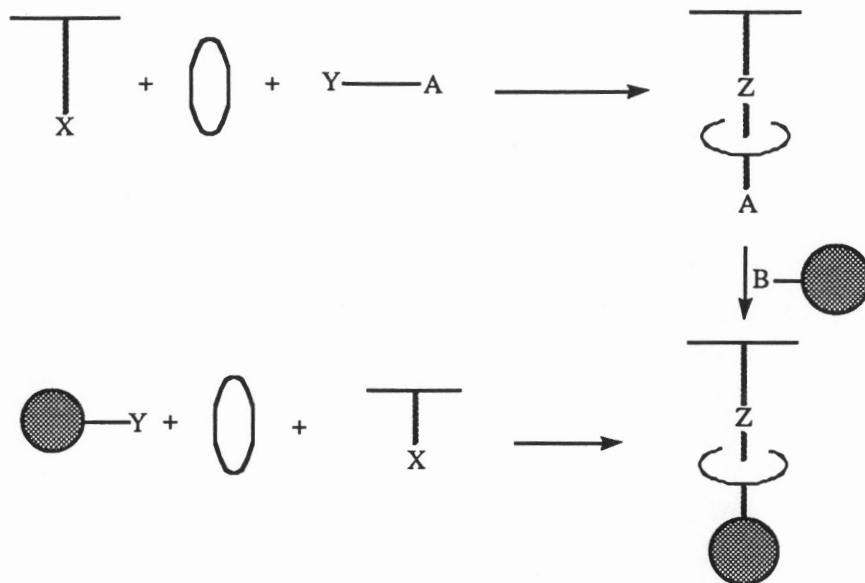
### 5.3.3 Synthetic approaches to the side chain rotaxanes 100

Similar to the main chain polyrotaxanes, side chain polyrotaxanes can be synthesized via 6 routes.

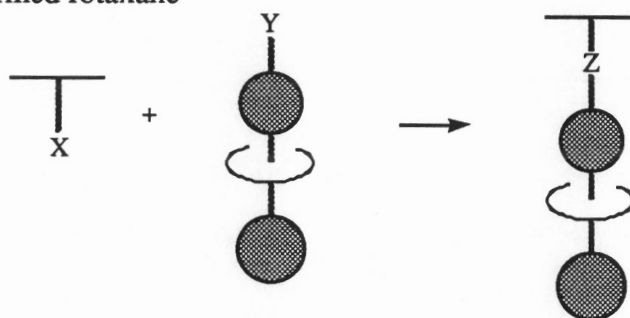
#### 1. Threading of preformed graft copolymer



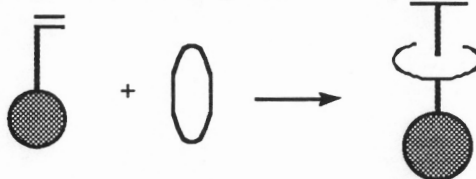
#### 2. Grafting in the presence of cyclic



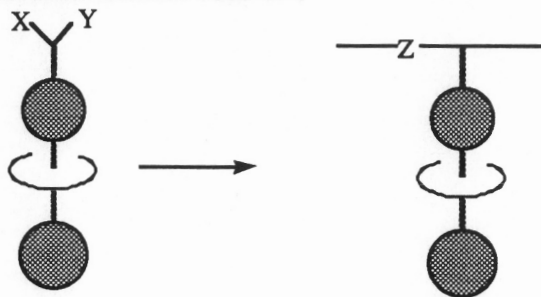
### 3. Grafting of preformed rotaxane



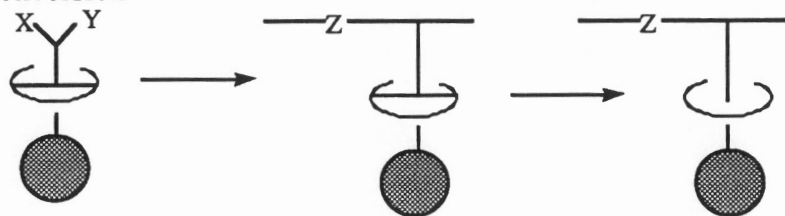
### 4. Polymerization of macromonomer in the presence of cyclic



### 5. Polymerization of macromonomeric rotaxane

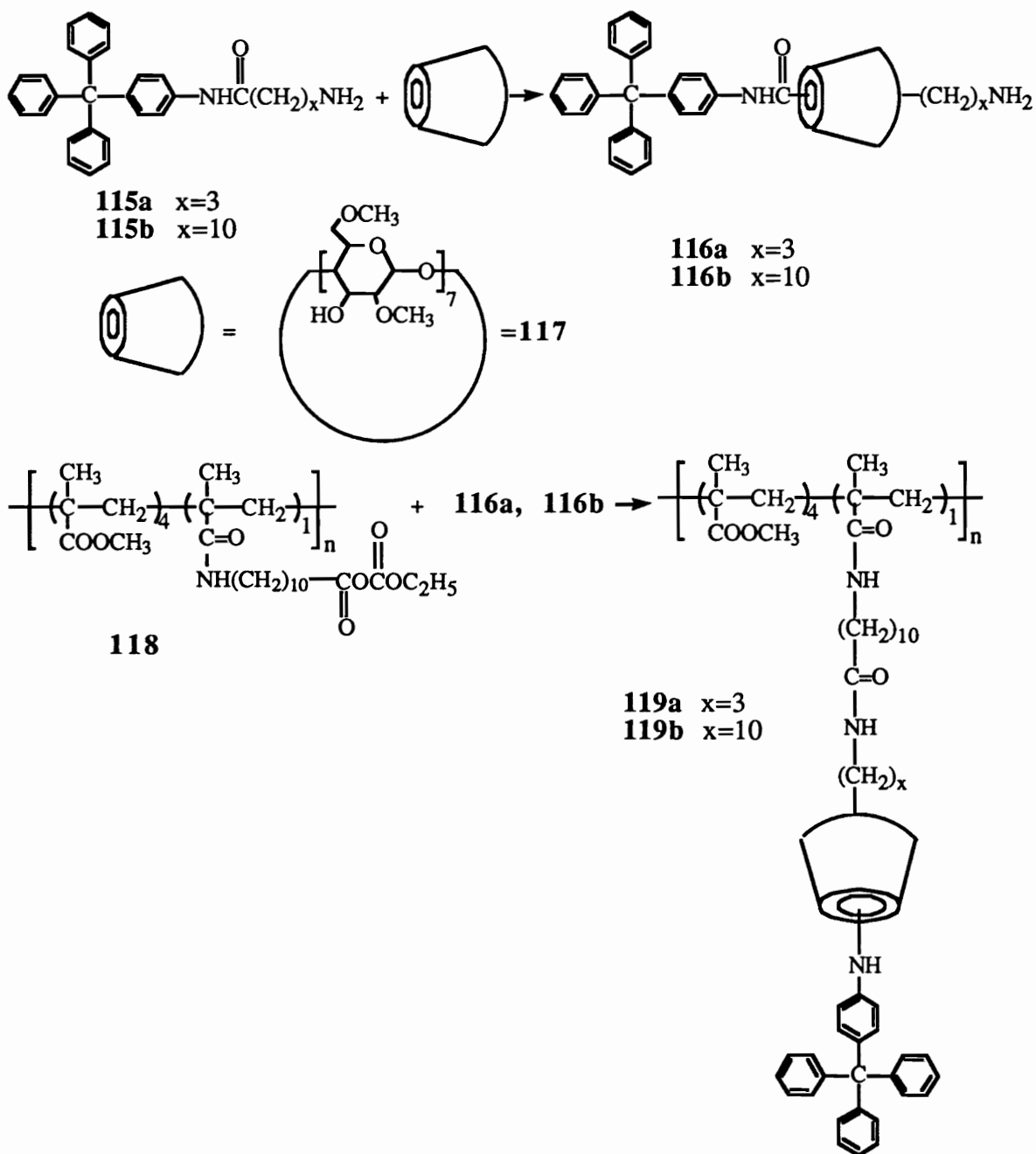


## 6. Chemical Conversion



The first route is to thread the side chains of a graft copolymer with macrocycles and end block them. The second method is to attach linear chains to the backbone polymers in the presence of macrocycles which may be threaded. The following end-cap gives polyrotaxanes. The third way is to attach the preformed rotaxanes onto the polymer chains. The fourth one is to polymerize or copolymerize the macromonomers with one blocking group at the end in the presence of the macrocycles. Similar to the fourth method, the fifth method is to polymerize the preformed macromonomeric rotaxanes. The sixth method is to polymerize the preformed semirotaxanes in which the macrocycles are chemically bonded to the chains, followed by bond breaking of the semirotaxane units.

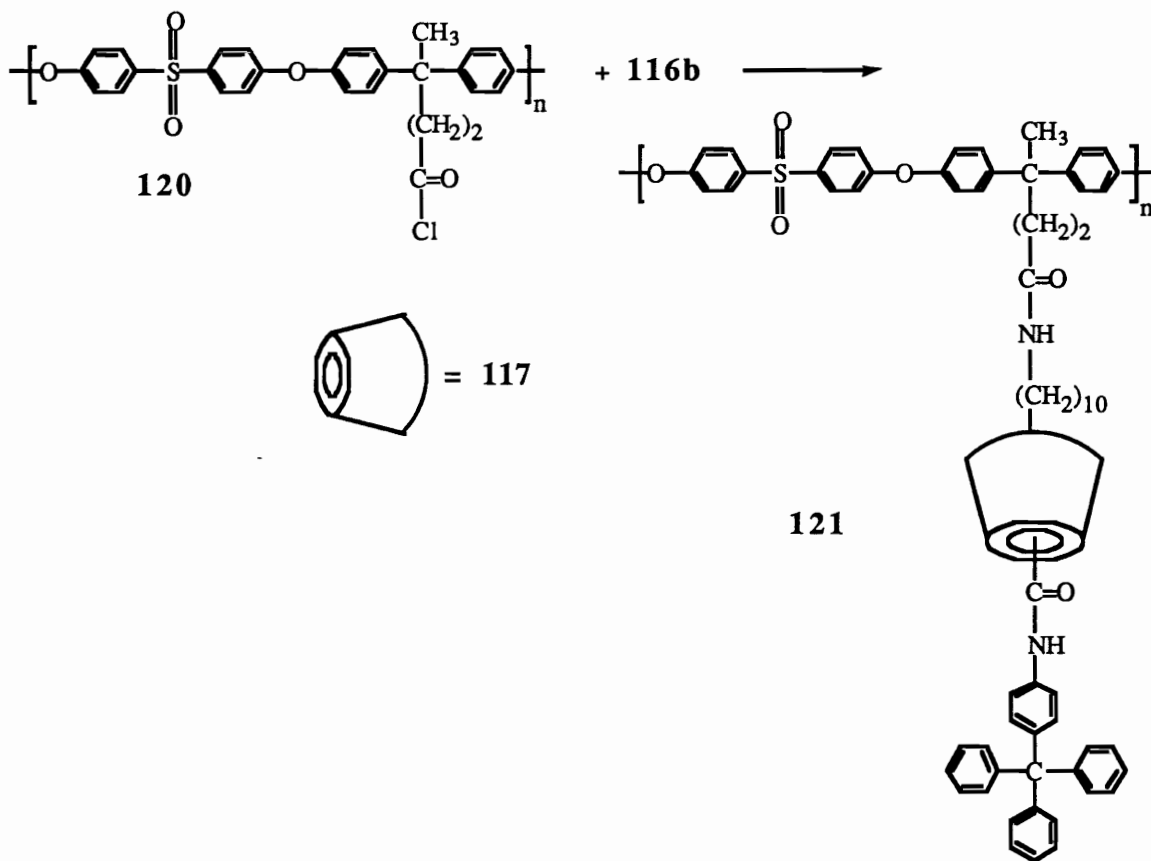
Up to now, the only side chain polyrotaxanes have been reported by Born and Ritter.<sup>99</sup> The semirotaxanes were first prepared by mixing aminoamide **115a** and **115b** with 2,6-dimethyl- $\beta$ -cyclodextrin via route 2. The structure of **116a** was confirmed by FAB/MS, which showed the parent ion at  $m/z$  1767, and  $^1\text{H}$  NMR, in which a doublet of aromatic aniline protons in 2,6-positions was shifted and broadened to a singlet. These semirotaxanes **116a** and **116b** were reacted with a copolymer of methyl methacrylate and 11-methacryloylaminoundecanoic acid bearing an anhydride terminated pendant group (**118**) to give side chain polyrotaxanes **119a** and **119b**. A model compound with no cyclodextrin was also prepared by reacting **118** with **115a**.



The structure of **119a** was supported by IR, NMR and TLC, which showed no free cyclodextrin present. The polyrotaxane **119a** was found to have different solubility and viscosity compared to the model compound. The polyrotaxanes were soluble in diethyl ether, while the model compound was not. The polyrotaxanes also had lower reduced

viscosity than the model compound. This can be explained by the presence of a cyclodextrin “sleeve” around the amide linkage of the polyrotaxanes which reduced the amide-amide hydrogen bonding that led to insolubility of the model compound in ether and increased reduced viscosity at low concentrations.

Ritter also reported another side chain polyrotaxane system.<sup>100</sup> This side chain polyrotaxane was made by the reaction of a polysulfone backbone bearing an activated acyl chloride in the side group (**120**) with semirotaxane **116b**. A model compound was also synthesized by reacting **120** with **115b**. The semirotaxane **116b** was characterized by IR, NMR and FAB/MS, which detected the  $[M+H]^+$  of the complex at  $m/z=1851$ . Polyrotaxane structure **121** was confirmed by  $^1H$  NMR, which showed the downfield shift of the doublet of the aromatic proton near the sulfone group as compared to the model compound, elemental analysis and TLC. The DSC curve showed polyrotaxane **121** had higher  $T_g$  (135 °C) than that of the model compound (111 °C) which might arise from the ability of the cyclodextrin to lower the mobility of the polysulfone chains in the solid state. Similar to the polyrotaxane **119a**, **121** showed a maximum of reduced viscosity at low concentrations. Solubility differences were also observed between **121** and the model compound. The model compound can not be dissolved in acetone, while **121** can. The GPC measurements of **121** and the model compound indicated **121** had a higher coil volume than the model compound.



## 6. Conductive polymers

The field of conductive polymers has emerged in the last two decades as one of the most exciting and interdisciplinary areas of physical science. Most of the early investigations in this field were motivated by the excellent electrical and optical properties and high potential of practical applications of the conducting polymers. After years of study, only a few conducting polymers are still under investigation because of their good conductivities and stabilities. They include poly(1,4-phenylenevinylene), polythiophene, polypyrrole, polyaniline, and their derivatives.

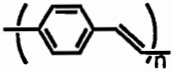
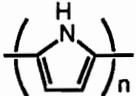
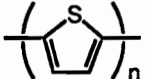
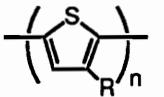
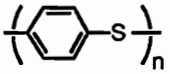
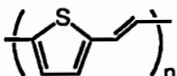
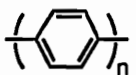
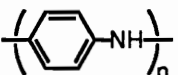
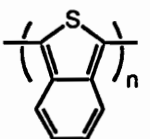
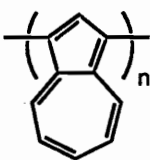
As a class of materials, polymers have been viewed as insulators by the electronics and electrical industries for a long time. Most synthetic polymers are insulators and have found lots of their applications in this area. Accordingly, conductivity and polymers were generally viewed as mutually exclusive. This view was

shown to be incorrect when the first breakthrough was made by Heeger and MacDiarmid at the end of 1970s. They discovered that polyacetylene, synthesized by the Shirakawa method, could undergo a 12 orders of magnitude increase in conductivity upon charge transfer oxidative doping. This exciting discovery resulted in a tremendous amount of investigation into conductive polymers.

Conductive polymers refer to the polymers containing loosely held electrons in their backbones. These polymers can achieve high conductivity by removing or adding electrons to their backbones (n-type, p-type doping). Most of the conducting polymers synthesized so far are highly rigid, with essential structural characteristics of their conjugated  $\pi$  electrons extending over their backbones. Neutral conjugated polymers are generally insulating materials due to the lack of charge carriers. To make these polymers electrically conductive, mobile charge carriers must be introduced. This is typically done by oxidation or reduction of the conjugated backbone, commonly termed doping. Table I-1 lists some of conducting polymers and their electrical conductivity after doping.

Although conjugated polymers exhibit amazing electrical properties, their physical and material properties, including solubility, fusibility and stability, are usually quite limited. The common advantage of the syntheses of the polymers, the ability to cheaply produce a material that can be cast or molded into a desired shape from melt or from solution, is not achievable for most conjugated polymers. Their conformational rigidities give rise to their insolubility and infusibility which become one of the largest obstacles in conductive polymer application.

**Table I-1. CONDUCTIVITIES OF CONDUCTING POLYMERS**

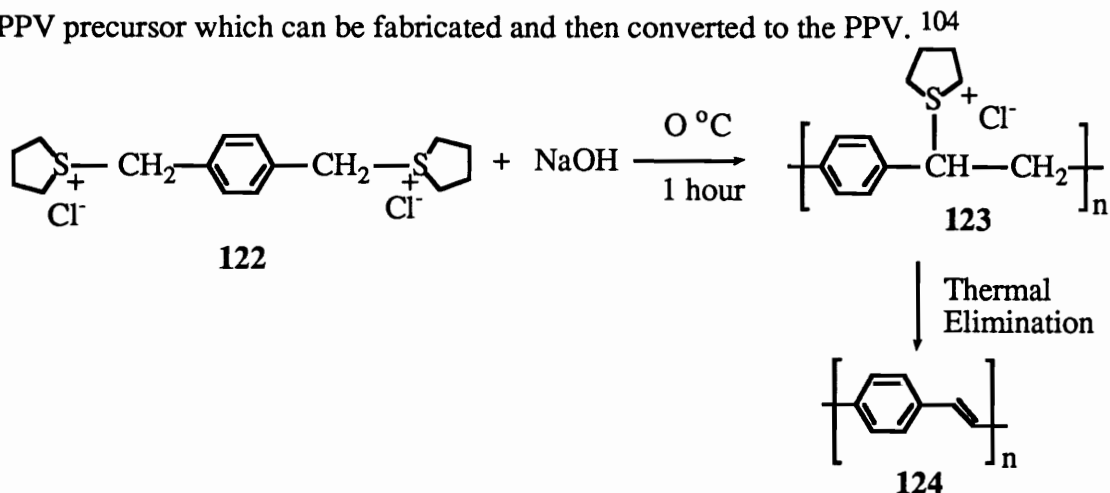
Polymer	Structure	Doping Materials	Approximate Conductivity (S/cm)
Polyphenylenevinylene		AsF <sub>5</sub>	10,000 <sup>a</sup>
Polyacetylene	(CH) <sub>n</sub>	I <sub>2</sub> , Br <sub>2</sub> , Li, Na, AsF <sub>5</sub>	10,000 <sup>a</sup>
Polypyrrole		BF <sub>4</sub> <sup>-</sup> , ClO <sub>4</sub> <sup>-</sup> , tosylate	500-7500
Polythiophene		BF <sub>4</sub> <sup>-</sup> , ClO <sub>4</sub> <sup>-</sup> , tosylate, FeCl <sub>4</sub> <sup>-</sup>	1000
Poly(3-alkylthiophene)		BF <sub>4</sub> <sup>-</sup> , ClO <sub>4</sub> <sup>-</sup> , FeCl <sub>4</sub> <sup>-</sup>	1000-10,000 <sup>a</sup>
Polyphenylene sulfide		AsF <sub>5</sub>	500
Polythienylenevinylene		AsF <sub>5</sub>	2700 <sup>a</sup>
Polyphenylene		AsF <sub>5</sub> , Li, K	1000
Polyaniline		HCl	200 <sup>a</sup>
Polyfuran		BF <sub>4</sub> <sup>-</sup> , ClO <sub>4</sub> <sup>-</sup>	100
Polyisothianaphthene		BF <sub>4</sub> <sup>-</sup> , ClO <sub>4</sub> <sup>-</sup>	50
Polyazulene		BF <sub>4</sub> <sup>-</sup> , ClO <sub>4</sub> <sup>-</sup>	1

a: Conductivity of oriented polymer (ref. 102)

To overcome this obstacle, two methods have been developed. The first one was to synthesize soluble precursors of the intended conducting polymers followed by thermal conversion of the polymer precursors to the final conducting polymers. For example, the synthesis of poly(1,4-phenylenevinylene) (PPV) was done via a two-step precursor route in which a water soluble PPV precursor was made in the first step followed by thermal elimination to convert the precursor to the PPV after fabrication. The second method was to incorporate flexible alkyl or alkoxide chains onto the rigid linear chains.

### 6.1 Synthesis of poly(1,4-phenylenevinylene)

Poly(1,4-phenylenevinylene) (PPV) (**124**) is a perfectly alternating copolymer of p-phenylene and trans-vinylene units. It shows extremely high electrical conductivity ( $10^5$  S/cm) and good optical features after stretching and doping.<sup>102</sup> Poly(1,4-phenylenevinylene) was first synthesized by Campbell and McDonald using a Wittig reaction.<sup>103</sup> However, the extended  $\pi$  conjugated system rendered it insoluble and infusible. This limited the ability of fabricating this material into different forms after synthesis. This problem was first circumvented by Wessling who prepared a processible PPV precursor which can be fabricated and then converted to the PPV.<sup>104</sup>



To circumvent the dilemma of a potential material which can't be processed, two well established ways in material science can be used, including either modifying the molecular structure so as to retain the property of interest while rendering the material's good processibility, or processing the material at a precursor stage which can subsequently be converted to the desired material. Wessling's soluble precursor method is based on the second strategy and the procedure was further optimized by Lenz et al. In fact, it is now one of the most successful ways to synthesize PPV.<sup>105</sup>

Lenz's procedure to synthesize PPV precursor **123** started from the addition of an argon-purged aqueous NaOH solution to the equal molar argon purged aqueous monomer solution, aqueous p-xylylene tetrahydrothiophenium chloride solution (**122**), stirred with pentane. Gel formation was found shortly after addition of the NaOH solution when the concentration of the monomer solution exceeded 0.1 M. The reaction was allowed to proceed at 0 °C for 1 hour.

The reaction was quenched by adding 1 M HCl solution to neutralize the solution to slightly acidic. Most of pentane was decanted off and nitrogen was bubbled through the solution overnight to eliminate residual pentane. The colorless solution obtained was dialyzed against deionized water for 2-3 days to remove the unreacted monomers, oligomers and salt.

The key feature of this reaction is that the true monomer is the p-xylylene sulfonium salt which is in equilibrium with the deprotonated monomer. Although the equilibrium of the true monomer formation is well established, the mechanism of polymerization is still under investigation. It was assumed that tetrahydrothiophene produced in the reaction would compete with the active center of the growing polymer chains for reaction with true monomers. If this was the case, the concentration of the true monomer would be reduced by the reverse reaction and thereby the formation of a high molecular weight polymer was limited. Based on the competition assumption, an

immiscible organic solvent, pentane, was used to extract the by product, organic sulfide, from the water layer which would increase the concentration of the true monomer. The result, up to 90% polymer yield, verified the assumption. <sup>106</sup>

The initial concentration of the monomer, which is another key factor in the polymerization reaction, also showed large effects on the polymer yield and molecular weight of the polymer. Table I-2 High yields were obtained with high concentrations of the original monomer up to 0.2 M. The gel formation when the monomer concentration exceeded 0.1 mol/L, did not prevent the reaction in the presence of pentane, but did influence the polymer yield and molecular weight of the polymer. <sup>106</sup> This is understandable because even though the gel formation limits the extraction of organic sulfide from the reaction solution, the presence of pentane can still help to remove the organic sulfide in order to form the true monomer.

Table I-2 Conditions and products for the polymerization reactions of 1,1'-[1,4-phenylene-bis(methylene)]bis(thiolanylium) dichloride

Monomer <sup>a)</sup> concentration in mol/L	Reaction <sup>b)</sup> conversion in %	$\frac{[\eta]}{dL/g}$ <sup>c)</sup>	Polymer <sup>d)</sup> yield in %	$\frac{[\eta]}{dL/g}$ <sup>e)</sup>	Polymer state
0.05	88	2.0	57	4.1	solution
0.1	92	8.1	70	10.1	gel
0.2	96	--	91	7.1	gel
0.3	93	--	68	14.3	gel

a) Ratio [Monomer]:[NaOH]=1:1.1.

b) Based on the amount of NaOH consumed.

c) Intrinsic viscosity of polymer solutions measured before dialysis.

d) Determined gravimetrically from the concentration of polymer in the dialyzed solution after evaporation before conversion to PPV.

e) Intrinsic viscosity measured after dialysis.

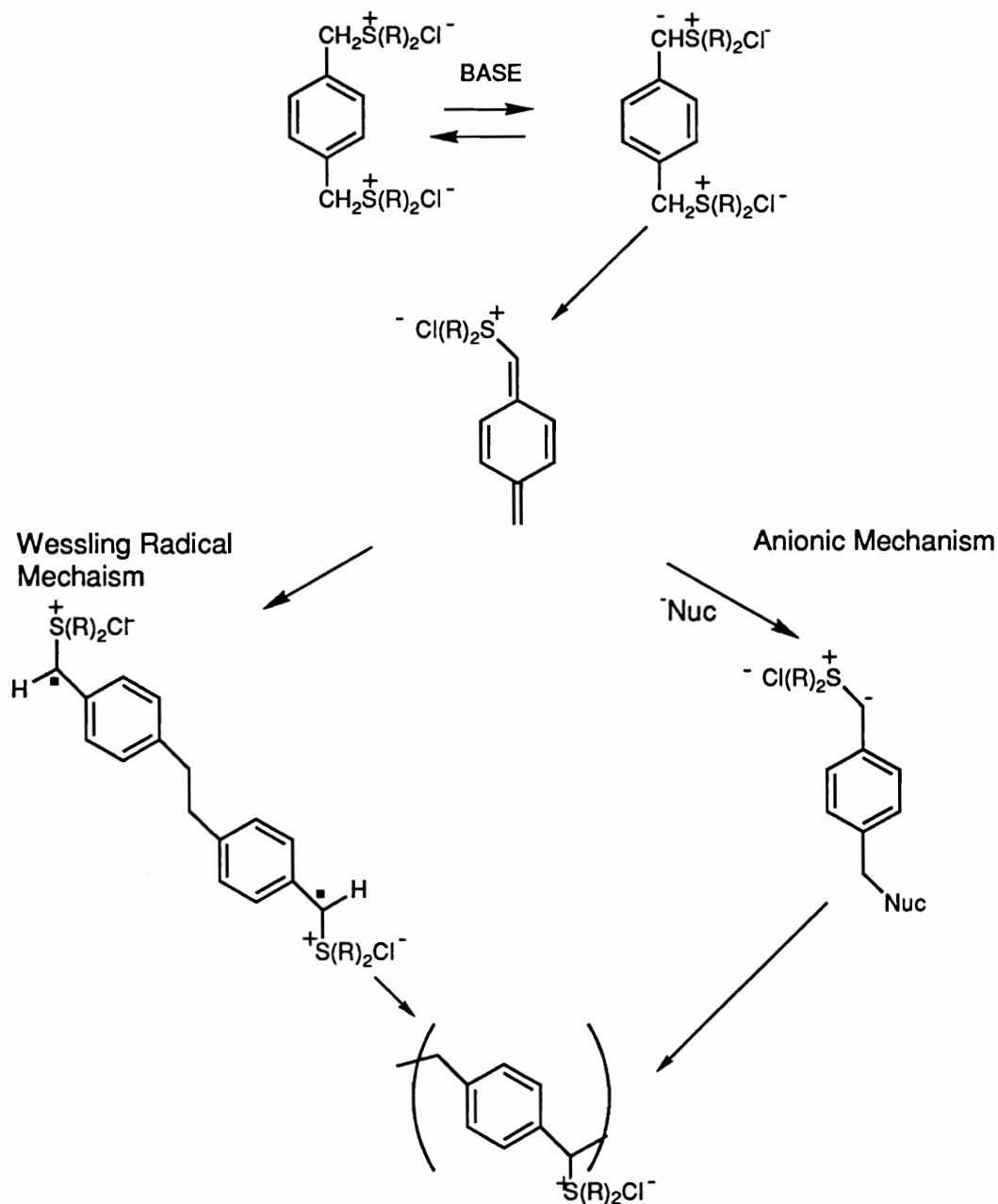
Although two polymerization mechanisms, diradical and anionic, were postulated at early stages, the diradical mechanism seems to be favored by the latest

evidence.<sup>104, 107</sup> The examination of the polymerization mechanism was performed by adding radical trap reagents into the polymerization reaction. The greatly reduced degree of polymerization and ESR studies of the polymerization suggested that the production of a high molecular weight PPV proceed through a radical chain propagation step. (Scheme I-2)

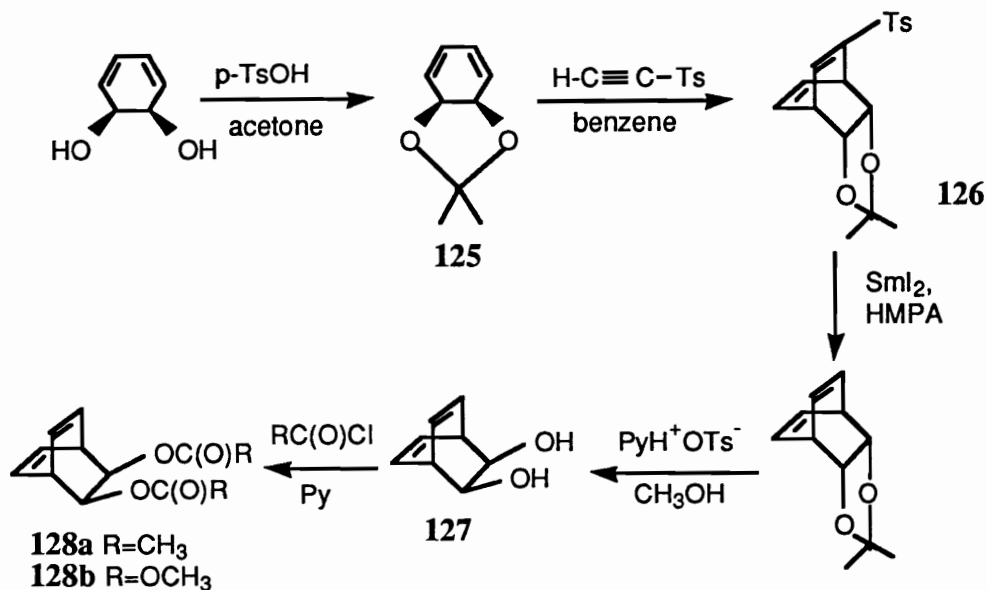
The polymer precursor solution obtained after dialysis can be cast into a film on the glass and heated under vacuum at around 250 °C for 20 hours to eliminate the organic sulfide and afford the final product: poly(1,4-phenylenevinylene). The elimination was postulated to proceed by E1 mechanism.<sup>108</sup> High conductivity can be achieved at this stage by doping and stretching the polymer while elimination occurs.

Although Wessling's soluble precursor polymerization provided high molecular weight polymer, certain polymer features, including degree of polymerization and polydispersity, were difficult to control. Recently, Grubbs reported a new precursor route to synthesize PPV via a living ring opening metathesis polymerization which gave better control over the structure of PPV.<sup>109</sup> Diel-Alder reaction between the acetone protected 3,5-cyclohexadien-cis-1,2-diol (**125**) and ethynyl p-tolyl sulfone gave totally anti cycloadduct **126**. Reductive desulfonylation followed by acid catalyzed hydrolysis generated bicyclic diol **127**, which can be converted to the monomers **128a** and **128b** by reacting with acetyl chloride or methyl chloroformate, respectively.

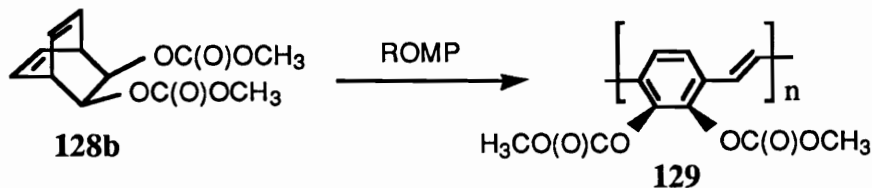
**SCHEME I-2. POSSIBLE MECHANISMS OF PPV PRECURSOR POLYMERIZATION**



The polymerization of these monomers was carried out with the olefin metathesis catalyst,  $\text{Mo}(=\text{NAr})(=\text{C}(\text{H})\text{CMe}_2\text{Ph})-(\text{OCMe}_2(\text{CF}_3))_2$  ( $\text{Ar}=2,6\text{-diisopropylphenyl}$ ), and dry dichloromethane as a solvent in a glove box.

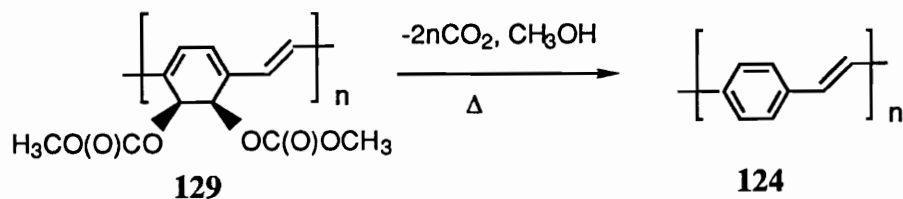


The reaction proceeded for 24 hours at 25 °C and was terminated by capping with benzaldehyde. The polymer (**129**) solution was precipitated in methanol and isolated by filtration and vacuum dried.



A high yield of polymerization was only obtained for **128b** monomer. However, relatively narrow molecular weight distributions were obtained (PDI=1.2-1.3). Almost equal amounts of cis- and trans-vinylene units were detected on the polymer backbones by <sup>1</sup>H NMR.

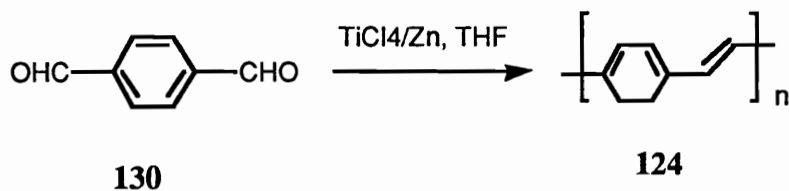
This polymer precursor (**129**) can be converted to PPV (**124**) by isothermal pyrolysis (280 °C) to eliminate carbon dioxide and methanol. PPV film obtained via this route contained only trans vinyl linkages, suggesting isomerization took place during the pyrolysis.



Compared to Wessling's method, ring opening metathesis has several advantages. It is compatible with the conventional non-aqueous fabrication techniques and the living polymerization provides better control of the PPV structure, including a closely defined degree of polymerization, molecular weight distribution, end group and sequence structure of copolymers. However, due to the high sensitivity of the catalyst, the polymerization must be performed under extremely dry conditions, in a glove box, which is inconvenient. The multistep monomer syntheses are also relatively complicated.

Besides the two methods introduced above, several other methods were also reported in the literature, including the McMurry reaction and acyclic metathesis polymerization.<sup>110, 111</sup>

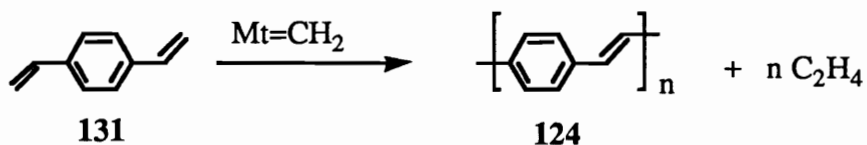
Deoxygenative coupling of aldehyde and ketone to yield olefins on treatment with low valent titanium is usually referred to as the McMurry reaction. This reaction is well established in organic chemistry and was optimized recently by McMurry.<sup>112</sup> Extending this reaction into polymer chemistry, PPV can be synthesized, starting from terephthalaldehyde (**130**).



The active species in this reaction are low valent titaniums, Ti (0), Ti (1), which are formed from TiCl<sub>4</sub>. Aldehyde groups present in the reaction can be concurrently

deoxygenated and coupled with one another to give the PPV (124). The PPV obtained was a yellow-brown material which was identified by the IR spectra and thermal analysis, differential scanning calorimetry (DSC), and thermogravimetric analysis (TGA). A quantitative yield was obtained in this reaction. But due to insolubility, molecular weight and molecular weight distribution could not be determined. <sup>110</sup>

Acyclic metathesis polymerization was successfully used by Wagener to synthesize unsaturated polyethers, polyesters etc., using Schrock's catalysts. This reaction was also applied to synthesize the PPV by Kumar and Eichinger recently, using Schrock's catalysts and 1,4-divinyl benzene (131) as the monomer. <sup>111</sup>



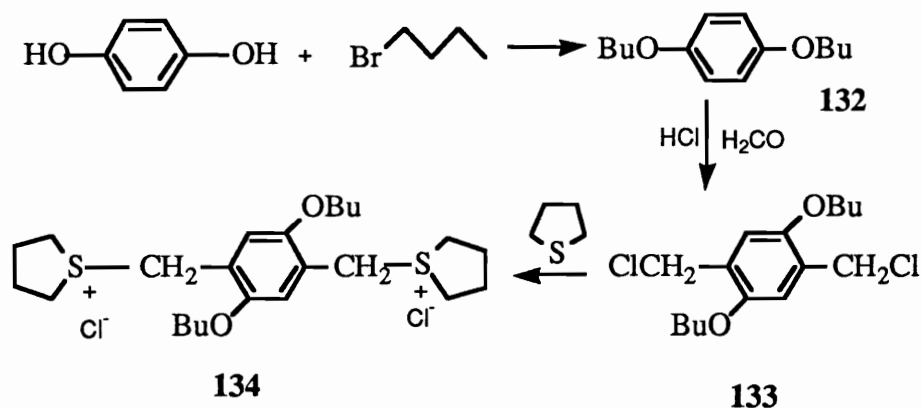
Though different PPV synthetic routes have been reported in the literature, Wessling's soluble precursor route is still a promising method for synthesizing PPV. However, much research needs to be done to truly understand this reaction, especially the mechanism of the reaction which can be utilized to optimize the reaction conditions and get better control of the polymer structure. Grubbs' ring opening metathesis polymerization is also a plausible method. However, relatively strict requirements for the polymerization reaction and multistep syntheses of the monomer may limit its application.

## 6.2 Synthesis of modified PPV

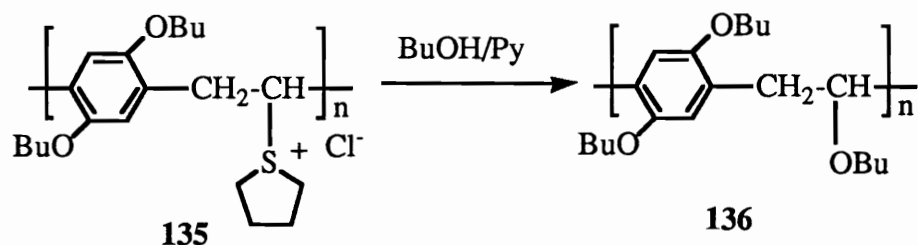
As mentioned early in this chapter, two strategies can be used to improve the processibility of the materials. Instead of making a soluble precursor, synthesis of modified PPV with high processibility is also possible. That is, the polymers can be

processed in their highly conductive forms. Two structural modifications of poly(1,4-phenylenevinylene) are discussed herein, including introduction of alkoxy and alkanesulfonate side chains onto the benzene rings. The introduction of the flexible side chains can not only reduces the interchain interactions, but can also cause a large entropy change of the polymer because of the variety of conformations of the side chains in the solution. Therefore, the processibility of the rigid conductive polymer can be improved.

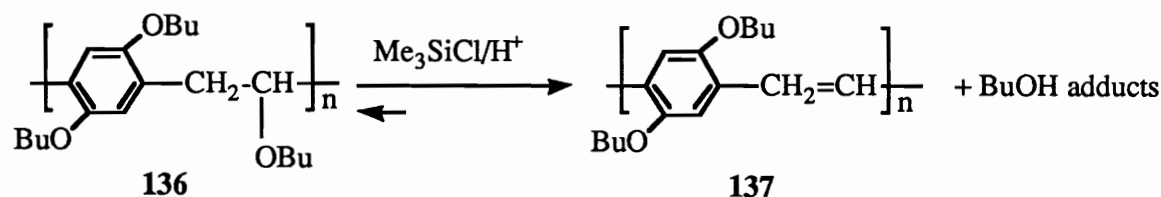
The synthesis of processible poly(dibutoxyphenylenevinylene) (**137**), which was reported by Elsenbaumer, had remarkable importance in the synthesis of conductive polymers.<sup>113</sup> For the first time, an electrically conductive polymer was synthesized from a non-ionic polymer precursor which was further converted to its conductive form by protonic acid doping in solution at room temperature. Another important discovery in this reaction was that the ionic precursor can be stabilized for a long time before being converted to a non-ionic precursor by the addition of a weak base such as pyridine. The monomer **134** was prepared from hydroquinone and n-butyl bromide via a Williamson ether synthesis route. The 1,4-dibutoxybenzene (**132**) obtained can react with formaldehyde and HCl to give 1,4-bis(chloromethyl)-2,5-dibutoxybenzene (**133**) following Wood and Gibson's procedure.<sup>114</sup> Further reaction of 1,4-bis(chloromethyl)-2,5-dibutoxybenzene (**133**) with 3 equivalents of tetrahydrothiophene in methanol at 50°C gave the monomer **134**.



The monomer **134** was polymerized by treatment with equimolar NaOH. The polymer **135** obtained can be dissolved in organic solvents and kept in solution for a long time by adding small amounts of weak base such as pyridine. When this ionic polymer precursor (**135**) was dialyzed against butanol in the presence of small amounts of pyridine, a new non-ionic polymer was obtained, which was poly(1,4-dibutoxyphenylene-2,5-diyl-1'-butoxy-1',2'-ethylenediyl) (**136**).



The final step, the conversion of non-ionic precursor **136** to its conductive form, was completed by reacting the precursor with strong acid in the presence of butanol scavenger such as  $\text{Me}_3\text{SiCl}$  in solution at room temperature.

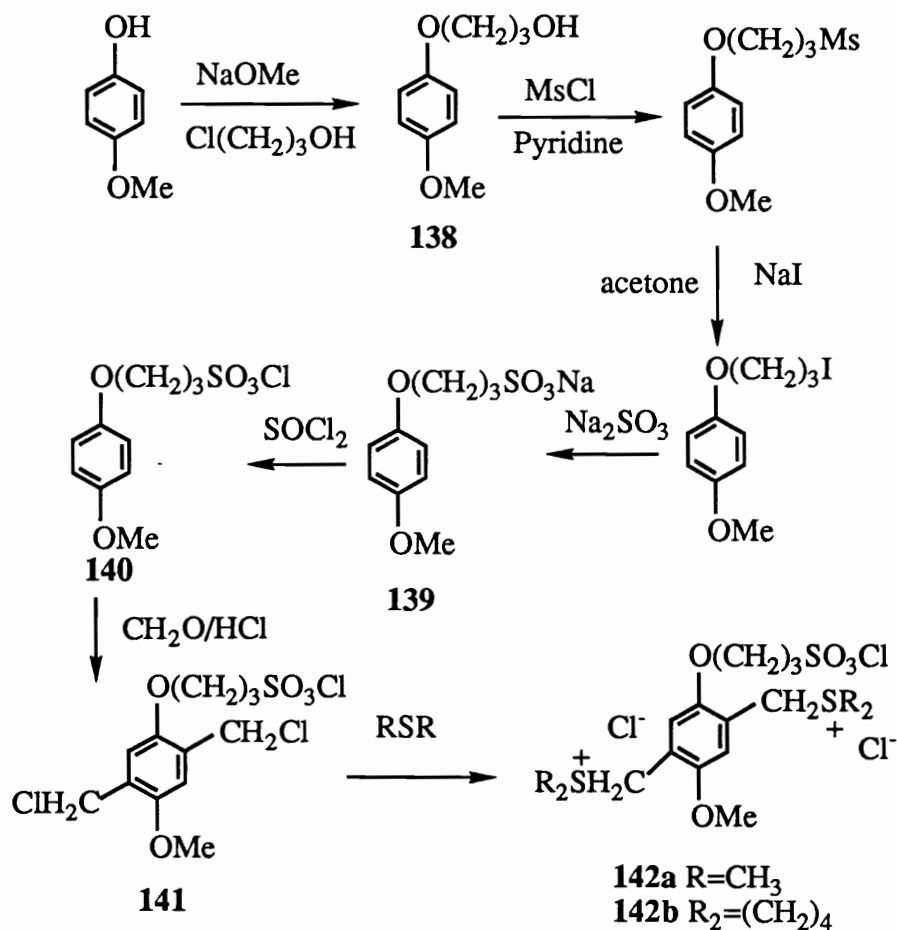


The conductivity of polymer **137** was high after stretching and doping, 98 S/cm.

Therefore, the final goal, improving the processibility of the conductive polymer while retaining its high conductivity, was achieved by modification of the molecular structure.

Although the modified PPVs which are soluble in organic solvents have already been synthesized in the past, <sup>115</sup> successful synthesis of water soluble PPV derivatives was not found in the literature until 1990. <sup>116</sup> The idea of synthesis water soluble PPV derivatives was also based on the modification strategy. Instead of alkoxy side chains, new alkanesulfonate chains were introduced onto the benzene rings which resulted in high solubility of the polymer in aqueous solution.

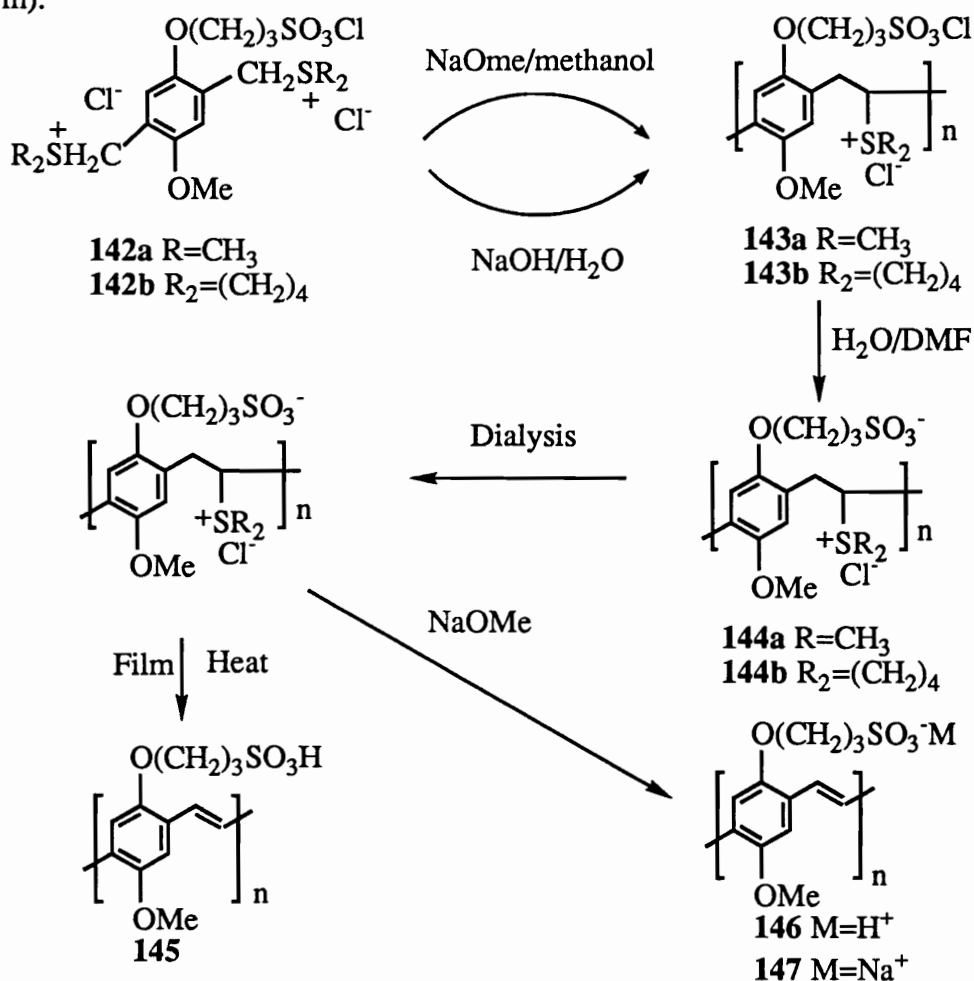
The monomer synthesis started from 4-methoxyphenol which was alkylated by 3-chloropropanol in the presence of sodium methoxide to give **138**. This compound was converted to **139** via mesylation, halogenation and sulfonation. Since **139** didn't undergo chloromethylation, it was first converted to **140** by reacting with thionyl chloride. The compound **140** was directly used in the chloromethylation to produce dichloro compound **141** without purification. Upon treatment of **141** with dimethyl sulfide or tetrahydrothiophene, hygroscopic bis(sulfonium) chloride monomers **142a** and **142b** were obtained in quantitative yield. The monomers **142a** and **142b** were purified by recrystallization from methanol/acetone.



The polymerizations were carried out in both organic solvent ( $\text{NaOMe}/\text{methanol}$ ) and aqueous solution ( $\text{NaOH}/\text{H}_2\text{O}$ ) to give polymers **143a** and **143b**. The polymers **143a** and **143b** can be hydrolyzed by refluxing with  $\text{DMF}/\text{water}$  to get sulfonate precursors **144a** and **144b**. After dialysis, the precursors can be converted to the final conjugated form in three ways. Method A was to heat the precursor films under vacuum at  $200\text{ }^\circ\text{C}$  for 4 hours to give fully conjugated polymer **145** which was the same as the procedure generally used for thermal elimination of a conducting polymer.

Method B was to reflux precursor solutions in  $\text{DMF}/\text{H}_2\text{O}$  in the presence of small amounts of acid (dopant) to yield a red solution of polymer **146**. In method C, the precursor was treated with excess sodium methoxide in ethylene glycol and then heated

to 190 °C under nitrogen for 26 hours to get a red solution of polymer **147** (the sodium salt form).



The polymers obtained from methods B and C can be easily redissolved in water. However, the polymer obtained by thermal elimination was found to be insoluble in any solvent, presumably due to the crosslinking at high temperature. The conductivity of polymer film **145** was around  $2 \times 10^{-6}$  S/cm. The conductivity of polymer **146**, which was relatively humidity dependent, ranged from  $10^{-4}$  to  $10^{-2}$  S/cm. The weight average molecular weight ( $M_w$ ) for polymer **146** was around  $1.12 \times 10^6$  g/mol with polydispersity of 16, measured from GPC.

Although some other modification reactions were also reported in the literature, the basic principles are the same: introducing flexible side chains on the polymer backbone to prevent the interchain interaction, and interrupting the coplanar topology of the conjugated backbone. However, for the same reason the high conductivity of the original polymer, which also results from the high conjugation along the backbone (good p electron overlap) and interchain electron transfer, may be decreased, as in the water soluble PPV derivative case. In fact, the modification of a highly conductive polymer is an attempt to get the best compromise between conductivity and processibility.

### **6.3 Luminescence of PPV and its applications**

In addition to its high conductivity, PPV also has other promising prospects for applications, e.g., optoelectronic and nonlinear optical devices. These applications are based on another important feature of PPV, luminescence. PPV can be both electroluminescent and photoluminescent.<sup>117,118</sup> The electroluminescence is obtained by injection of electrons into the conduction band and holes into the valence band, which capture one another with emission of visible radiation. This feature allows the PPV to be used as an active element in a large-area light-emitting diodes. Inorganic semiconductors with direct band gaps, such as GaAs, have been used in light-emitting devices. However, they are not easily or economically used in large-area displays. Organic molecular semiconductors have also been used in light-emitting devices because of their high photoluminescence quantum yield. However, there are problems associated with the long-term stability of these organic films which were generated by sublimation. Compared to the organic films, the PPV films offers better structural stability and higher quantum efficiency for the luminescence. All these remarkable properties make PPV an intensively investigated material for optical applications.<sup>117,118,119</sup>

Our research interest is to take advantage of the polyrotaxane architecture which can offer the combined characters of the two components to synthesize conducting polyrotaxanes. By choosing the conducting polymer as the backbone of the polyrotaxane and flexible crown ethers as the macrocycles, the polyrotaxanes are expected to have improved processibility than the rigid linear backbones. This idea is similar to the second modifying method for the conducting polymers because the flexible macrocycles act as side chains on the conducting polymer backbones. The only difference between these two methods is that the macrocycles are physically trapped, instead of chemically bonded, to the linear chains; this allows the rings to move along the linear chains. The threaded crown ethers may complex with the dopant such as sodium naphthlite which can stabilize the dopant. However, because of the crown ether incorporation, the distance between the linear chains will be increased which results in less electron hopping between the chains. This can cause anisotropic conduction (molecular wires) instead of 3 dimensional conduction. The luminescence of rotaxanes are expected to be different from the PPV backbone as well because of the structure difference. Therefore, the conductivities and photoluminescence of the polyrotaxanes are investigated to compare with the PPV. In this research, poly(1,4-phenylenevinylene) was chosen as the conducting polymer and the 42-crown-14 and 60-crown-20 were used as macrocycles. The syntheses and characterization of the crown ethers, poly(1,4-phenylenevinylene) and poly(1,4-phenylenevinylene)-crown ether rotaxanes via statistical threading are going to be reported in the following chapters.

## REFERENCES

1. J. Furukawa, *Encycl. Polym. Sci Eng.*, Wiley, NY, **1985**, 2nd ed., vol.4, 233-261
2. G. Riess, G. Hurtrez, P. Bahadur, *Encycl. Polym. Sci. Eng.*, Wiley, NY, **1985**, 2nd ed., vol.2, 324-434
3. J. E. McGrath, ed., *Anionic Polymerization, No. 166*, Symposium Series, American Chemical Society, Washington, DC, **1981**
4. M. van Beylen, S. Bywater, G. Smets, M. Szwarc, D. J. Worsfold, *Adv. Polymer. Sci.*, **1988**, 86, 87-143
5. H. G. Elias, *Macromolecules*, Plenum Press, New York, **1984**, pp.50
6. J. Roovers, *Encycl. Polym. Sci. Eng.*, Wiley, NY, **1985**, 2nd ed., vol.2, 478-499
7. P. Dregfuss, R. P. Quirk, *Encycl. Polym. Sci. Eng.*, Wiley, NY, **1985**, 2nd ed., vol.7, 551-579
8. D. M. Kulich, P. D. Kelley, J. E. Pace, *Encycl. Polym. Sci. Eng.*, Wiley, NY, **1985**, 2nd ed., vol.1, 388-426
9. D. A. Tomalia, D. M. Hedstrand, L. R. Wilson, *Encycl. Polym. Sci. Eng.*, Wiley, NY, **1990**, 2nd ed., index vol., 46-92
10. D. A. Tomalia, A. M. Naylor, W. A. Goddard, *Angew. Chem. Int. Ed. Engl.*, **1990**, 29, 138
11. H. B. Meikelburger, W. Jaworek, F. Vogtle, *Angew. Chem. Int. Ed. Engl.*, **1992**, 31, 1571
12. I. Gitsov, J. M. J. Frechet, *Macromolecules*, **1993**, 26, 6536
13. J. M. G. Cowie, *Polymers: Chemistry and Physics of modern Materials*, 2nd ed., Blackie, London, **1991**
14. G. Odian, *Principle of Polymerization*, 2nd ed., Wiley, NY, **1981**
15. W. J. Freeman, *Encycl. Polym. Sci. Eng.*, Wiley, NY, **1985**, 2nd ed., vol.3, 290-327
16. L. H. Sperling, *Interpenetrating Polymer Networks and Related Materials*, Plenum Press, **1981**
17. D. Klempner, L. H. Sperling, L. A. Utracki ed., *Interpenetrating Polymer Networks*, Advances in Chemistry, series 239, American Chemical Society, Washington, DC, **1994**

18. D. Klempner, L. Berkowski, *Encycl. Polym. Sci. Eng.*, Wiley, NY, **1985**, 2nd ed., vol.8, 279-341
19. D. R. Paul, J. W. Barlow, H. Keskkula, *Encycl. Polym. Sci. Eng.*, Wiley, NY, **1985**, vol.12, 399-461
20. L. A. Utracki, *Polymer Alloys and Blends*, Hanser Publisher, NY, **1990**
21. F. M. Sweeny ed., *Polymer Blends and Alloys*, Technomic Publishing, Lancaster, **1988**
22. D. B. Amabslio, I. W. Parsons, J. F. Stoddart, *TRIR*, **1994**, vol.2, No.5, 146
23. H. L. Frisch, E. Wasserman, *J. Amer. Chem. Soc.*, **1961**, 83, 3789
24. H. Frisch, I. Martin, H. Mark, *Monatsh*, **1953**, 84, 250
25. F. Patat, P. Derst, *Angew. Chem.*, **1959**, 71, 105
26. A. Luttringhaus, F. Cramer, H. Prinzbach, F. M. Henglein, *Leibigs Ann. Chem.*, **1958**, 613, 185
27. G. Schill, *PhD Thesis*, Universitat Freiburg **1959**
28. G. Schill, A. Luttringhaus, *Angew. Chem. Int. Ed. Engl.*, **1964**, 3, 546
29. E. Wasserman, *J. Amer. Chem. Soc.*, **1960**, 82, 4433
30. E. Wasserman, *Sci. American*, **1962**, 207, No.5, 94
31. I. T. Harrison, S. Harrison, *J. Amer. Chem. Soc.*, **1967**, 89, 5723
32. I. T. Harrison, *J. Am. Chem. Soc.*, **1972**, 231
33. I. T. Harrison, *J. Chem. Soc. Perk. Tran.*, **1974**, 1, 301
34. G. Schill, W. Beckmann, N. Schweickert, H. Fritz, *Chem. Ber.*, **1986**, 119, 2647
35. G. Schill, *Catenanes, Rotaxanes and Knots*, Academic Press, New York, **1971**
36. G. Schill, H. Zollenkopf, *Nachr. Chem. Techn.*, **1967**, 79, 149
37. G. Schill, H. Zollenkopf, *Ann. Chem.*, **1969**, 721, 53
38. C.J. Pedersen, *J. Am. Chem. Soc.*, **1967**, 89, 2495; C. J. Pedersen, *J. Am. Chem. Soc.*, **1967**, 89, 7017; D. J. Cram, *Angew. Chem. Int. Ed. Engl.*, **1988**, 27, 1009; J-M. Lehn, *Angew. Chem. Int. Ed. Engl.*, **1988**, 89, 27; J-M. Lehn, *Angew. Chem. Int. Ed. Engl.*, **1990**, 29, 1304
39. R. Hoss, F. Vogle, *Angew. Chem. Int. Ed. Engl.*, **1994**, 33, 375
40. M. C. Thompson, D. H. Busch, *J. Am. Chem. Soc.*, **1962**, 84, 1762
41. C. O. Dietrich-Buchecker, J-P. Sauvage, *Chem. Rev.*, **1987**, 87, 795; J. C. Chambron, C. O. Dietrich-Buchecker, J. P. Sauvage, *Top. Curr. Chem.*, **1993**, 165, 131
42. C. O. Dietrich-Buchecker, J. P. Sauvage, J. M. Kerm, *J. Am. Chem. Soc.*, **1984**, 106, 3043

43. A. M. Albrecht-Gary, C. O. Dietrich-Buchecker, Z. Saad, J. P. Sauvage, *J. Am. Chem. Soc.*, **1988**, *110*, 1467
44. M. Casario, C. O. Dietrich-Buchecker, J. Guilhem, C. Pascard, J. P. Sauvage, *J. Chem. Soc., Chem. Commun.*, **1985**, 244
45. C. O. Dietrich-Buchecker, B. Frommberger, I. Luer, J. P. Sauvage, F. Vogtle, *Angew. Chem. Int. Ed. Engl.*, **1993**, *32*, 1434
46. J. F. Stoddart, *Angew. Chem. Int. Ed. Engl.*, **1992**, *31*, 846
47. D. Armspach, P. R. Ashton, C. P. Moore, N. Spencer, J. F. Stoddart, T. J. Wear, D. J. Williams, *Angew. Chem. Int. Ed. Engl.*, **1993**, *32*, 854
48. H. Ogino, *J. Am. Chem. Soc.*, 1981, 103, 1303; H. Ogino, *New J. Chem.*, **1993**, *17*, 683-688
49. R. Isnin, A. E. Kaifer, *J. Am. Chem. Soc.*, 1991, 113, 8188-8190; R. Isnin, A. E. Kaifer, *Pure & Appl. Chem.*, **1993**, *vol.65*, 495
50. R. S. Wylie, D. H. Macartney, *J. Am. Chem. Soc.*, **1992**, *114*, 3136
51. G. Wenz, E. Von der Bey, *Angew. Chem. Int. Ed. Engl.*, **1992**, *31*, 783; G. Wenz, F. Wolf, M. Wagner, S. Kubik, *New J. Chem.*, **1993**, *17*, 729
52. G. Wenz, G. Keller, *Angew. Chem. Int. Ed. Engl.*, **1992**, *31*, 199
53. A. Harada, J. Li, M. Kamachi, *Nature*, **1993**, *364*, 516
54. G. Wenz, *Angew. Chem. Int. Ed. Engl.*, **1994**, *33*, 803
55. C. Wu, P.R. Lecavalier, Y. X. Shen, H. W. Gibson, *Chem. Mater.*, **1991**, *3*, 569
56. J-C. Chambron, A. Harriman, V. Heitz, J. P. Sauvage, *J. Am. Chem. Soc.*, **1993**, *115*, 7419
57. K. Yamamari, Y. Shimura, *Bull. Chem. Soc. Jpn.*, **1988**, *57*, 1596
58. T. V. S. Rao, D. S. Lawrence, *J. Am. Chem. Soc.*, **1990**, *112*, 3614
59. H. M. Colquhoun, E. P. Goodings, J. M. Maud, J. F. Stoddart, O. J. Williams, J. B. Wolstenholme, *J. Chem. Soc. Chem. Commun.*, **1983**, 1140
60. H. M. Colquhoun, E. P. Goodings, J. M. Maud, J. F. Stoddart, J. B. Wolstenholme, D. J. Williams, *J. Chem. Soc., Perkin Trans.*, **1985**, 607
61. B. L. Allwood, N. Spencer, H. Shahriari-Zavareh, J. F. Stoddart, D. J. Williams, *J. Chem. Soc., Chem. Commun.*, **1987**, 1058
62. B. L. Allwood, N. Spencer, H. Shahriari-Zavareh, J. F. Stoddart, D. J. Williams, *J. Chem. Soc., Chem. Commun.*, **1987**, 1064
63. P. R. Ashton, A. M. Z. Slawin, N. Spencer, J. F. Stoddart, D. J. Williams, *J. Chem. Soc., Chem. Commun.*, **1987**, 1066

64. P. R. Ashton, A. M. Z. Slawin, N. Spencer, J. F. Stoddart, D. J. Williams, *J. Chem. Soc., Chem. Commun.*, **1987**, 1061
65. J. Y. Ortholand, A. M. Slawin, W. Spencer, J. F. Stoddart, D. J. Williams, *Angew. Chem. Int. Ed. Engl.*, **1989**, 28, 1394
66. B. Odell, M. V. Reddington, A. M. Z. Slawin, N. Spencer, J. F. Stoddart, D. J. Williams, *Angew. Chem. Int. Ed. Engl.*, **1988**, 27, 1547
67. P. R. Ashton, B. Odell, M. V. Reddington, A. M. Z. Slawin, J. F. Stoddart, D. J. Williams, *Angew. Chem. Int. Ed. Engl.*, **1988**, 27, 1550
68. P. R. Ashton, T. T. Goodnow, A. E. Kaifer, M. V. Reddington, A. M. Z. Slawin, N. Spencer, J. F. Stoddart, C. Vincent, D. J. Williams, *Angew. Chem. Int. Ed. Engl.*, **1989**, 28, 1396; P-L. Anchli, P. R. Ashton, R. Ballardini, V. Balzani, M. Delgado, M. T. Gandolphi, T. T. Goodnow, A. E. Kaifer, D. Philp, M. Pietraszkiewicz, L. Prodi, M. V. Reddington, A. M. Z. Slawin, N. Spencer, J. F. Stoddart, C. Vicent, D. J. Williams, *J. Am. Chem. Soc.*, **1992**, 114, 193
69. P. R. Ashton, C. L. Brown, E. J. T. Chrystal, T. T. Goodnow, A. E. Kaifer, K. P. Parry, D. Philp, A. M. Z. Slawin, N. Spencer, J. F. Stoddart, C. Vincent, D. J. Williams, *J. Chem. Soc., Chem. Commun.*, **1991**, 634
70. P. R. Ashton, C. L. Brown, E. J. T. Chrystal, T. T. Goodnow, A. E. Kaifer, K. P. Parry, M. Pietraszkiewicz, N. Spencer, J. F. Stoddart, *Angew. Chem. Int. Ed. Engl.*, **1991**, 30, 1042
71. P. R. Ashton, C. L. Brown, E. J. T. Chrystal, T. T. Goodnow, A. E. Kaifer, K. P. Parry, A. M. Z. Slawin, N. Spencer, J. F. Stoddart, D. J. Williams, *Angew. Chem. Int. Ed. Engl.*, **1991**, 30, 1039
72. D. B. Amabilino, P. R. Ashton, A. S. Reder, N. Spencer, J. F. Stoddart, *Angew. Chem. Int. Ed. Engl.*, **1994**, 33, 433
73. P. L. Ancli, N. Spencer, J. F. Stoddart, *J. Am. Chem. Soc.*, **1991**, 113, 5131
74. P. R. Ashton, M. Groguz, A. M. Z. Slawin, J. F. Stoddart, D. J. Williams, *Tetrahedron Lett.*, **1991**, 32, 6235
75. R. A. Bissell, E. Cordova, A. E. Kaifer, J. F. Stoddart, *Nature*, **1994**, vol. 369, 133
76. P. L. Anelli, P. R. Ashton, D. Philp, M. V. Reddington, A. M. Z. Slawin, N. Spencer, J. F. Stoddart, D. J. Williams, *Angew. Chem. Int. Ed. Engl.*, **1991**, 30, 1036
77. P. R. Ashton, D. Philp, M. V. Reddington, A. M. Z. Slawin, N. Spencer, J. F. Stoddart, D. J. Williams, *J. Chem. Soc., Chem. Commun.*, **1991**, 1680

78. Y. X. Shen, P. T. Engen, M. A. G. Gerg. J. S. Merola, H. W. Gibson, *Macromolecules*, **1992**, *25*, 2786
79. P. R. Ashton, D. Philp, N. Spencer, J. F. Stoddart, *J. Chem. Soc., Chem. Commun.*, **1992**, 1124
80. Y. X. Shen, *PhD Dissertation*, Virginia Polytechnic Institute and State University, **1992**
81. P. R. Ashton, M. Belohradsky, D. Philp, J. F. Stoddart, *J. Chem. Soc., Chem. Commun.*, **1993**, 1269
82. P. R. Ashton, D. Philp, N. Spencer, J. F. Stoddart, D. J. Williams, *J. Chem. Soc., Chem. Commun.*, **1994**, 181
83. G. Agam, D. Gravier, A. Zilkha, *J. Am. Chem. Soc.*, **1976**, *98*, 5206
84. G. Agam, A. Zilkha, *J. Am. Chem. Soc.*, **1976**, *98*, 5214
85. A. Harada, M. Kamachi, *Macromolecules*, **1990**, *23*, 2821
86. A. Harada, M. Kamachi, *J. Chem. Soc., Chem. Commun.*, **1990**, 1322
87. A. Harada, J. Li, M. Kamachi, *Nature*, **1993**, *vol.314*, 516
88. A. Harada, J. Li, T. Nakamitsu, M. Kamachi, *J. Org. Chem.*, **1993**, *58*, 7524
89. A. Harada, J. Li, M. Kamachi, *Macromolecules*, **1993**, *26*, 5698
90. A. Harada, J. Li, S. Suzuki, M. Kamachi, *Macromolecules*, **1993**, *26*, 5267
91. N. Ogata, K. Sanui, J. Wada, *J. Polym. Sci., Polym. Lett. Ed.*, **1975**, *14*, 459
92. I. T. Harrison, *J. C. S. Chem. Comm.*, **1977**, 384
93. M. Maciejewski, *J. Macromol. Sci-Chem.*, **1979**, *A13*, 77
94. M. maciejewski, A. Gwizdowski, P. Peczak, A. Pietrzak, *J. Macromol. Sci-Chem.*, **1979**, *A13*, 87
95. T. E. Lipotova, L. F. Kosyanchuk, V. V. Shilov, Y. P. Gomza, *Polymer Science U. S. S. R.*, **1985**, *vol.27*, 622
96. T. E. Lipotova, L. F. Kosyanchuk, Y. P. Gomza, V. V. Shilov, Y. S. Lipatov, *Dokl. Akad. Nauk S. S. S. R (Engl. Tr.)*, **1982**, 263, 140
97. Y. X. Shen, D. H. Xie, H.W. Gibson, *J. Am. Chem. Soc.*, **1994**, *116*, 537
98. J. Y. Sze, H. W. Gibson, *Polym. Prepr., J. Am. Chem. Soc. Div. Polym. Chem.*, **1992**, *33(2)*, 331
99. M. Born, H. Ritter, *Makromol. Chem. Rapid Commun.*, **1991**, *12*, 471
100. M. Born, H. Ritter, *Acta Polymer*, **1994**, *45*, 68
101. M. C. Bheda, *PhD Dissertation*, Virginia Polytechnic Institute and State University, **1992**

102. M. G. Kanatzidis, *C&EN*, **1990**, Dec.3
103. R. N. McDonald, T. W. Campbell, *J. Am. Chem.Soc.*, **1960**, *82*, 4669
104. R. A. Wessling, *J. Polym. Sci., Polym. Symp.*, **1985**, *72*, 55-66
105. R. O. Garay, R. W. Lenz, *J. Polym. Sci.: Part A: Polym. Chem.*, **1992**, *30*, 977
106. R. W. Lenz, C. C. Han, J. S. Smith, F. E. Karasz, *J. Polym. Sci.: Part A: Polym. Chem.*, **1988**, *26*, 3241; R. Garay, R. W. Lenz, *Macromol. Chem., Suppl.*, **1989**, *15*, 1-7; F. R. Denton III, P. M. Lahti, F. E. Karasz, *J. Polym. Sci.: Part A: Polym. Chem.*, **1992**, *30*, 2223
107. P. M. Lahti, D. A. Modarelli, F. R. Denton III, R. W. Lenz, F. E. Karasz, *J. Am. Chem. Soc.*, **1988**, *110*, 7258
108. D. A. Halliday, P. L. Burn, R. H. Friend, A. B. Holmes, *J. Chem. Soc., Chem. Commun.*, **1992**, *22*, 1686
109. V. P. Conticello, D. L. Gin, R. H. Grubbs, *J. Am. Chem. Soc.*, **1992**, *114*, 9708
110. F. Cataldo, *Polym. Commun.*, **1991**, *32*, 354
111. A. Kumar, B. E. Eichinger, *Makromol. Chem., Rapid Commun.*, **1992**, *13*, 311
112. J. E. McMurry, T. Lectka, J.G.Rico, *J. Org. Chem.*, **1989**, *54*, 3748
113. C. C. Han, R. L. Elsenbaumer, *Mol. Cryst. Liq. Cryst.*, **1990**, *189*, 183
114. J. H. Wood, R. E. Gibson, *J. Am. Chem. Soc.*, **1947**, *71*, 393
115. S. H. Askari, S. D. Rughroputh, F. Wudl, *Proc. Acs Div, Polym. Mat. Sci. Eng.*, **1988**, *59*, 1068
116. S. Shi, F. Wudl, *Macromolecules*, **1990**, *23*, 2119
117. D. D. C. Bradley. *Chem. Br.*, **1991**, *27*, 719
118. N. C. Greenham, S. C. Moratti, D. D. C. Bradley, R. H. Friend, A. B. Holmes, *Nature*, **1993**, *vol. 365*, 628
119. J. H. Burroughes, D. D. Bradley, A. R. Brown, R. N. Marks, K. Mackay, R. H. Friend, P. L. Burns, A. B. Holmes, *Nature*, **1990**, *vol. 347*, 539

# CHAPTER II BLOCKING GROUP SYNTHESIS AND CHARACTERIZATION

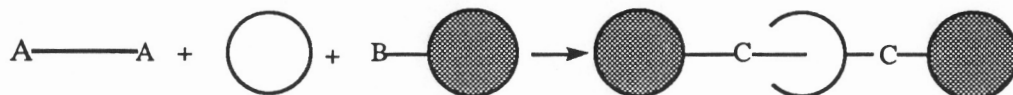
## 1. INTRODUCTION

As one of the important components in the rotaxanes and polyrotaxanes, blocking groups are used to prevent the slippage of the threaded macrocycles and to control the molecular weight of the polyrotaxanes. Since end-capping is the major function of the blocking groups, the size of blocking groups is the most important factor in the design. Obviously, the sizes of the blocking groups should be larger than the cavities of the macrocycles to be blocked. This can be theoretically calculated and demonstrated by CPK models.

As different types of monomeric and polymeric rotaxanes were prepared, various blocking groups have been developed. In 1967, Harrison investigated the statistical formation of the rotaxanes by reversible cleavage of blocking group, triphenylmethyl, to allow the threading of a cyclohydrocarbon mixture and then reblocked the linear chain.<sup>1</sup> The largest macrocycle that could be blocked by this blocking group was a 29-membered ring. The next blocking groups Harrison studied were cyclohexylacetyl chloride and tris(tert-butylphenyl)methanol. His results showed that the cyclohexylacetate group could only block macrocycles with less than 28 methylene units. However, the tris(tert-butylphenyl)methanol could block macrocycles with up to 33 methylene units. These results were confirmed by Schill in his rotaxane experiments using triphenyl blocking group.<sup>2</sup>

Besides the size factor shown in Harrison's and Schill's results, another factor to be considered in the design of the blocking groups is functionality. To end-cap the linear chain, the functional end of the blocking groups must be reactive toward the chain ends of the linear backbones. This requires the blocking groups to be compatible with the

reaction system and have monofunctionality on the ends (B) to react with the functional group on the linear chain ends (A). The functional groups include halo, phenolic, alcoholic and amino groups that can fit into the rotaxane and polyrotaxane.

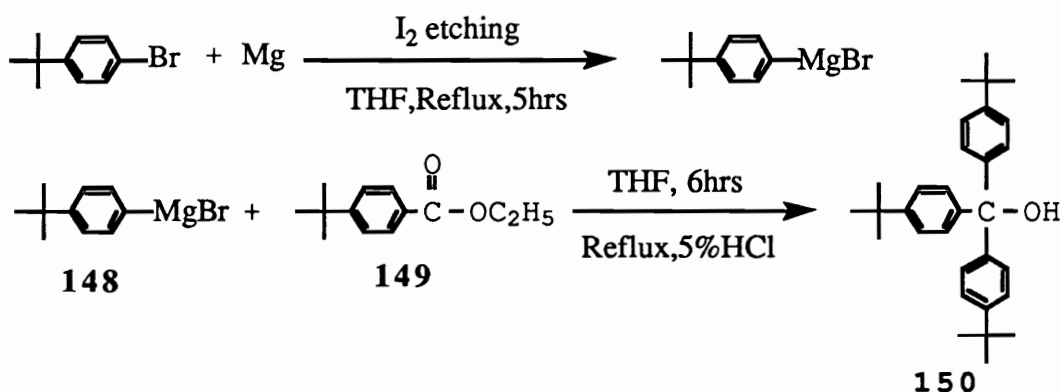


The last factor that needs to be addressed in blocking group design is the solubility of the blocking group. The blocking groups must be soluble in the reaction solvents, either melted macrocycles or other solvents, so that the blocking can take place during the reactions.

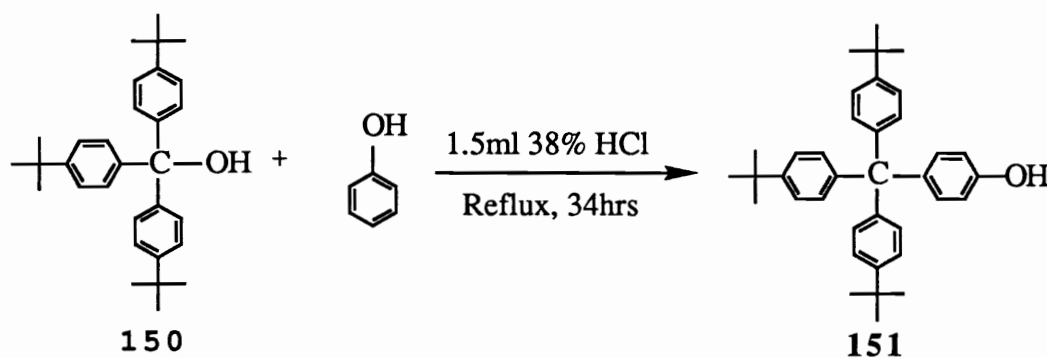
In addition to the early reported trityl blocking group, Stoddart reported rotaxanes with porphyrins as stoppers.<sup>3</sup> Cobalt and iron complexes and other compounds were also reported to be used as blocking groups in the monomeric or polymeric rotaxanes syntheses.<sup>4,5,6</sup> Considering the crown ethers we used in the polyrotaxane syntheses that have very large cavities and the compatibility of the reaction systems, we decided to focus on the very bulky triarylmethyl compounds. They can provide both steric hindrance and solubility in the reaction solvents.

## 2. RESULTS & DISCUSSION

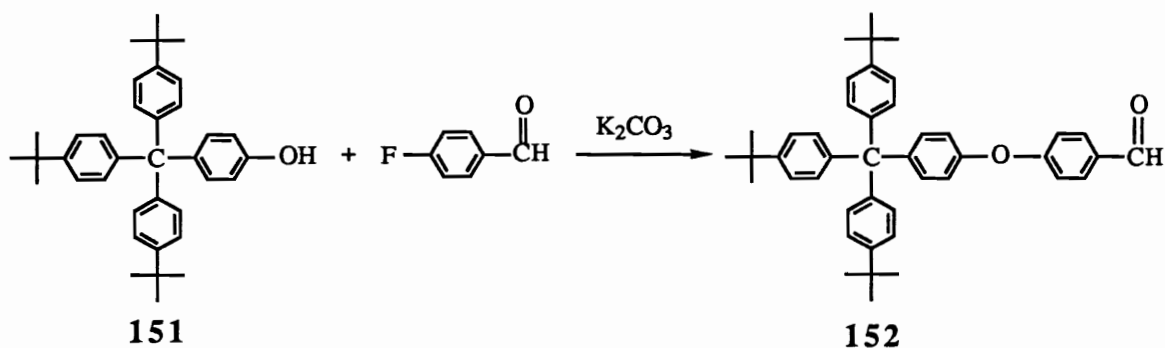
The triarylmethyl blocking groups syntheses start from benzoate ester **149** which can react with Grignard reagent **148** derived from p-bromo-tert-butylbenzene in refluxing of tetrahydrofuran to give tris-p-t-butylphenylmethanol (**150**) in good yield.



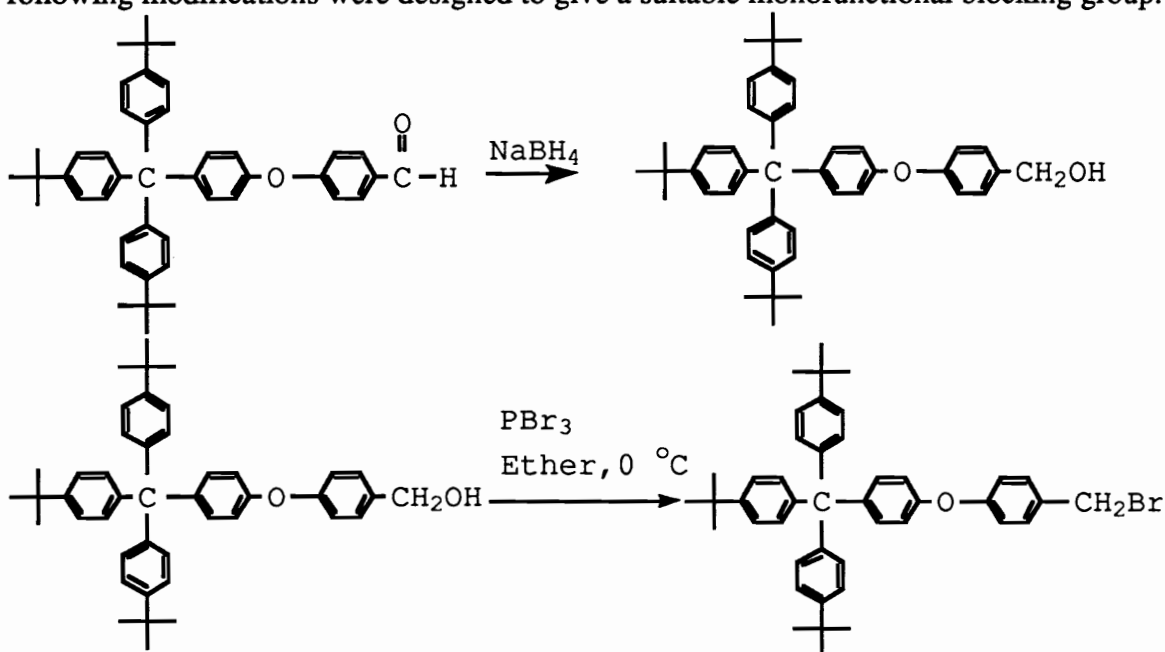
This compound was purified by recrystallization in cyclohexane. The purified product was characterized by  $^1\text{H}$  NMR (Fig. II-1) and IR (Fig. II-2). The compound **150** with OH functionality at one end can be used as a blocking group. However, because of steric hindrance of the bulky side groups, the reactivity of this functional group was reduced. To extend the end group, carbocation chemistry was adopted. This method was based on the work reported by Milkroyannidis.<sup>7</sup> The compound **150** was reacted with an excess of phenol with a small amount of concentrated HCl as a catalyst under reflux conditions to give blocking group **151** with extended functionality.

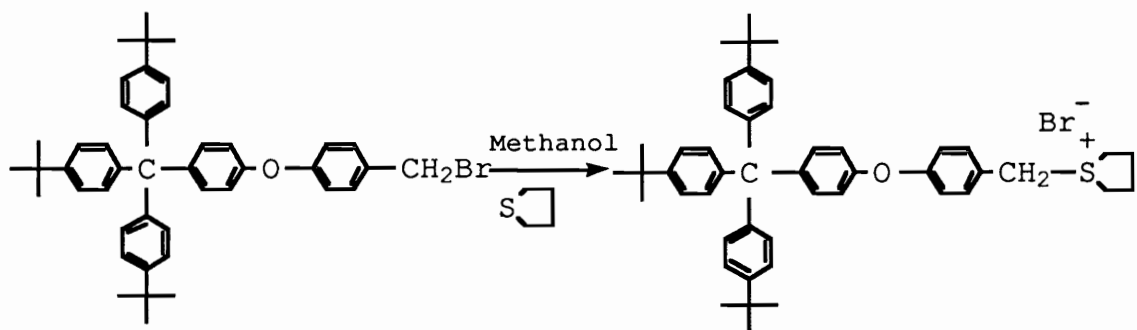


The compound was purified by washing with hot hexane and methanol. The purified **151** was characterized by  $^1\text{H}$  NMR (Fig. II-3). The end group of **151** was further extended by reaction with 4-fluorobenzaldehyde via a nucleophilic substitution to give compound **152**.



This compound was purified by column chromatography and characterized by  $^1\text{H}$  NMR (Fig. II-4a), IR (Fig. II-4b) and elemental analysis. All the results agree very well with the structure. To make the blocking group compatible with the polymerization, the following modifications were designed to give a suitable monofunctional blocking group.





However, the molecular weight of the linear polymer backbone was found to be very high. (see chapter IV) Therefore, it seems the end blocking is not very necessary and sometimes it may have the opposite effect on the threading--pushing the threaded macrocycles off the linear chains. The high threading yields in the later polyrotaxanes syntheses confirmed that the blocking group is not necessary in this system. Therefore, the last three steps were aborted.

### 3. EXPERIMENTAL

The starting materials were bought from Aldrich Chemical Co. and used with no further purification. Melting points were taken in capillary tubes and have been corrected. Proton and carbon NMR spectra, reported in ppm, were obtained on a 270 MHz spectrometer using chloroform solutions with tetramethylsilane as an internal standard. Elemental analysis was performed by Atlantic Microlab of Norcross, GA

#### 1. Synthesis of Tris-(p-t-butylphenyl)methanol (150)

Because the Grignard reagent is very sensitive to water, all glassware was dried by free flame. The Mg (4.86 g, 0.2 mol) and a few crystals of iodine were added first. The iodine was vaporized by free flame. When the purple vapor condensed and the flask was still warm, the solution of p-t-butylbromobenzene (42.62 g, 0.2 mol) in THF (120 mL) was added. The reaction started immediately, indicated by the disappearance of brown color and spontaneous boiling. The solution was heated at reflux for 5 hours. A solution of ethyl p-t-butyl-benzoate (20.9 g, 0.1 mole) in THF (50 mL) was added slowly from the dropping funnel. The reaction solution was heated at reflux for another 6 hours. The reaction was worked up by pouring the reaction solution into 700 mL 5% HCl solution and extracted with dichloromethane (3x650 mL). The dichloromethane was dried with sodium sulfate. The product, a yellow solid, was obtained by rotary evaporating the solvent. The compound was purified by recrystallizing from cyclohexane to give 29.58 g (69.3% ) of white powder: mp 207-210 °C; reported mp 212-213 °C;<sup>8</sup> IR 3550 (sharp, OH), 3084, 3056, 3029 (arom), 2959, 2903, 2865 (aliph), 1507, 1400 (arom), 1269 (OH bend), 1008, 1005 (C-O), 826; <sup>1</sup>H NMR  $\delta$  1.31 (s, 27H, CH<sub>3</sub>), 2.71 (s, 1H, OH), 7.17 (d, J=11, 6H, arom), 7.33 (d, J=11, 6H, arom).

## 2. Synthesis of Tri-(p-t-butylphenyl)-4-hydroxyphenylmethane (151)

Tris-(p-t-butylphenyl)methanol (29.06 g, 56.7 mmol) was added into a 500 mL one neck flask with a condenser. Excess phenol (95.13 g, 1.01 mol) was used and 1.5 mL of 38% HCl was added to catalyze the reaction. The solution became solid in 30 minutes and more phenol (36 g, 380 mmol) was added with increasing temperature. After 34 hours of refluxing, the reaction solution was poured into a 500 mL 5% NaOH solution to remove the excess phenol. The product was extracted with toluene (4x200 mL). The toluene solution was washed with NaOH (3x500 mL) and water (3x500 mL) until pH=7. The toluene solution was dried with sodium sulfate. The product was obtained by rotary evaporating toluene. It was purified by boiling in n-hexane, methanol and recrystallized from the mixture of toluene/hexane (3:1) to afford 16.5 g (56.8%) of light yellow powder: mp 302.5-303 °C; reported mp 304-305.8 °C;<sup>9, 10</sup>. IR 3596, 3487 (OH), 3029 (arom), 2961, 2899, 2865, (aliph) 1504, 1361, 841, 828; <sup>1</sup>H NMR  $\delta$  1.30 (s, 27H, CH<sub>3</sub>), 6.72 (d, J=11, 2H, arom), 7.03-7.21 (m, 14H, arom).

## 3. Synthesis of p-[p-(tris-(p-t-butylphenyl)methyl)phenoxy]benzaldehyde (152)

A 250 ml 4 neck flask equipped with a condenser and a Dean-Stark trap was dried by free flame. It was charged with tris-(p-t-butylphenyl)-4-hydroxyphenylmethane (5 g, 1 mmole), K<sub>2</sub>CO<sub>3</sub> (0.823 g, 5.94 mmole) (ground), DMAC (100 mL) and toluene (60 mL). The solution was stirred with a magnetic stirring bar and heated at reflux for 4 hours. After 4 hours of refluxing, toluene was distilled and p-fluorobenzaldehyde (1.23g, 1 mmol) was added by syringe. The reaction temperature was controlled at 140 °C and the reaction was run for 4 hours. The solution was precipitated into 800 mL 10% H<sub>2</sub>SO<sub>4</sub> solution. The precipitate was washed with water and extracted with dichloromethane. The compound was purified by column chromatography and recrystallized from ethyl acetate 3 times to give 3.4 g (56.5 %) of white powder: mp 277-278 °C (dec.); IR 3031, 3029 (arom), 2959, 2903, 2869 (aliph), 1700 (C=O), 1496 (arom), 1236, 1208, 1018 (C-

O), 821;  $^1\text{H NMR } \delta$  1.30 (s, 27H,  $\text{CH}_3$ ), 6.92 (d,  $J=8.6$ , 2H, arom), 7.10, 7.25 (m, 16H, arom), 7.82 (d,  $J=8.6$ , 2H, arom), 9.91 (s, 1H,  $\text{O}=\text{CH}$ ); Anal. calcd for  $\text{C}_{44}\text{H}_{48}\text{O}_2$ : C, 86.80; H, 7.95. found: C, 86.60; H, 7.95.

## REFERENCE

1. I. T. Harrison, S. Harrison, *J. Am. Chem. Soc.*, **1967**, *89*, 5723; I. T. Harrison, *J. Am. Chem. Soc.*, **1972**, 231
2. G. Schill, W. Beckmann, N. Schweickert, H. Fritz, *Chem. Ber.*, **1986**, *119*, 2647
3. P. R. Ashton, M.R.Johnson, J. F. Stoddart, M. S. Tolly, J. W. Wheeler, *J. Chem. Soc. Chem. Commun.*, **1992**, 1128
4. H. Ogino, *J. Am. Chem. Soc.*, 1981, 103, 1303; H. Ogino, *New J. Chem.*, **1993**, *17*, 683-688
5. R. Isnin, A. E. Kaifer, *J. Am. Chem. Soc.*, **1991**, *113*, 8188-8190; R. Isnin, A. E. Kaifer, *Pure & Appl. Chem.*, **1993**, *vol.65*, 495
6. R. S. Wylie, D. H. Macartney, *J. Am. Chem. Soc.*, **1992**, *114*, 3136
7. J. A. Mikroyannidis, *Eur. Poly. J.*, **1985**, *21*, 895
8. C. S. Marvel, J. F. Kaplan, C.M. Himel, *J. Am. Chem. Soc.*, **1941**, *63*, 1892
9. H. W. Gibson, S. H.Lee, P. T. Engen, P. Lecavalier, J. Sze, Y. X. Shen, M. Bheda, *J. Org. Chem.*, **1993**, *58*, 3748
10. J. Sze, Master Thesis, Virginia Polytechnic Institute & State University, 1992

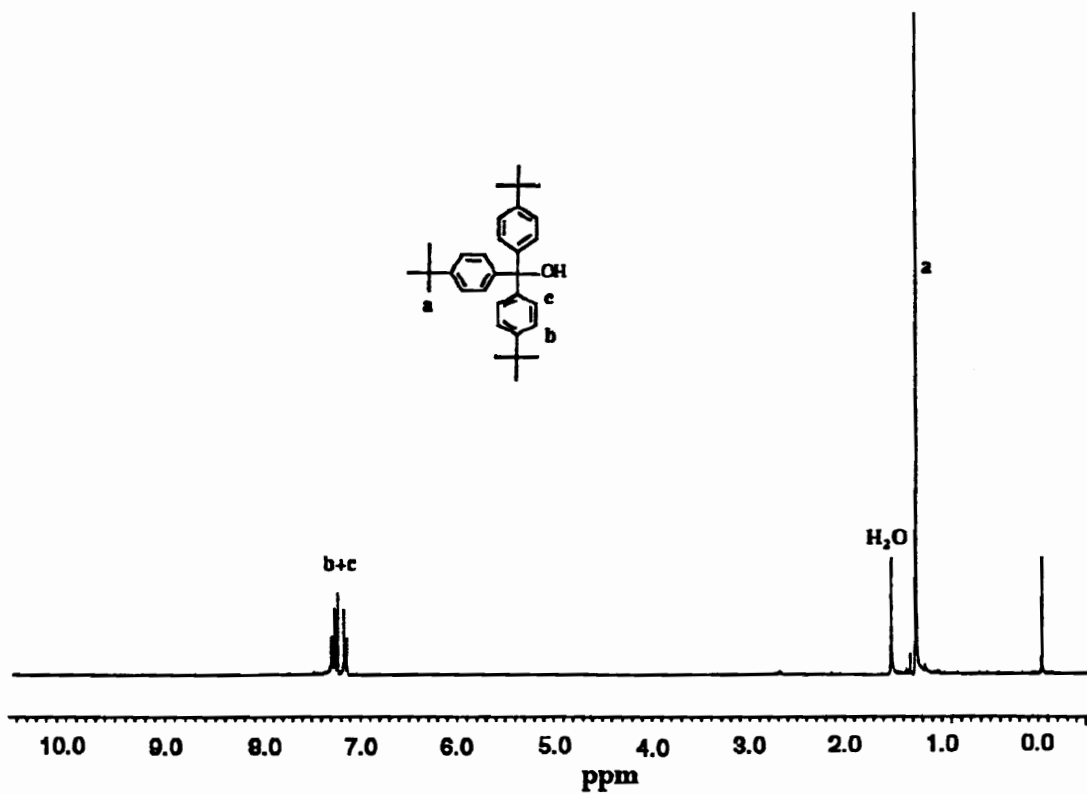


**Figure II-1. 270 MHz <sup>1</sup>H NMR spectrum of tris-p-t-butylphenylmethanol in CDCl<sub>3</sub>.**

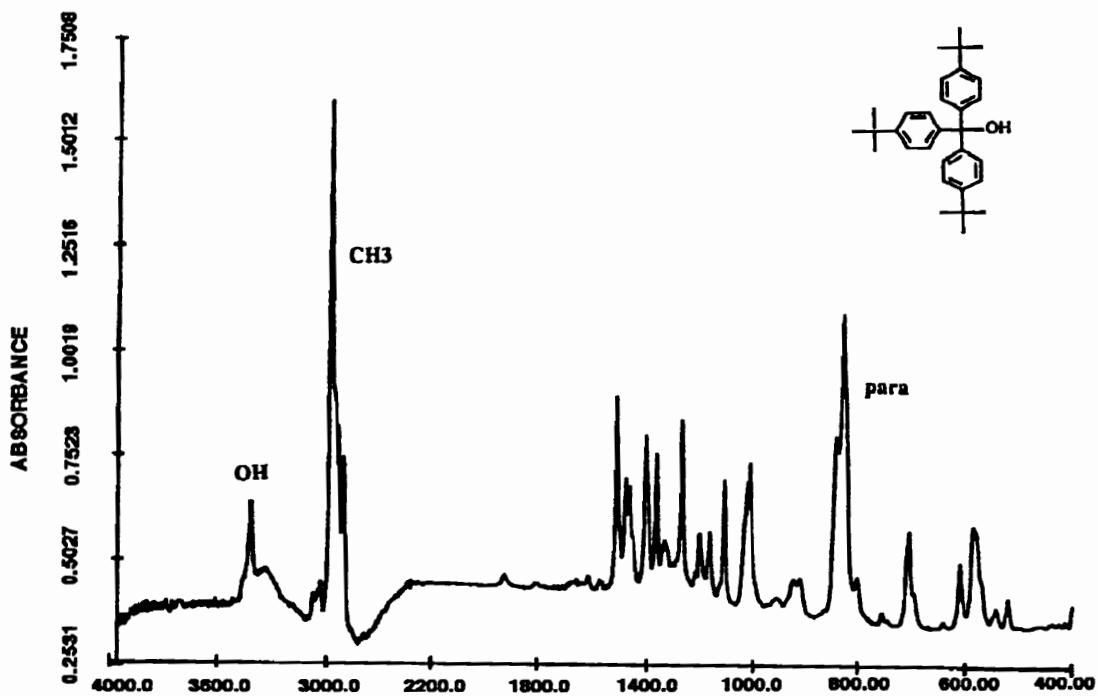
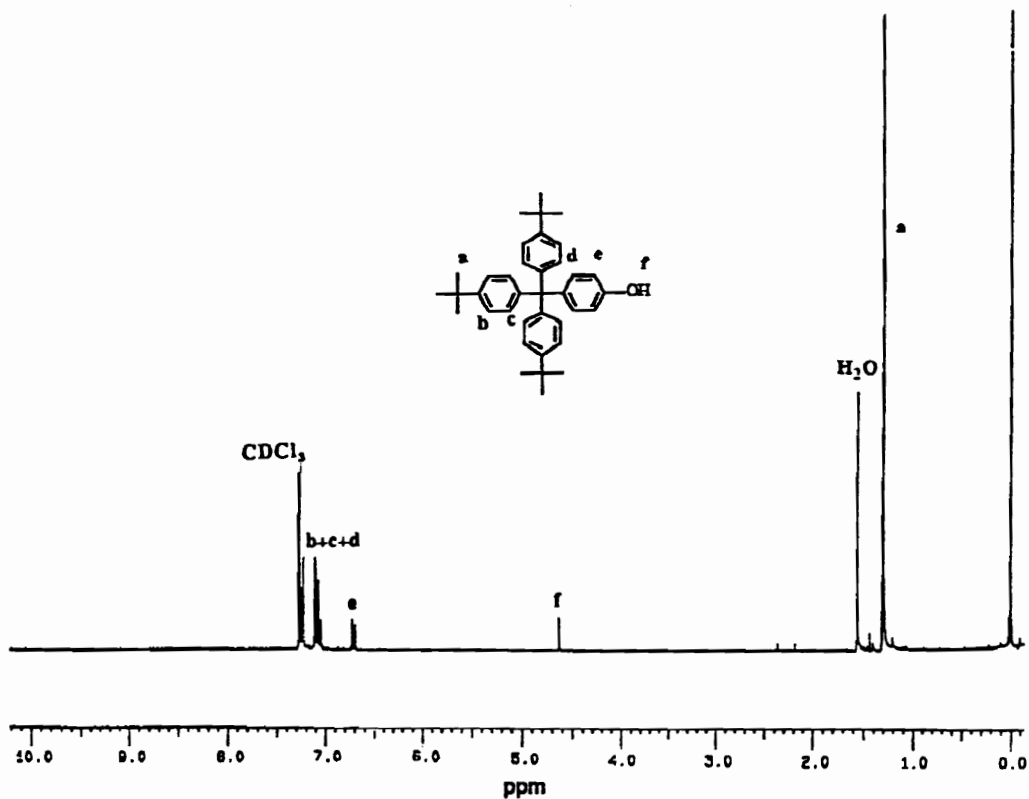


Figure II-2. FTIR spectrum of tris-p-t-butylphenylmethanol in KBr pellet.



**Figure II-3. 270 MHz <sup>1</sup>H NMR spectrum of tri-(p-t-butylphenyl)-4-hydroxyphenylmethane in CDCl<sub>3</sub>.**

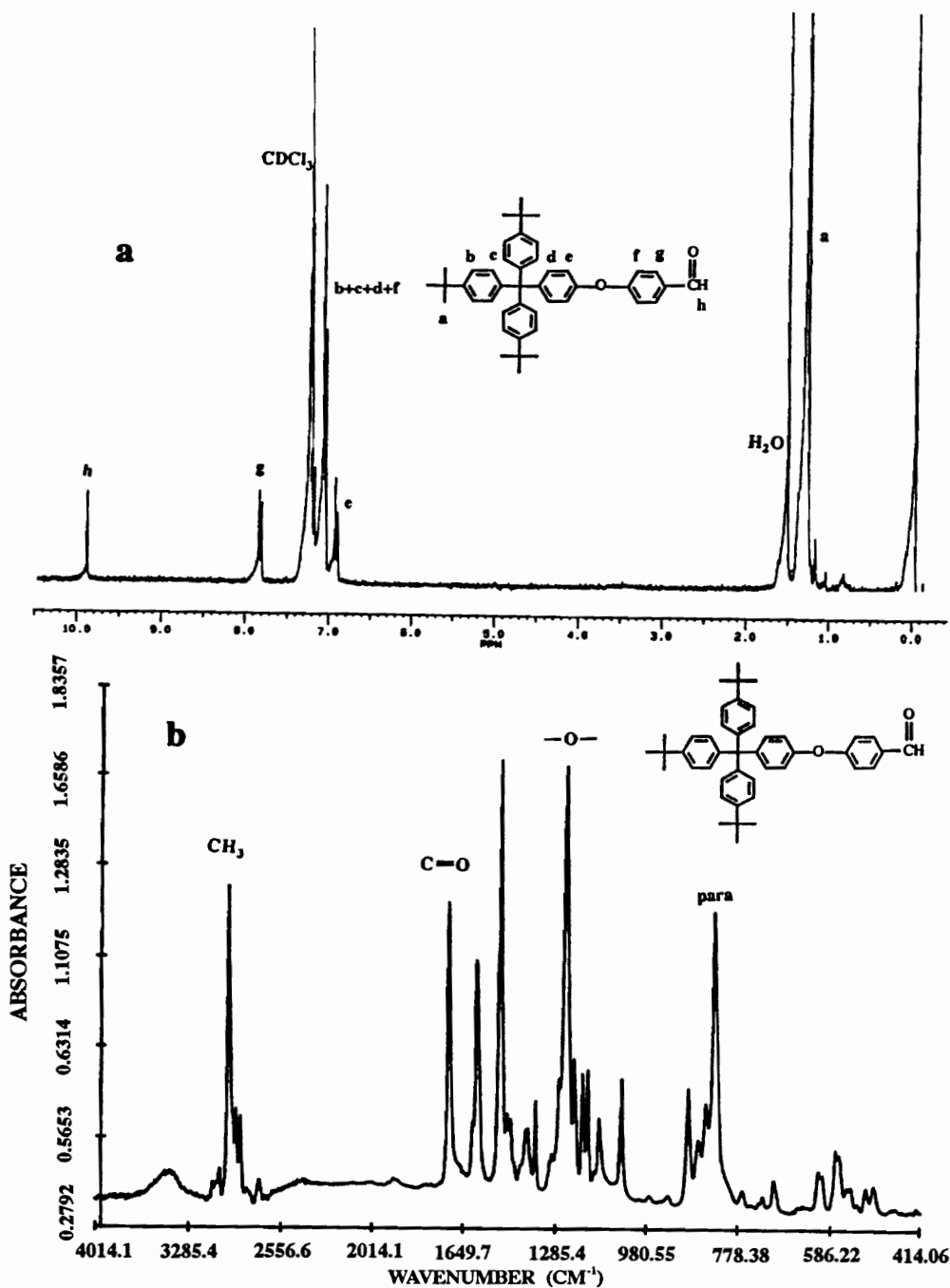


Figure II-4. a) 270 MHz <sup>1</sup>H NMR spectrum of p-[p'-(tris-(p''-t-butylphenyl)methyl)phenoxy]benzaldehyde in CDCl<sub>3</sub>; b) FTIR spectrum of p-[p'-(tris-(p''-t-butylphenyl)methyl)phenoxy]benzaldehyde in KBr pellet.

# CHAPTER III. CROWN ETHER SYNTHESSES AND CHARACTERIZATION

## 1. INTRODUCTION

Ring structures have been found to exist widely in nature, such as cycloantibiotics, cyclodextrins and circular DNA macrocycles. However, they were not well investigated until the rapid development of molecular recognition, that is, the rings can selectively complex with or organize the ligands. The intensive research activities in this area started from late 1960's when Pederson first synthesized crown ethers, dibenzo-18-crown-6, 18-crown-6 and other crown ether macrocycles.<sup>1-4</sup> To bind specific cations, several structural parameters of the crown ethers can be modified. They include size of the cavity, number of ether oxygen atoms, length of aliphatic chains connecting ether oxygens, aromatic groups and incorporation of heteroatoms other than O, such as N and S, into the ring structure.

The ring structures we are interested in are the macrocycles suitable for polyrotaxane syntheses. Since the polyrotaxanes are going to be made by polymerizing the linear chain in the presence of the macrocycles, the following characteristics should be possessed by the selected macrocycles:

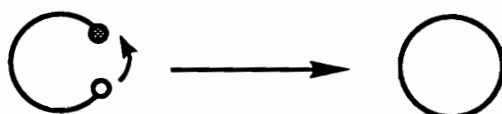
1. More than 22 members to be threaded by a polymethylene backbone.
2. Chemically different from the linear species to maximize the property difference between the two components.
3. No functionality should be present to interfere with the polymerization reaction.
4. Containing donor center capable of coordination with the monomer and/or polymer.
5. Can be easily synthesized in multigram scale.

Considering the above requirements, we chose different sizes of aliphatic crown ethers to be the macrocycles in polyrotaxanes syntheses. Although various aliphatic and

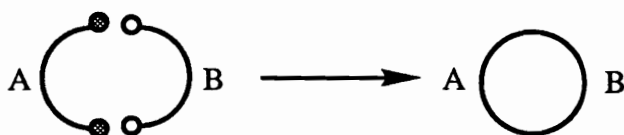
aromatic crown ethers and analogs containing hetero-atoms with less than 27 atoms have been synthesized,<sup>5, 6</sup> there are not many large aliphatic crown ethers (>27) syntheses reported in the literature. For this reason, we developed an efficient method to synthesize different sizes of large aliphatic crown ethers.

The aliphatic crown ethers can be achieved in at least three ways:

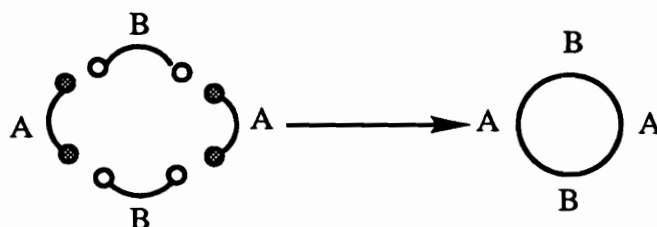
1. Cyclization of one linear chain with two functionalities at the chain ends.



2. Cyclization of two linear chains with totally four functionalities at the chain ends.



3. Cyclization of four linear chains with totally eight functionalities at the chain ends



The first method starts from making a long oligo(ethylene glycol) chain with two functional groups, such as hydroxyl and tosyl chloride. The ring can be formed by reacting the two functional groups (A and B) at the chain ends. The drawback of this method is the necessity to prepare and purify the long oligo(ethylene glycol) chain which is very difficult when the chain contains more than six oxyethylene units. Fractional distillation and other purification methods become more and more difficult as the molecular weight of the chain is increased. The second method requires two linear chains with two functional groups (A or B). The ring closure is carried out by reacting the four functionalities. This method also faces the same drawback of method 1 because

long chain synthesis (even though just half of the chain length is required as in method 1) is still unavoidable. In the third method, four short pieces of linear chains with functionality at each end are connected to give one ring. Obviously, this method does not require long chains and thus avoids the purification difficulties. By reacting hexa(ethylene glycol) with hexa(ethylene glycol) ditosylate, crown ethers up to 72C24 (first number indicates the number of atoms in the ring, "C" stands for crown and the second number indicates the number of oxygen atoms in the ring) can be synthesized.

Since the ring closure reaction always competes with the oligomerization of the short linear species, the yields were low in most cases reported in the literature. For example, in a one-pot reaction (method 1) between oligo(ethylene glycol) and one equivalent of *p*-toluensulfonyl chloride in the presence of base, giving the monotosylate in situ, crown ethers ranging from 12-crown-4 to 60-crown-20 have been obtained.<sup>9</sup> However, the yields of large size crown ethers were low; 12% yield for 30-crown-10 was obtained from penta(ethylene glycol). To improve the yields of the rings, the reactions can be modified to favor the ring closure. High dilution conditions and the template method are the two well known and most effective methods among these modifications.<sup>10, 11</sup> Other modifications including the rigid group principle<sup>12</sup> (in which the rotation is restricted by the rigid groups), the cesium effect,<sup>13</sup> and the gauche effect have also been reported.

Another way to synthesize large crown ether **155** with (x+y) ethyleneoxy units is by the condensation reaction of one mole of oligo(ethylene glycol) **153** having x units with one equivalent of oligo(ethylene glycol) ditosylate **154** having y units in the presence of a base (method 2)<sup>14</sup> (Scheme 1). Obviously, large macrocycle **156** can also be formed by reacting two oligo(ethylene glycol) units with two oligo(ethylene glycol) ditosylate units at the same time.

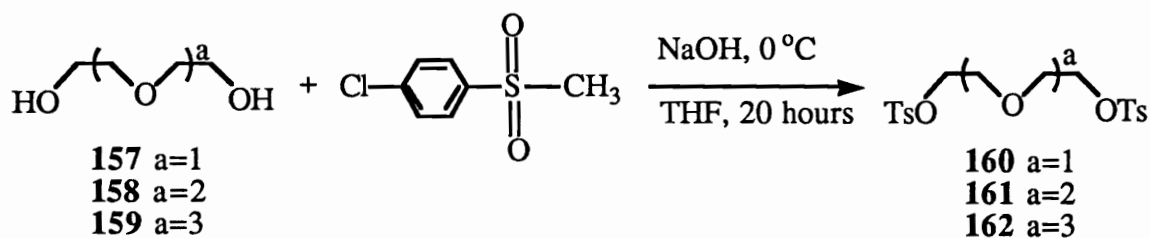


## 2. RESULTS & DISCUSSION

### 2.1 Linear precursor synthesis

To circumvent the difficulties in the synthesis of long linear glycols, we chose method 3 as our approach to make large size crown ethers. The large size crown ether **156** was generated by connecting two linear glycols with two ditosylate units, instead of one glycol unit reacting with one ditosylate unit as in method 2. Besides the commercially available triethylene glycol and tetraethylene glycol, the linear precursors we used in large size crown ethers (36C12, 42C14, 60C20) syntheses, including di(ethylene glycol) ditosylate, tri(ethylene glycol) ditosylate, tetra(ethylene glycol) ditosylate and hexa(ethylene glycol), can all be obtained from cheap starting materials.

Di(ethylene glycol) ditosylate (**160**), tri(ethylene glycol) ditosylate (**161**), tetra(ethylene glycol) ditosylate (**162**), were synthesized by reacting di(ethylene glycol) (**157**), tri(ethylene glycol) (**158**), tetra(ethylene glycol) (**159**), respectively, with p-toluenesulfonyl chloride, in the presence of sodium hydroxide in THF at 0 °C for 20 hours.



This is a modified procedure which was reported by Ouchi et al.<sup>15</sup> The products were purified by recrystallizations in acetone after workup, except tetra(ethylene glycol) ditosylate which was a viscous oil after the crude product was washed with hot hexane to remove the unreacted p-toluenesulfonyl chloride. The yields of these reactions were all above 90%. The purified di(ethylene glycol) ditosylate and tri(ethylene glycol) ditosylate were characterized by <sup>1</sup>H NMR (Fig. III-1a, Fig. III-1b)

Hexa(ethylene glycol) was synthesized via Bartsch's procedure using a phase transfer catalyst.<sup>16</sup> The reaction was done by stirring 50% aqueous sodium hydroxide solution with a solution of tetra(ethylene glycol) in Cl-CH<sub>2</sub>CH<sub>2</sub>O-THP (THP=tetrahydropyanyl) in the presence of tetrabutylammonium hydrogen sulfate at 65 °C for 3 days. The yield of this reaction was as high as 92%.

## 2.2 Crown ether synthesis and purification

Large size crown ethers (36C12, 42C14, 60C20) were synthesized via method 3 in a one-pot reaction. Generally, the reactions were carried out at modest dilution (ca 0.1M) using NaH as a base in THF. Obviously, in addition to the large size crown ethers, small size crown ethers with half the size of the intended large size crown ethers can also be generated by "two-piece combination" of the corresponding glycol and ditosylate units. The yields of the small size crown ethers sometimes may be higher than the yields of large size crown ethers, especially in the 36C12 case.<sup>17</sup>

To optimize the reaction condition, 36C12 was synthesized from different starting materials: di(ethylene glycol) ditosylate reacted with tetra(ethylene glycol), and tri(ethylene glycol) reacted with tri(ethylene glycol) ditosylate. The reactions were carried out in THF and dioxane under reflux conditions (THF, bp 67 °C; dioxane, bp 101 °C respectively). The results are shown in Table 1.

**Table III-1. Results of 36C12 syntheses by multiple condensation (Scheme III-1).**

Solvent	x	y	36-crown-12		18-crown-6
			Yield	Melting Point	Yield
THF	2	2	10.6%	54.5-56.5 °C	—
Dioxane	2	2	13.1%	54.5-56.0 °C	43.6%
THF	3	1	8.9%	55.0-57.0 °C	46.9%
Dioxane	3	1	6.5%	54.0-56.0 °C	32.2%

The results of the 36C12 syntheses indicated that linear glycol and ditosylate with similar lengths gave higher yields. Moreover, the yields of cyclic products in these

reactions were higher than 50% due to the dilution condition and template effect. The purification of crown ethers is potentially difficult because the byproducts of the reaction are diol and ditosylate oligomers. The products can not be vacuum distilled because of high boiling points and decomposition of crown ethers at high temperatures. Column chromatography using silica gel is also not practical on such large scale syntheses. However, we found 36C12 could be isolated from the solution by multiple recrystallizations in acetone at low temperatures. The linear impurities are soluble in acetone even at low temperature. Therefore, the 36C12 was isolated by recrystallization in acetone at 0 °C to -20 °C. Since 18C6 does not recrystallize from the acetone solution, it was isolated and purified by extraction of the crude product with hot hexane which dissolves 18C6.

The obtained 36C12 and 18C6 were characterized by <sup>1</sup>H NMR (Fig. III-2a, Fig. III-2b) which gave single peaks at 3.644 ppm and 3.689 ppm, respectively. The <sup>13</sup>C NMR of 36C12 (Fig. III-3) also showed only one peak at 70.698 ppm. 36C12 was characterized by thermogravimetric analysis (Fig. III-4) with 5% weight loss at 214 °C in air and 374 °C in nitrogen.

Another large size crown ether, 42C14, was synthesized under similar conditions. The reactions were carried out by reacting tetra(ethylene glycol) with tri(ethylene glycol) ditosylate in THF and glyme (THF, bp 67 °C; glyme, bp 85 °C respectively) under reflux conditions. The results are shown in Table 2.

**Table III-2. Results of 42C14 syntheses by multiple condensations (Scheme III-1)**

Solvent	42-crown-14	
	Yield	Melting Point
THF	33%	55.5-57.8 °C
Glyme	52%	55.1-56.2 °C

The results clearly show that 42C14 can be synthesized in much higher yields than that of the 36C12 which might result from the templet effect of the Na<sup>+</sup> which favors the

ring closure of the 42C14. The 42C14 was also purified by multiple recrystallizations in acetone at a low temperature. The purified 42C14 was characterized by  $^1\text{H}$  NMR (Fig. III-5) which gave a single peak at 3.65 ppm. The IR spectrum of 42C14 showed the strong C-O-C stretch. (Fig. III-6) 42C14 was characterized by thermogravimetric analysis which showed 5% weight loss at 369 °C in nitrogen. (Fig. III-7)

Because of its large ring cavity, the 42C14 was chosen to be the macrocycle in the poly(1,4-phenylenevinylene) rotaxane construction. Moreover, its flexibility can help to reduce the rigidity of the linear PPV once the polyrotaxane is formed. The possibility of threading was supported by CPK modeling.

Under similar reaction conditions, 60C20 was synthesized by reacting hexa(ethylene glycol) with tetra(ethylene glycol) ditosylate in dioxane under reflux. This crown ether was purified by multiple recrystallizations in acetone after passing through a short silica gel column. Further purification was carried out by reacting the 60C20 with poly(methacryloyl chloride) which can react with the important byproducts, oligo-diols. The small amount of linear diols was removed by precipitating the reaction solution into methanol. The yield of the reaction was 20%. The purified product was characterized by  $^1\text{H}$  NMR which gave one peak at 3.645 ppm. (Fig. III-8) The thermogravimetric analysis showed the 5% weight loss at 376 °C in nitrogen (Fig. III-9) and 5% weight loss at 205°C in air (Fig.III-10).

This crown ether was also used in the poly(1,4-phenylenevinylene) rotaxane synthesis and it was expected to give a higher threading efficiency than that of 42C14 because of its larger cavity. Therefore, a more obvious processibility improvement in the PPV rotaxane was expected.

### 3. EXPERIMENTAL

#### 1. Synthesis of di(ethylene glycol) ditosylate (160)

NaOH (100g, 2.5 mol) was dissolved in deionized water (200 mL) and charged into a 5 L 3 neck flask equipped with mechanical stirrer and thermometer. Di(ethylene glycol) (106.12 g, 1 mol) was transferred into the flask with THF (400 mL). The flask was kept in an acetone ice bath (acetone+ice+dry ice) to keep the solution temperature below 0 °C. Tosyl chloride (400.26 g, 2.1 mol) was dissolved in THF (600 mL) and added dropwise into the flask from an addition funnel. The solution was stirred for 30 hours at 0 °C. The crystals in the reaction solution were filtered. Most of the solvent (mixture of THF and water) in the filtrate was removed by rotary evaporation. The rest of the filtrate was mixed with the crystals obtained and extracted with dichloromethane. The crude product was obtained after the dichloromethane was removed. Recrystallizations of the crude product in acetone afforded di(ethylene glycol) ditosylate (391.2 g, 94.5%): mp 89-89.5 °C; reported mp 88-89 °C;<sup>15</sup> <sup>1</sup>H NMR:  $\delta$  2.45 (s, 6H, CH<sub>3</sub>), 3.60 (t, J=4.6, 4H, OCH<sub>2</sub>), 4.09 (t, J=4.6, 4H, CH<sub>2</sub>OTs), 7.33 (d, J=8.3, 4H, arom), 7.79 (d, J=8.3, 4H, arom).

#### 2. Synthesis of tri(ethylene glycol) ditosylate (161)

NaOH (168 g, 4.20 mol) was dissolved in deionized water (400 mL) and charged into a 5 L 3 neck flask equipped with mechanical stirrer and thermometer. Tri(ethylene glycol) (225 g, 1.50 mol) was transferred into the flask with THF (500 mL). The flask was kept in an acetone ice bath (acetone+ice+dry ice) to keep the solution temperature below 0 °C. Tosyl chloride (644 g, 3.38 mol) was dissolved in THF (1500 mL) and added dropwise into the flask from an addition funnel. The solution was stirred for 25 hours at 0 °C. The solvent (mixture of THF and water) was removed by rotary evaporation. The solid obtained was dissolved in dichloromethane and washed with water (3x1000 mL). The aqueous solution was extracted with dichloromethane (3x300

mL). The organic solutions were combined and dichloromethane was removed to give a crude product. Recrystallizations of the crude product in acetone afforded tri(ethylene glycol) ditosylate, 604 g (88%): mp 83.5-84.2 °C; reported mp 80.5-81.5 °C;<sup>15</sup> <sup>1</sup>H NMR  $\delta$  2.45 (s, 6H, CH<sub>3</sub>), 3.53 (s, 4H, CH<sub>2</sub>O), 3.65 (t, J=4.7, 4H, OCH<sub>2</sub>), 4.14 (t, J=4.7, 4H, CH<sub>2</sub>OTs), 7.35 (d, J=8.1, 4H, arom), 7.77 (d, J=8.1, 4H, arom)

### 3. Synthesis of 36-crown-12 (156, x+y=6)

NaH (4.8g, 0.12 mol) was washed with hexane (3x40 mL) and transferred into a 1 L 3 neck flask with dry dioxane (10 mL) under nitrogen. Tri(ethylene glycol) (4.51 g, 30 mmol) in dioxane (15 mL) was charged into the flask and the mixture was mechanically stirred for 3 hours. Tri(ethylene glycol) ditosylate (6.87g, 15 mmol) in dioxane (20 mL) was added into the flask quickly (20 mins). The solution was stirred for 8 hours at reflux. The system was then diluted to 400 mL and the rest of the tetra(ethylene glycol) ditosylate (6.87g, 15 mmol) in dioxane (120 mL) was added. The addition took 2 hours. The mixed system was stirred for another 36 hours at reflux. Water (10 mL) was added to destroy the unreacted NaH. The precipitate was filtered and washed with dioxane. The dioxane was removed to afford the crude product, a greenish yellow oil, which was dried under vacuum at room temperature for 24 hours. Recrystallizations of the crude product in acetone at -20°C gave 1.04 g 36C12 (13.1%): mp 54.5-56.0 °C; reported mp 36.5-38.0 °C, <sup>9</sup> <sup>1</sup>H NMR  $\delta$  3.647 (s). Extracting the crude product with hot hexane after recrystallization gave 3.46 g (43.6%) oily 18-crown-6 (155, x+y=6). <sup>1</sup>H NMR  $\delta$  3.689 (s)

### 4. Synthesis of 42-crown-14 (156, x+y=7)

NaH (40 g, 1 mol) was washed with hexane (3x200 mL) and transferred into a 5 L 3 neck flask with THF (50 mL) under nitrogen. Tetra(ethylene glycol) (48.56g, 250 mmol) in THF (60 mL) was charged into the flask and the mixture was mechanically stirred for 3 hours. Tri(ethylene glycol) ditosylate (57.25 g, 125 mmol) in THF (300 mL) was

added into the flask quickly (45 mins). The solution was stirred for 5 hours at reflux. The system was then diluted to 3.5 L and the rest of the tetra(ethylene glycol) ditosylate (57.25 g, 125 mmol) in THF (500 mL) was added. The addition took 2 hours. The mixed system was stirred for another 36 hours at reflux. Water (10 mL) was added to destroy the unreacted NaH. The precipitate was filtered and washed with THF. The THF was removed to give the crude product which was dried under vacuum at room temperature for 24 hours. Recrystallizations of the crude product in acetone at -20°C afforded 25.4 g of 42C14 (33%): mp 55.1-56.2°C; reported mp 28.5-31.0 °C, <sup>14</sup> <sup>1</sup>H NMR δ 3.64 (s); IR 2930 (aliph), 1485, 1290, 1120 (C-O-C), 854. A small scale reaction was also carried out with the same procedure. The yield (52%) was higher than that of the large scale.

#### **5. Synthesis of 60-crown-20 (156, x+y=10)**

NaH (12.59 g, 0.319 mole) was washed with hexane (3x20 mL) and transferred into a 1L 3 neck flask equipped with mechanical stirrer and condenser. Hexa(ethylene glycol) (16.94 g, 60 mmole) in dry dioxane (40 mL) was added dropwise into the flask. The solution was kept stirring at room temperature for 2 hours. Tetra(ethylene glycol) ditosylate (15.08 g, 0.0300 mole) in dioxane (40 mL) was added into the flask over a period of 2 hours at reflux temperature. After 6 hours of refluxing, the reaction solution was diluted to 900 mL. The rest of the tetra(ethylene glycol) ditosylate (15.08 g, 30 mmole) in dioxane (40 mL) was added into the flask over a period of 5 hours. The solution was stirred under reflux for 40 hours. The precipitate of the solution was filtered through the Celite. The yellow filtrate was decolorized four times with active charcoal. The white solid obtained after removing the solvent by rotary evaporation was washed with HPLC acetone twice and it was recrystallized from acetone. Further reaction with poly(methacryloyl chloride) gave 5.2 g of white powder (20%) <sup>17</sup>: mp 58.3-60.5 °C; reported mp 46.0-50.5 °C, <sup>14</sup> <sup>1</sup>H NMR δ 3.646(s).

## 6. Synthesis of poly(methacryloyl chloride)

Distilled methacryloyl chloride (72.13g, 690 mmol) and azobis(isobutyronitrile) (AIBN) (1.133 g, 6.9 mmol) were dissolved in dried ( $\text{CaSO}_4$ ) toluene and charged into a 250 mL 1 neck flask equipped with a condenser, nitrogen inlet and magnetic stirring bar. The solution was stirred at 90 °C under nitrogen for 22 hours. After the solution was cooled to room temperature, it was concentrated and precipitated into dried (4 Å molecular sieves) n-hexane (1.6 L). The polymer was filtered and vacuum dried. The light yellow powder weighed 31 g (43%).

## REFERENCES

1. C. J. Pedersen, *J. Am. Chem. Soc.*, **1967**, *89*, 2495
2. C. J. Pedersen, *J. Am. Chem. Soc.*, **1967**, *89*, 7017
3. C. J. Pedersen, *J. Am. Chem. Soc.*, **1970**, *92*, 391
4. C. J. Pedersen, *J. Org. Synth.*, **1972**, *52*, 66
5. S. Patai, Z. Rappoport, Eds., "*Crown Ethers and Analogues*", John Wiley & Sons, New York, NY, **1989**
6. U. Inoue, G. W. Gokel, Eds., "*Cation Binding by Macrocycles*", John Wiley & Sons, New York, NY, **1990**
7. B. Dietrich, P. Viout, J.-M. Lehn, "*Macrocyclic Chemistry*", VCH, NY, **1993**
8. C. Wu, M. Bheda, C. Lim, Y. X. Shen, J. Sze, H. W. Gibson, *Polym. Commun.*, **1991**, *32*, 204; H. W. Gibson, M. Bheda, P. T. Engen, Y. X. Shen, J. Sze, C. Wu, S. Joardar, T. C. Ward, P. R. Lecavalier, *Makromol. Chem. Macromol. Symp.*, **1991**, *42/43*, 395; Y. X. Shen, H. W. Gibson, *Macromolecules*, **1992**, *25*, 2058; Y. X. Shen, P. T. Engen, M. A. G. Berg, J. S. Merola, H. W. Gibson, *Macromolecules*, **1992**, *25*, 2786; H. W. Gibson, H. Marand, *Adv. Mater.*, **1993**, *5*, 11
9. C. A. Vitali, B. Masci, *Tetrahedron*, **1989**, *45*, 2201
10. D. Knops, N. Sendhoff, H. B. Meikelburger, F. Vogtle, *Topics Curr. Chem.*, **1992**, *161*, 3
11. D. A. Laidler, J. F. Stoddart, "*Synthesis of Crown Ethers and Analogues*" in The chemistry of functional group, Suppl. E., Part 1, S. Patai, Ed., Wiley, **1980**
12. W. Baker, J. F. W. Mac-Omie, W. D. J. Ollis, *J. Chem. Soc.*, **1951**, 200
13. A. Ostrowicki, E. Koeppe, F. Vogtle, *Topics Curr. Chem.*, **1992**, *161*, 39
14. R. Chenevent, L. D'Astous, *J. Heterocyclic Chem.*, **1986**, *23*, 1785
15. M. Ouchi, Y. Inoue, T. Kanzaki, T. Hakushi, *J. Org. Chem.*, **1984**, *49*, 1408
16. R. A. Bartsch, C. V. Cason, B. P. Czech, *J. Org. Chem.*, **1989**, *54*, 857
17. H. W. Gibson, M. C. Bheda, P. Engen, Y. X. Shen, J. Sze, H. Zhang, M. D. Gibson, Y. Delaviz, S. H. Lee, S. Liu, L. Wang, D. Nagvekar, J. Rancourt and L. Taylor, *J. Org. Chem.*, **1994**, *59*, 2186

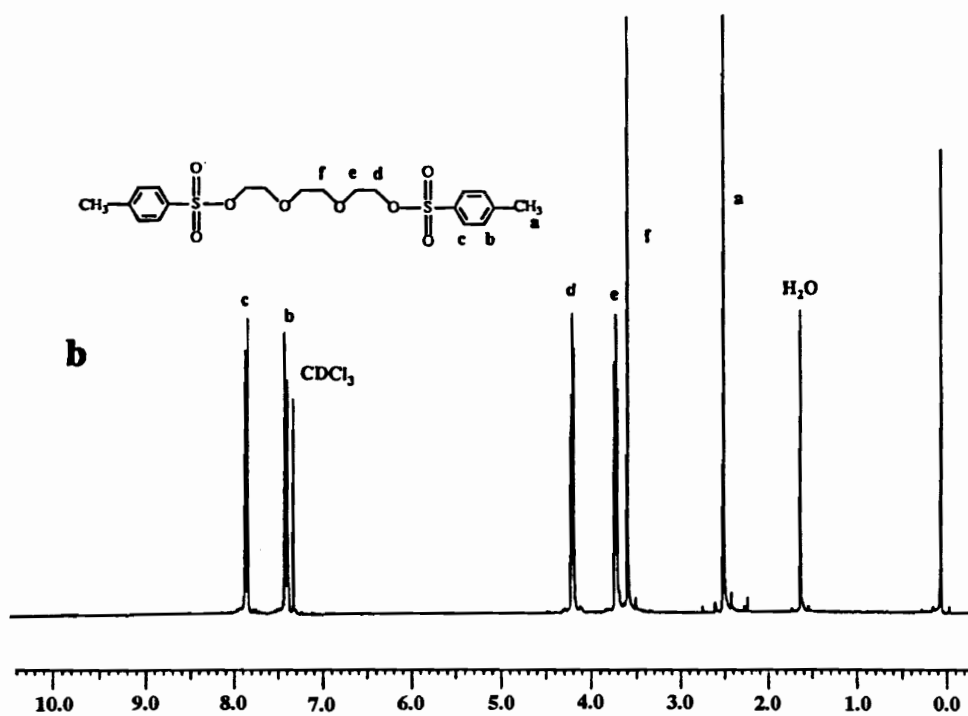
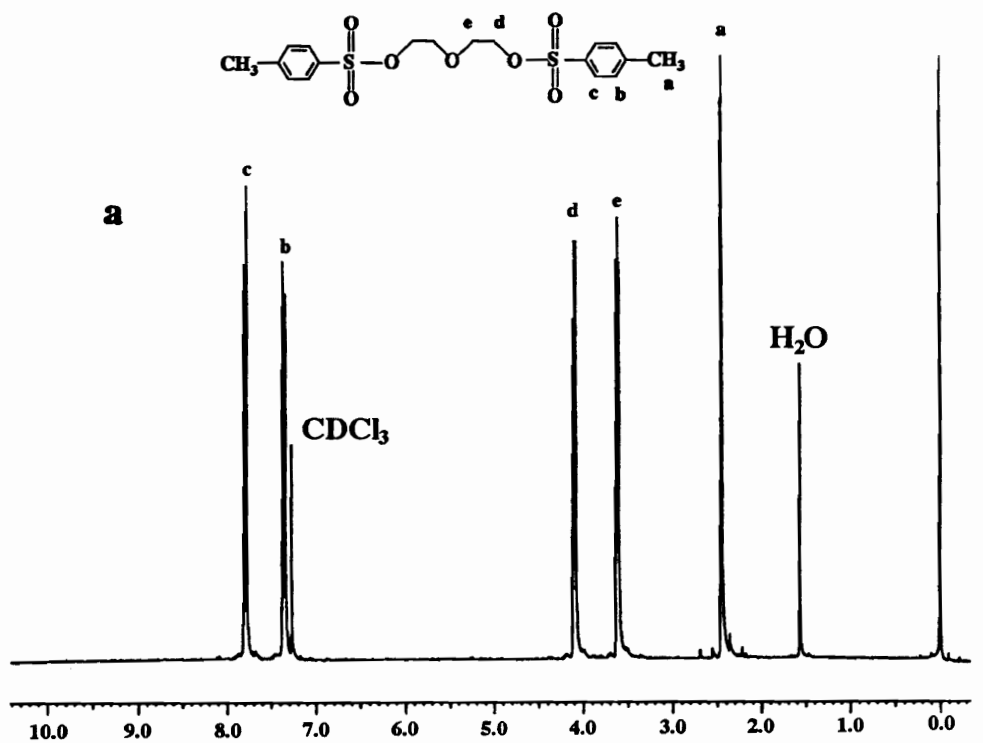


**Figure III-1. 270MHz  $^1\text{H NMR}$  spectra of a) di(ethylene glycol) ditosylate; b) tri(ethylene glycol) ditosylate in  $\text{CDCl}_3$ .**

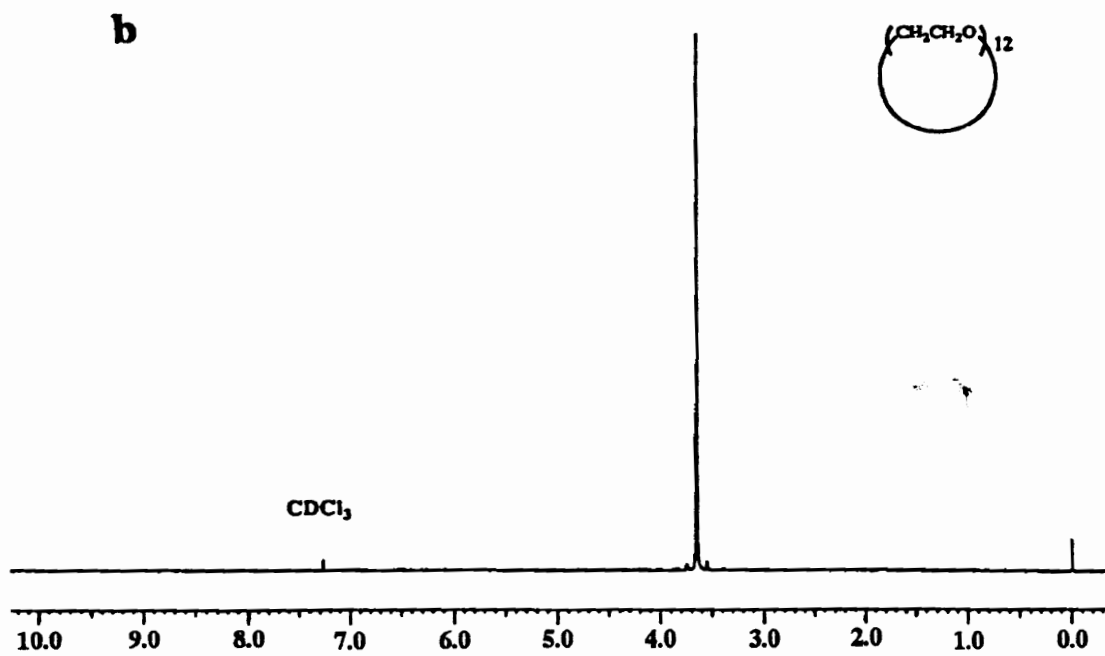
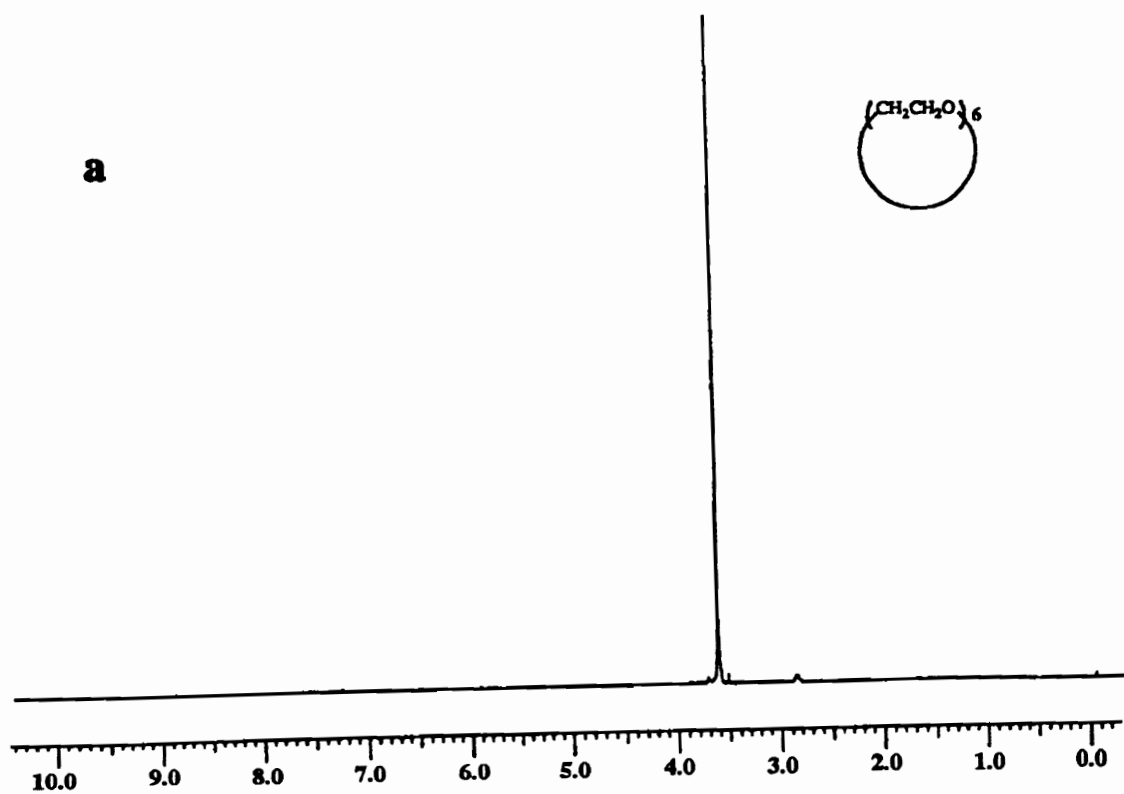


Figure III-2. 270 MHz  $^1\text{H}$  NMR spectra of a) 36-crown-12; b) 18-crown-6 in  $\text{CDCl}_3$ .

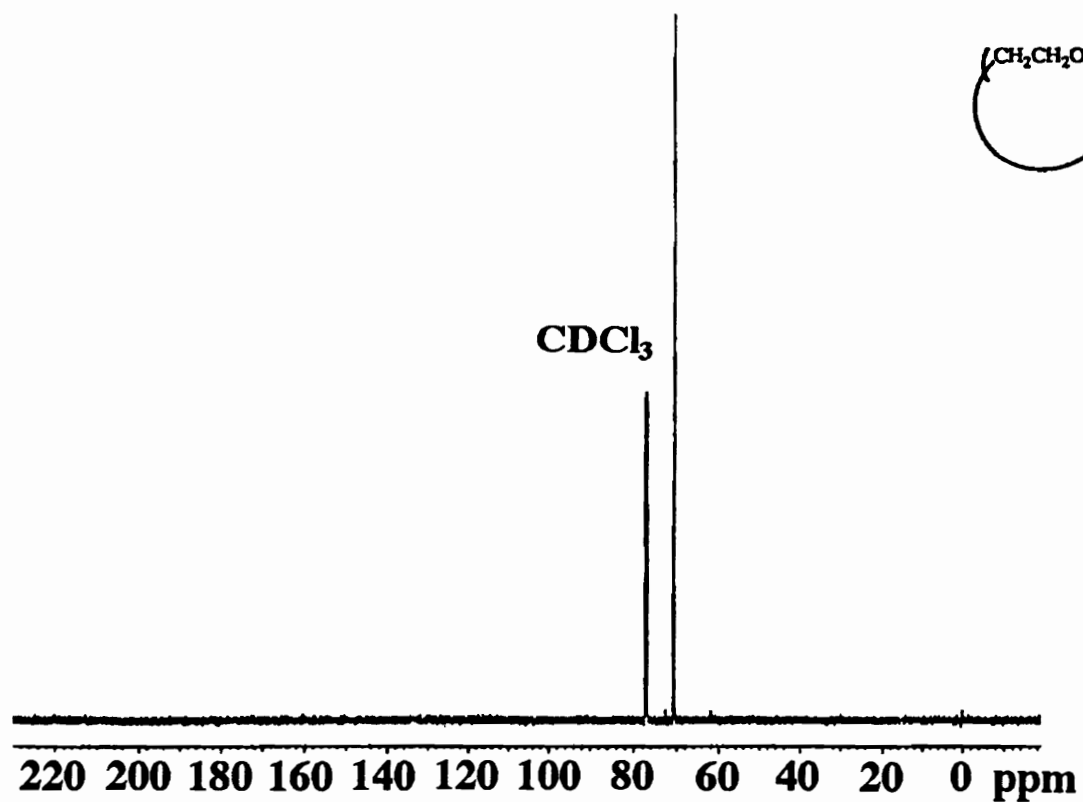


Figure III-3.  $^{13}\text{C}$  NMR spectrum of 36-crown-12 in  $\text{CDCl}_3$ .

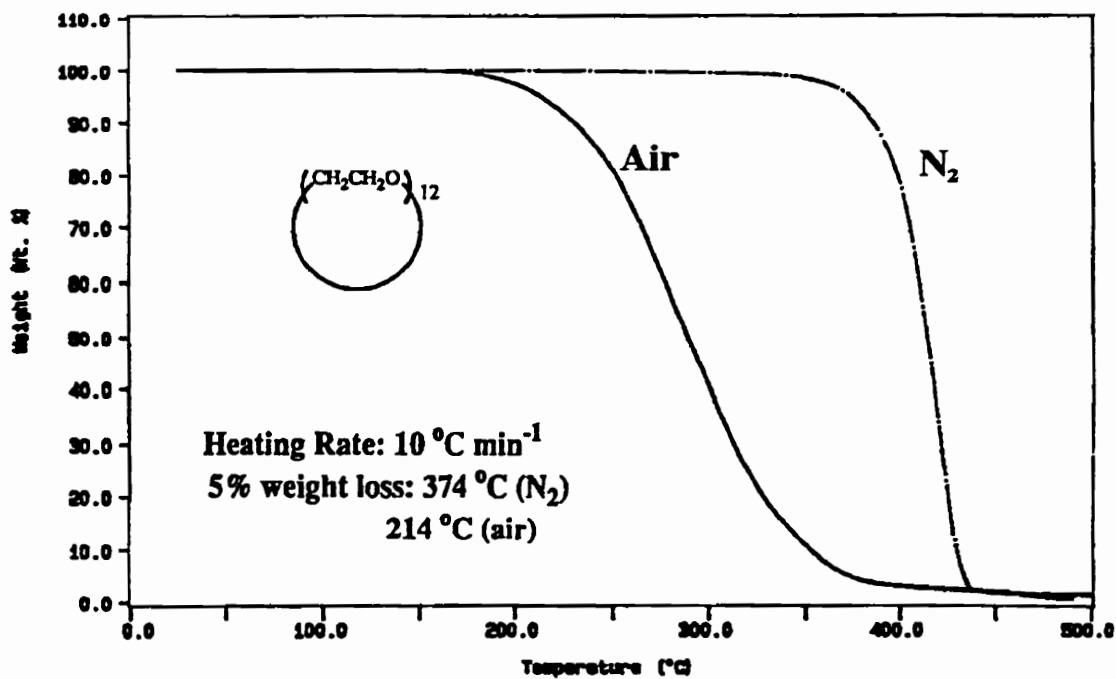


Figure III-4. Thermogravimetric analysis of 36-crown-12 in nitrogen and air.

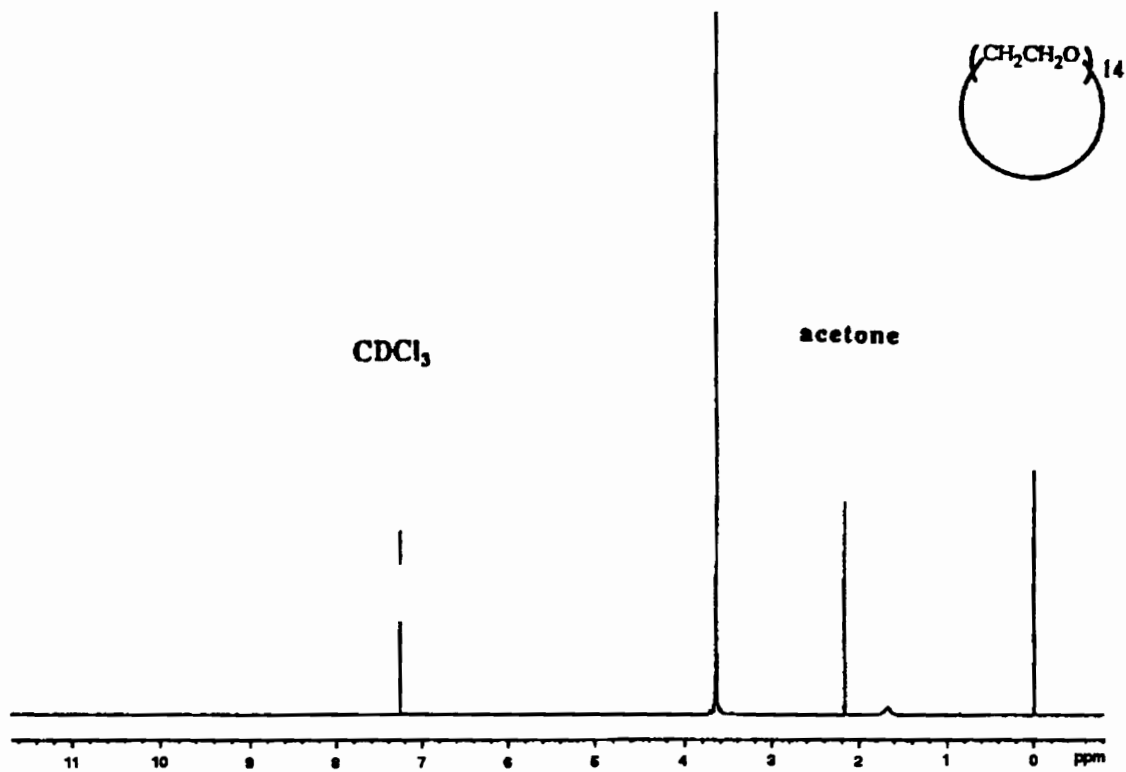


Figure III-5. 270 MHz  ${}^1\text{H}$  NMR spectrum of 42-crown-14 in  $\text{CDCl}_3$ .

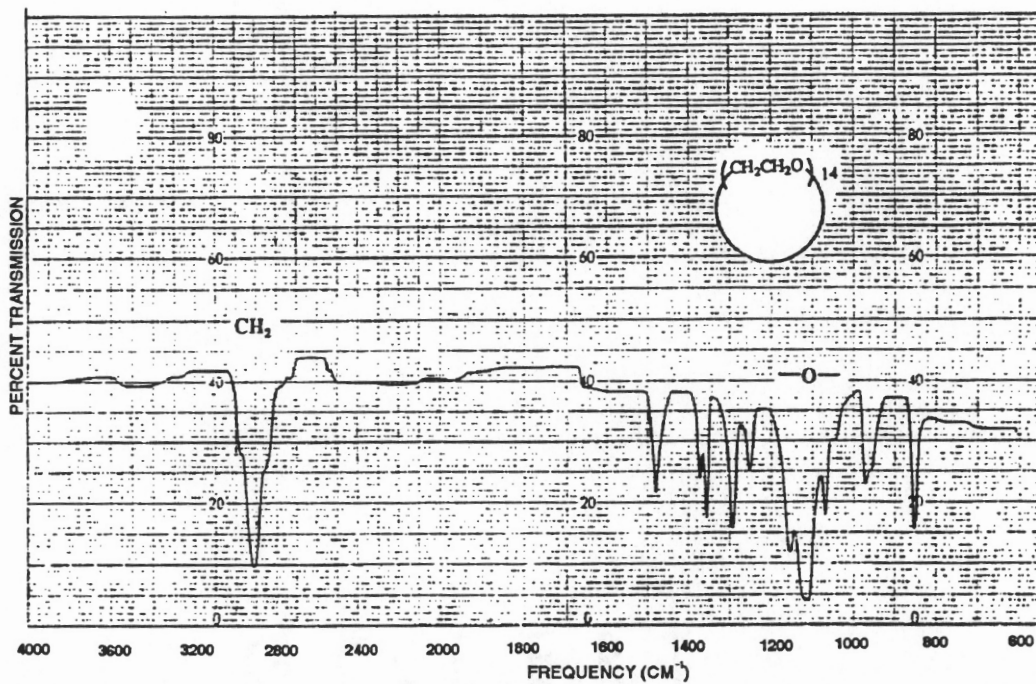


Figure III-6. IR spectrum of 42-crown-14 in KBr pellet.

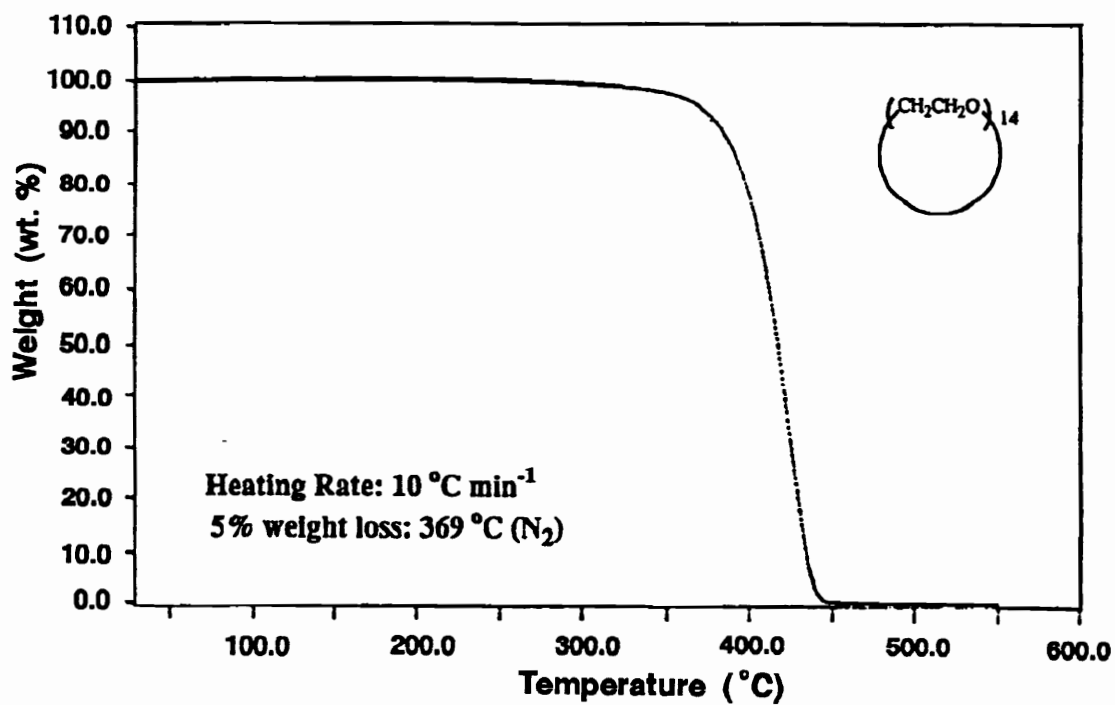


Figure III-7. Thermogravimetric analysis of 42-crown-14 in nitrogen.

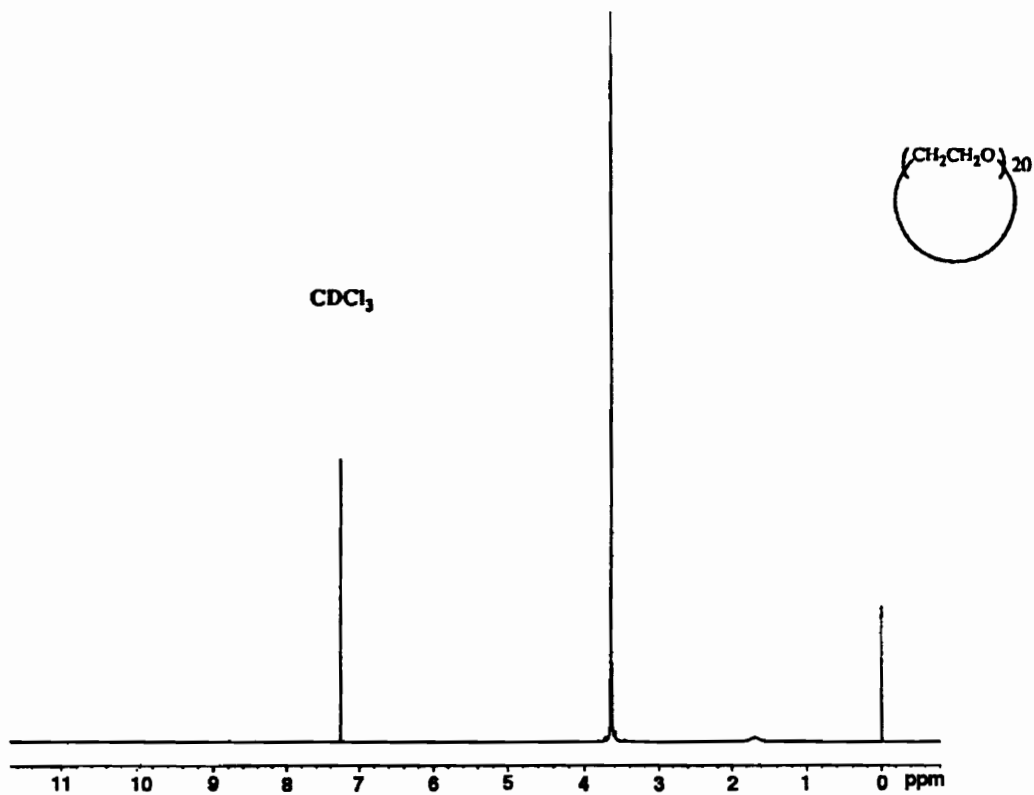


Figure III-8. 270 MHz  $^1\text{H}$  NMR spectrum of 60-crown-20 in  $\text{CDCl}_3$ .

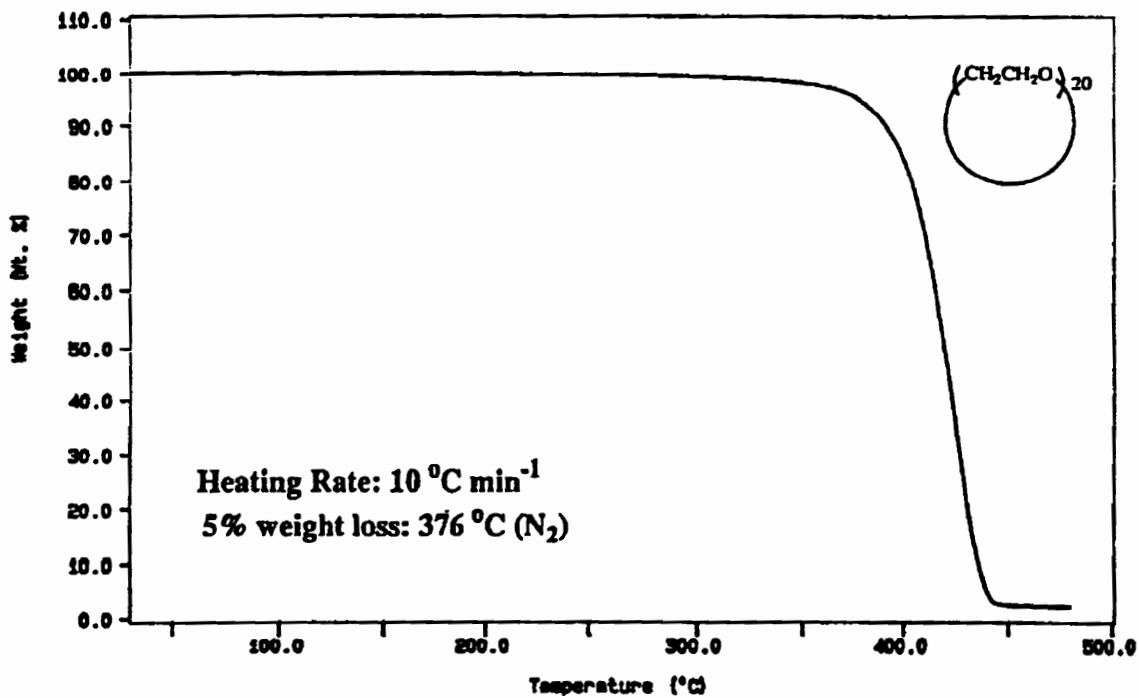


Figure III-9. Thermogravimetric analysis of 60-crown-20 in nitrogen.

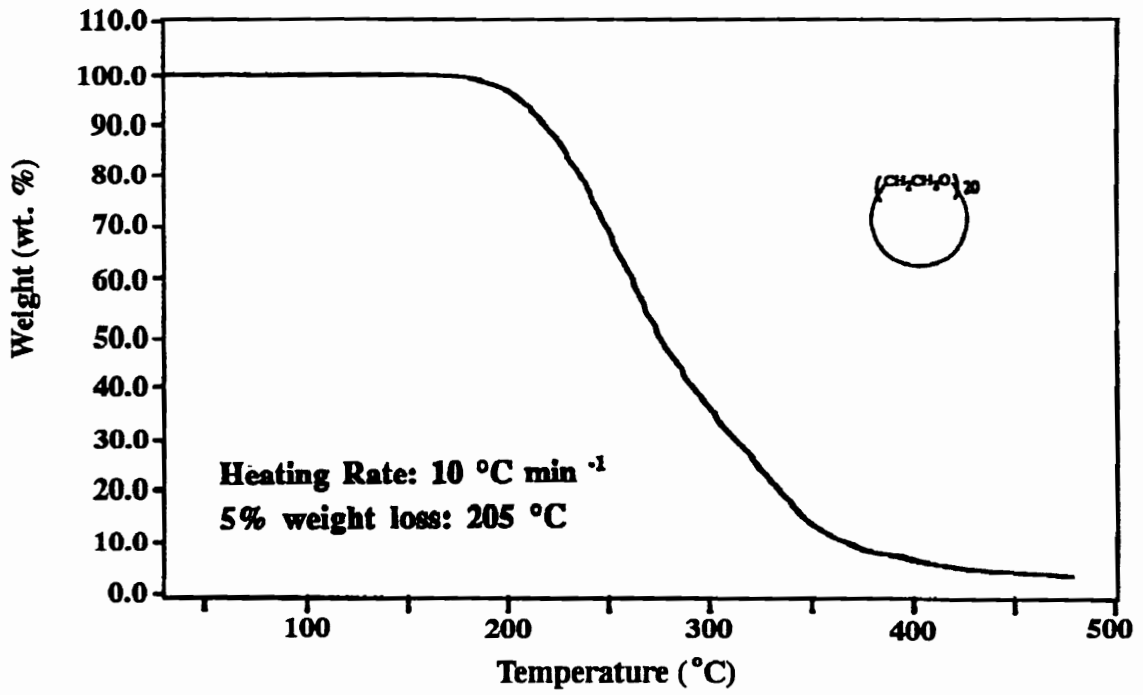


Figure III-10. Thermogravimetric analysis of 60-crown-20 in air.

# CHAPTER IV. SYNTHESSES AND CHARACTERIZATION OF POLY(1, 4-PHENYLENEVINYLENE) AND POLY- (1, 4-PHENYLENEVINYLENE) CROWN ETHER ROTAXANES

## 1. INTRODUCTION

Poly(1,4-phenylenevinylene) (PPV) **124** is one of the most attractive conducting polymers. Its high conductivity upon doping and luminescence characteristics due to  $\pi$ - $\pi$  conjugation make it a very promising material which may be applied in making conductors and large-area light-emitting diodes.

To improve the poor processibility of the PPV, PPV-rotaxa-42C14 **167** and PPV-rotaxa-60C20 **168** were synthesized. The flexible macrocycles were expected to improve the solubility of the PPV backbone. In order to compare the different properties between the PPV and PPV rotaxanes, the PPV **124** was synthesized via reported procedure. The obtained PPV was characterized by IR, UV-vis, photoluminescence spectroscopy, and TGA. The molecular weight of this polymer was measured by low angle laser light scattering. The polyrotaxanes were synthesized by polymerizing the PPV in the presence of the crown ethers (42-crown-14, 60-crown-20). To confirm that the crown ether will not interfere with the polymerization reaction, the polymerization was first carried out in the presence of 18-crown-6, whose cavity is too small to be threaded. The results showed that 18-crown-6 was not incorporated into the PPV backbone which indicated that the crown ethers do not interfere with the polymerization. The polyrotaxanes were isolated by dialysis and solid-liquid extraction. The polyrotaxanes were characterized by TGA, photoluminescence spectroscopy and solid state  $^{13}\text{C}$  NMR. The conductivity of the polyrotaxanes were also measured via four probe method.<sup>1</sup>

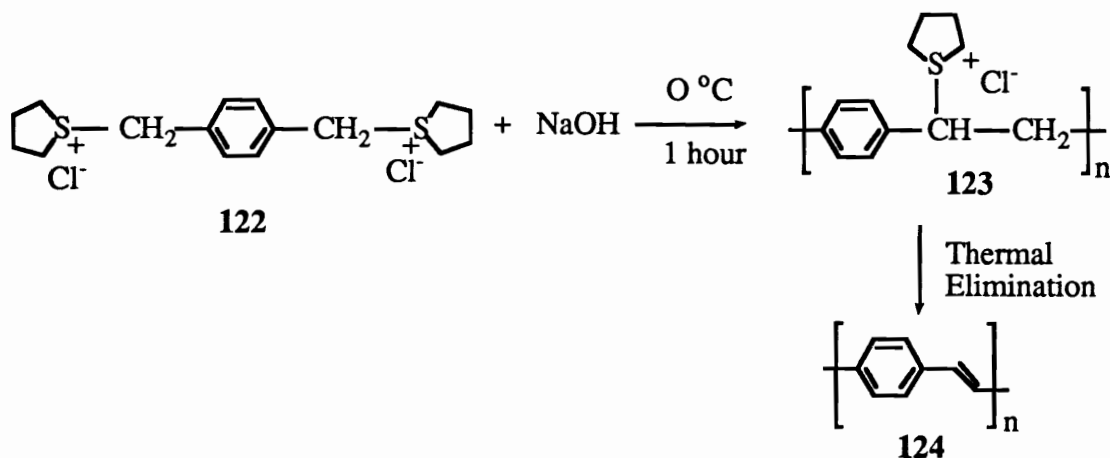
## 2. RESULTS AND DISCUSSION

### 2.1 Synthesis of Poly(1,4-phenylenevinylene)

#### 2.1.1 Synthesis of p-xylylene bis(tetrahydrothiophenium) chloride

Following conventional procedures in the literature,<sup>1</sup> the monomer for poly(1,4-phenylenevinylene), p-xylylene bis(tetrahydrothiophenium) chloride **122** was made by reacting  $\alpha, \alpha'$ -dichloroxylylene with an excess of tetrahydrothiophene in methanol at 50 °C for 20 hours. The product was isolated by precipitating the concentrated methanol solution into cold, dry acetone and purified by reprecipitating it from methanol into dry acetone. The final product, a hygroscopic white solid, was analyzed by <sup>1</sup>H NMR and <sup>13</sup>C NMR. (Fig. IV-1a, Fig. IV-1b).

#### 2.1.2 Synthesis of poly(1,4-phenylenevinylene) precursor



The polymerization was carried out by reacting p-xylylene bis(tetrahydrothiophenium) chloride (0.4 M) **122** with equimolar aqueous NaOH solution (0.4 M) at 0 °C for 1 hour under nitrogen. The reaction solution gelled in 5 minutes after the addition of NaOH. The gel was dissolved and the solution turned green gradually upon dilution at room temperature, indicating the formation of a conjugated backbone.

The solution was dialyzed (membran molecular weight cut off=6,000-8,000) against deionized water for 3 days. The polymer solution **123** after dialysis was cast into a film in a plastic pan and the water was evaporated slowly under N<sub>2</sub> at room temperature. The free standing film was characterized by FTIR. (Fig. IV-2a) The broad absorption peak which centered at 3325 cm<sup>-1</sup> is due to the absorbed water. The absorption peak at 965 cm<sup>-1</sup> indicates that trans vinyl bonds formed via the elimination reaction at room temperature. Actually, because of the elimination reaction, the film formed can not be redissolved in water.

This free standing film was converted to PPV **124** by heating in a drying pistol under vacuum at the reflux temperature of diethylene glycol (b.p. 245 °C). In the FTIR spectrum (Fig. IV-2b) the broad water peak disappeared after heating and the strong absorption peak at 965 cm<sup>-1</sup> showed the formation of trans vinyl bonds after elimination. In order to eliminate the tetrahydrothiophene substituent at a temperature at which the crown ether will not decompose, the precursor film was also converted to PPV at the reflux temperaure of ethylene glycol (b.p. 198 °C). The converted film was characterized by FTIR. The spectrum showed the same peaks as the one which was treated at high temperatures. The FTIR spectra agreed quite well with the literature reported values.<sup>4-7</sup>

The PPV precursor solution was also subjected to UV-vis and fluorescence analyses. In the UV-vis spectrum (Fig. IV-3), the peaks at 190 nm and 230 nm were associated with the phenyl group. The peak at 325 nm was assigned to the bathochromically shifted stilbene group, which came from the elimination of the tetrahydrothiophenium groups. The peak intensity ratio of the phenyl group to the shifted stilbene group indicates the extent of conjugation along the PPV backbone, i.e., the extent of elimination at room temperature. Less elimination was observed when the reaction solution was stored without light. The photoluminescence spectrum was obtained with 320 nm incident light. The wavelength of photoluminescent light was 490 nm. (Fig.IV-4a) However, lower

wavelength emission light was observed when the reaction solution was kept away from light. (Fig. IV-4b) This blue shift of the emission light can be interpreted as being due to the low conjugation along the polymer backbone which resulted in higher  $\pi$ - $\pi^*$  transition energy reflected by the lower wavelength of emission light. A similar observation was also reported in the literature by Holliday and Samuel et al.<sup>8,10</sup> Galvin et.al. found that the luminescence intensity decrease with increase of the carbonyl content in the backbone. The carbonyl groups are formed by oxidation of the -OH substituent on the backbone which can happen under the usual thermal elimination condition. This result suggests that the different luminescent intensities might be caused by the different carbonyl content on the PPV backbone.

The polymer precursor was analyzed by thermogravimetric analysis (TGA) which showed two weight loss processes from 100 °C to 200 °C (Fig. IV-5). The weight loss was due to 1) water and then 2) tetrahydrothiophene and HCl, respectively. The TGA spectrum also agreed very well with the reported literature values.<sup>10-12</sup>

### **2.1.3 Molecular weight of poly(1,4-phenylenevinylene)**

Because of the insolubility and infusibility of the PPV, the molecular weight of this polymer has to be measured at its precursor stage. However, due to the interactions between the PPV precursor and packing materials in the GPC column, accurate molecular weight measurement of PPV is impossible except by converting the PPV precursor to another polymer, such as the polymer precursor with tetrafluoroborate as the counterion, whose molecular weight can be measured by GPC.<sup>13</sup> Osmometry has also been reported to measure the molecular weight of the polymer precursor with disulfide substituent.<sup>14</sup> Another reported technique to measure the molecular weight is to combine low angle laser light scattering with centrifugation;<sup>14, 15</sup> however, the experimental details were not available. Low angle laser light scattering (LALLS) has not been utilized in the

molecular weight measurement of the PPV precursor with tetrahydrothiophene as a substituent.

The molecular weight measurement by light scattering is usually done by measuring the intensity of the scattering light at a series of scattering angles and with different concentrations. The molecular weight can be obtained by plotting the collected data, so called Zimm plot, and extrapolating the data to the 0 concentration and 0 angle. The intercept of the extrapolation gives the reciprocal of weight average molecular weight of the polymer. The principal equation is shown as follows:

$$Kc/R_{\theta} = (1/M + 2A_2c)[1 + 16\pi^2 r_g^2 \sin^2(\theta/2)/3\lambda]$$

where constant K includes determinable instrumental constants, solvent (n) and dn/dc; c is the concentration of the polymer solution;  $\lambda$  is the wavelength of the incident light;  $r_g$  is radius of gyration. However, if the scattering angle in the photometer is very small (1-6°),  $\sin^2(\theta/2)$  is almost 0, this equation can be simplified and it is not necessary to measure the scattering intensity at different angles. The simplified equation is shown as follows:

$$Kc/R_{\theta} = 1/M + 2A_2c$$

The constant K can be calculated as follows:

$$K = 2\pi^2 n^2 (dn/dc)^2 (1 + \cos^2\theta) / \lambda^4 N$$

where n is refractive index,  $\lambda$  is the wavelength, N is Avogadro's number, and dn/dc is the change in refractive index per unit change of concentration.

Combining the constants in the above equation for the instrument we used (KMX-6) results in:

$$K = 406.5e^{-8} n^2 (dn/dc)^2$$

By measuring  $dn/dc$ ,  $c$  and  $R(\theta)$ ,  $1/M_w$  can be obtained through the intercept of the plot  $Kc/R(\theta)$  vs  $c$ .

Since the low angle light scattering technique for molecular weight measurement requires a clear, dust free solution, the solution should be passed through a filter before use. However, the polymer, especially a high molecular weight polyelectrolyte, may also be removed by filtration. To check the filtration effect, the solution before and after filtration was analyzed by UV spectroscopy. The UV spectra showed about 20% loss of polymer during filtration by the intensity change measurement. The lost part of the polymer may be the highest molecular weight part whose loss may cause large experimental error in molecular weight determination. This problem was solved by the addition of a small amount of salt (NaCl) to suppress the polyelectrolyte effect by which the polymer chain was extended due to the charge repulsion, and changing the Teflon filter to an inorganic filter. The effect of salt addition was monitored by measuring the hydrodynamic size of the polymer chain, the diameter of the sphere of the polymer chain occupied, using dynamic light scattering measurement. (Fig. IV-13) When the salt (NaCl) concentration was in the 0.001-0.005 weight fraction range, the polyelectrolyte effect was efficiently suppressed. If the concentration was higher than 0.01 weight fraction, the polymer solution became cloudy or even precipitated out. According to the result of this experiment, we chose 0.002 salt (NaCl) concentration as a standard and measured light scattering and differential refractive indexes at this salt concentration.

Because of the easy elimination of the tetrahydrothiophene group at room temperature, the concentration of polymer solution can not be simply measured by drying the sample. It was done by drying and thermal elimination of PPV precursor to convert it to PPV. The concentration of PPV precursor can be obtained by calculating the weight of PPV in solution. However, because the substituent of PPV precursor can be eliminated at room temperature, two concentrations of PPV precursor were calculated, assuming no

elimination and 10% elimination, respectively. By this method, the concentrations of aqueous precursor solution were found to be 3.69 mg/mL and 3.88 mg/mL for 10% elimination and no elimination, respectively.

$R(\theta)$  was measured at different polymer concentrations at 25 °C. The results are shown as follows:

$10^{-5}C$	No elimination	6.05	9.18	12.15	18.1	24.3
g/mL	10% elimination	5.74	8.71	11.55	17.2	23.1
$10^{-6}R(\theta)$ ml <sup>-1</sup>		9.72	14.74	19.67	29.25	38.63

The differential refractive index was measured at 30 °C for different polymer concentrations vs. pure solvent. The refractive index can be calculated by the equation:

$$\Delta n = 1.3327e^{-7}[(L-R) - (L-R)_0]$$

where  $L-R$  is the refractive index change for polymer vs solvent, and  $(L-R)_0$  is the refractive index change for solvent vs solvent.

Because  $(L-R)_0$  varied with different measurements, 8 sets of  $\Delta n$  were obtained and they were used to calculate  $n$  respectively.

$$n = 1.3317 + \Delta n$$

Eight sets of  $n$  were used to draw the plot  $n$  vs  $c$ . From the slopes of these plots,  $dn/dc$  was found to be 0.211 and 0.200 for 10% elimination and no elimination cases, respectively. Also, the fluctuation of  $(L-R)_0$  was found to have little effect on the  $dn/dc$  calculation.

Finally,  $K$  was calculated and  $Kc/R(\theta)$  vs  $c$  was plotted. (Fig. 6) The intercepts,  $1/M_w$ , were  $1.795e^{-6}$  and  $1.88e^{-6}$  for no elimination and 10% elimination

conditions, respectively. The  $M_w$  was found to be  $557 \pm 22$  kg/mole for the no elimination case and  $530 \pm 21$  kg/mole for the 10% elimination case. These values agree with the reported molecular weight of PPV ( $M_w = 9.9 \times 10^5$  Da).<sup>14</sup>

## 2.2 Synthesis of PPV rotaxane

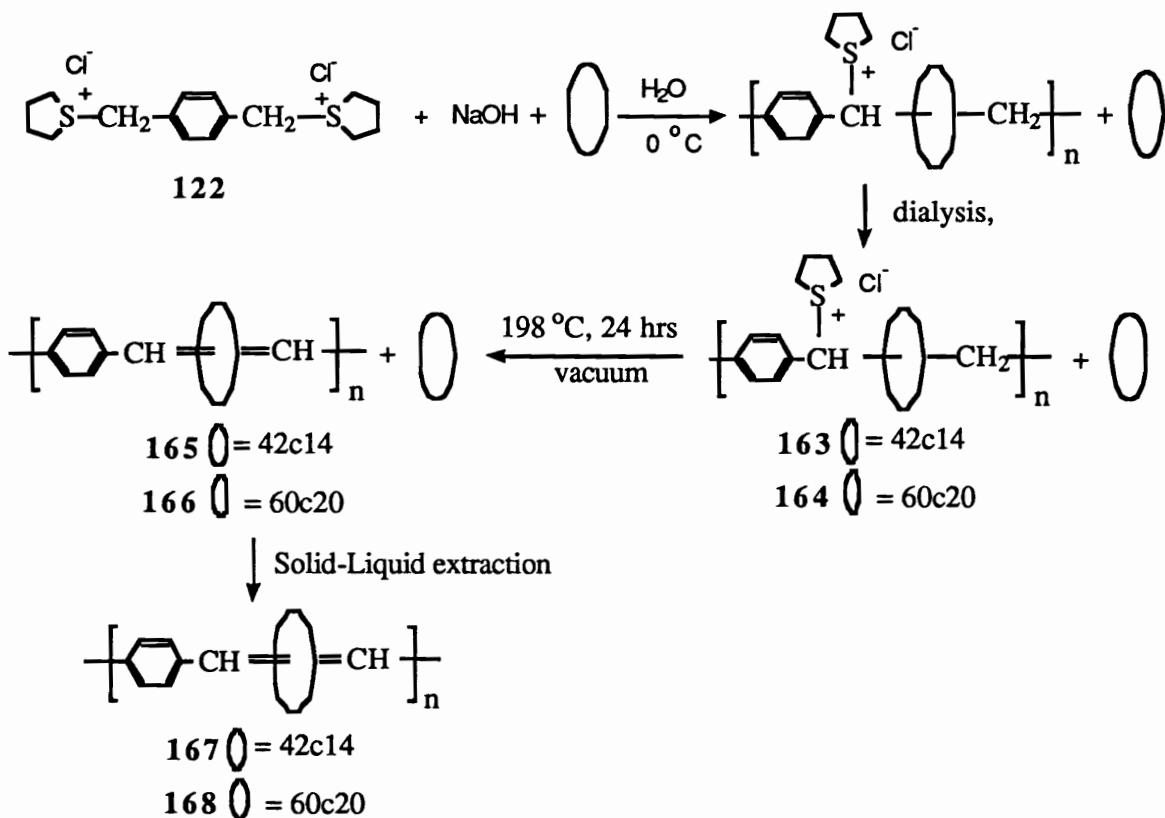
### 2.2.1 Synthesis of PPV in the presence of 18-crown-6

Because the mechanism of the polymerization of the PPV is free radical, there is the possibility of a chain transfer reaction which results in the ring opening of the macrocycle and the incorporation of the linear polyethylene oxide into the PPV backbone. If that is the case, the synthesized polymer is a copolymer of PPV and PEO instead of the PPV rotaxane. To investigate this possibility, p-xylylene bis(tetrahydrothiophenium) chloride was polymerized in the presence of 18-crown-6 under the same reaction conditions as in the PPV rotaxane synthesis. Because the cavity of the 18-crown-6 is too small to be threaded, if ether linkages were observed after removing the free 18-crown-6 by dialysis, chain transfer definitely happened. After polymerization was carried out in the presence of 18-crown-6 followed by 3 days of dialysis, no free crown ether could be detected by TLC. The reaction solution was cast into a film and characterized by IR. (Fig. IV-7a) No ether linkage was observed in the IR spectrum of the PPV film. Compared to the IR spectrum (Fig. IV-2a) of the PPV precursor, the film gave the same peaks and the strong ether stretch at  $1111 \text{ cm}^{-1}$  in 18-crown-6 (Fig. IV-7b) was not present. Therefore, we can conclude that no chain transfer or ring opening takes place in the polymerization reaction.

### 2.2.2 Synthesis of poly(1,4-phenylenevinylene) rotaxane

Since the presence of crown ether does not interfere with the polymerization of poly(1,4-phenylenevinylene), we carried out poly(1,4-phenylenevinylene) rotaxane (**167**)

synthesis by polymerizing the p-xylylene bis(tetrahydrothiophenium) chloride (**122**) in the presence of 42-crown-14, whose cavity is large enough to be threaded by the PPV chain.



Because the molecular weight of the linear backbone was very high according to the previous result, the dethreading process was assumed to have little influence on the threading yield. The entanglement and random coiling of the long chain polymer may greatly reduce the number of the threaded crown ethers to fall off the chain ends. Moreover, complexation of the crown ether with the sulfonium moieties was anticipated. Therefore, the blocking groups were not used in the polyrotaxanes syntheses. The reaction procedure was similar to the polymerization of PPV. Since the crown ether can complex with the monomer, which may increase the threading yield, the reaction was performed with prethreading, which can promote the complex by mixing the monomer and the crown ether, before the addition of the NaOH, and nonprethreading conditions. During the polymerization reaction, the solution didn't gel as in the pure PPV case. The

polyrotaxane solution was dialyzed against the deionized water after the reaction. The dialysis process was monitored by TLC which showed that the free crown ether still existed after 1 month of dialysis. This might be because the cationic substituent can complex with the crown ether which makes the free crown ether difficult to be removed by the dialysis. The polyrotaxane precursor solution **163** was analyzed by UV-vis and photoluminescence spectroscopy which showed similar characteristic peaks as the PPV precursor.

The poly[(1,4-phenylenevinylene)-rotaxa-(42-crown-14)] precursor **163** was converted to the polyrotaxane **165** by removing the solvent, followed by thermal elimination in a drying pistol at the reflux temperature of ethylene glycol (b.p. 198 °C) under vacuum for 24 hours. Because the unthreaded free crown ether can not be completely removed during the 3 day dialysis which was monitored by TLC, the poly(1,4-phenylenevinylene)-42-crown-14 rotaxane **165** actually obtained was a mixture of polyrotaxane, free 42-crown-14, and perhaps unthreaded poly(1,4-phenylenevinylene) linear chain. To remove the free 42-crown-14, the thermally converted poly[(1,4-phenylenevinylene)-rotaxa-(42-crown-14)] mixture **165** was transferred into a cellulose extraction thimble and extracted with hot methanol in a Soxhlet apparatus. The extract from the methanol was analyzed by <sup>1</sup>H NMR and IR spectroscopy which clearly demonstrated that the free 42-crown-14 was extracted out. (Fig. IV-8a) The extraction was continued until no crown ether could be extracted out, which was determined by weighing the extract after removal of the solvent. The yellow solid left in the thimble after extraction was pure PPV rotaxane **167** with perhaps some unthreaded PPV and it was dried in the vacuum overnight.

The PPV rotaxane **167**, after drying, was characterized by quantitative <sup>13</sup>C solid state NMR. (Fig. IV-8b) which clearly showed the PPV backbone peaks at 128 ppm and 136 ppm and the crown ether peak at 70 ppm. These values agree very well with the reported

$^{13}\text{C}$  solid state NMR peak position of PPV and  $^{13}\text{C}$  solid state NMR of 42-crown-14.(Fig. IV- 9a, 9b, 9c), (Fig. IV-10) Because of the low thermal elimination temperature, the resolution of different carbon atoms on the PPV backbone was low.<sup>16</sup> However, the threading yield and mass percent of the crown ether in the PPV rotaxane could still be calculated unambiguously from the NMR integration. Since in the nonprethreading case the integration of the carbon peak of PPV backbone is 748.9 and that of crown ether is 189.7, the number of repeating units per macrocycle (n/x) was calculated to be 13.8 which corresponded to 30% of the macrocycle content by mass in the poly[(1,4-phenylenevinylene)-rotaxa-(42-crown-14)]. Moreover, the mass content of crown ether in the prethreading case was found to be 34% which was almost the same as in the nonprethreading case, considering experimental error. This indicated that the prethreading did not have much influence on the threading efficiency. This could result from fast complex formation between the crown ether and the monomer.

The polyrotaxane architecture was also demonstrated by  $^{13}\text{C}$  solid state NMR. The threaded crown ether gave different chemical shift from the free crown ether (Fig. IV-21). The free crown ether gave a peak at 72.35 ppm in  $^{13}\text{C}$  solid state NMR, while the threaded crown ether gave a peak at 70.94 ppm.

The PPV rotaxane was characterized by TGA performed under nitrogen (Fig. IV-11a) and compared with TGA of PPV and 42-crown-14 performed under nitrogen. (Fig. IV-11b), (Fig. IV-11c) In the TGA diagram of 167, two weight losses were observed at 382 °C and 577 °C, respectively. The weight loss at 382 °C was associated with the thermal decomposition of 42-crown-14. From the diagram, at about 382 °C, 30% weight loss can be estimated, which agreed quite well with the quantitative  $^{13}\text{C}$  solid NMR results. The weight loss at 577 °C is associated with the decomposition of PPV itself.

The obtained polyrotaxane was found to be insoluble in common solvents, including toluene, hexane, acetone, ethyl acetate, methanol, THF, and chloroform. Even

concentrated sulfuric acid and trifluoroacetic acid could not dissolve the PPV rotaxane. The PPV rotaxane turned black in these strong solvents but not dissolve. This obvious lack of improvement in solubility of PPV after threading the flexible 42-crown-14 is because of the relatively low threading yield on the PPV backbone. The 30% of flexible macrocycle is not high enough to change the rigidity of the PPV backbone. To improve the solubility of this rigid backbone, at least 60% mass of the flexible side chains needs to be incorporated into the backbone as reported in the literature. 2, 3, 17

To increase the threading yield, the larger macrocycle, 60-crown-20, was considered in the polyrotaxane synthesis. The 60-crown-20 has a larger cavity than that of the 42-crown-14 and it was expected to have more threadable conformations. This expectation was verified in the poly[(1,4-phenylenevinylene)-rotaxa-(60-crown-20)] (**168**) synthesis. The polymerization was carried out in the presence of the pure 60-crown-20. The reaction solution was dialyzed against the deionized water as in the previous case. The polyrotaxane precursor **164** after dialysis was thermally converted to poly[(1,4-phenylenevinylene)-rotaxa-(60-crown-20)] (**166**) under vacuum. The free 60-crown-20 contained in the obtained polyrotaxane mixture **166** was extracted out using hot methanol. The isolated poly[(1,4-phenylenevinylene)-rotaxa-(60-crown-20)] (**168**) was also characterized by quantitative solid  $^{13}\text{C}$  NMR. (Fig. IV-12) The mass content of the flexible crown ether was found to be 58% which corresponded to 6.15 repeating units per ring. The large increase in the threading yield clearly demonstrated the ring size factor in the polyrotaxane syntheses. Unfortunately, even with such a high threading yield of the flexible crown ether the obtained poly[(1,4-phenylenevinylene)-rotaxa-(60-crown-20)] (**167**) was still not soluble in the various organic solvents. There may be two reasons for this result. First, the mass content of the flexible crown ether was still not high enough. Compared to the mass content of the flexible side chains in the soluble PPV derivatives (>60 mass%), the mass content of the polyrotaxane is not enough. 2, 3, 17 The second reason might be crosslinking of poly(1,4-phenylenevinylene) during the thermal

elimination process which leaves no chance for the polyrotaxanes to be soluble. This phenomenon was also reported in the literature.<sup>3</sup>

The conductivity of both poly[(1,4-phenylenevinylene)-rotaxa-(42-crown-14)] (**165**) and poly[(1,4-phenylenevinylene)-rotaxa-(60-crown-20)] (**166**) were measured by a conventional four probe technique. The polyrotaxane precursor solutions were cast into films on glass. The precursor films were thermally converted to the final rotaxane under vacuum. The free crown ether trapped in the film was not removed. The conductivities of both polyrotaxane films were measured before and after being doped with the concentrated H<sub>2</sub>SO<sub>4</sub>. The doping was carried out by immersing the polyrotaxane films **165** and **166** into the concentrated H<sub>2</sub>SO<sub>4</sub> for 1 hour. The doped film was dipped into deionized water several times and dried under vacuum. The conductivity was found to be greatly affected by the dopant and the large incorporation of crown ether. The conductivities of the PPV-rotaxa-60-crown-20 (**166**) and PPV-rotaxa-42-crown-14 (**165**) were found to be 2.0x10<sup>-11</sup> S/cm and 8.5x10<sup>-11</sup> S/cm, respectively. The conductivity increased to 2.0 x 10<sup>-9</sup> S/cm for doped PPV-rotaxa-60-crown-20 (**166**) which has 58% crown ether by mass and to 1.06x10<sup>-5</sup> S/cm for doped PPV-rotaxa-42-crown-14 (**165**) which has 34% incorporation of crown ether. The decrease in conductivity with an increase in crown ether content can be explained by reduced concentration of the conducting polymer chains and the increase in interchain distance which prevents the electrons from hopping from one chain to the other. The literature reported values are 10<sup>10</sup> S/cm for undoped PPV and 27 S/cm for unstretched PPV doped with concentrated H<sub>2</sub>SO<sub>4</sub>.<sup>18,19</sup>

### 2.3 Photoluminescence of poly(1,4-phenylenevinylene) rotaxanes

The photoluminescence spectra of PPV rotaxanes were obtained from solid films of **165** and **166**. Compared to the photoluminescence spectra of poly(1,4-phenylenevinylene) rotaxane precursors, the photoluminescence spectra of poly(1,4-

phenylenevinylene) rotaxanes have red-shifted peaks due to the increased conjugation length along the polymer backbone. The PPV spectrum (Fig. IV-14) showed 3 bands centered at 505nm, 520 nm, and 530 nm which arise from transitions between different vibrational ground states and excited singlet states. The PPV-42C14 (Fig. IV-15) showed two major bands centered at 505 nm and 530 nm. The intensity of the 520 nm band at in the PPV spectrum was reduced. This is presumably because the threaded 42-crown-14 increased the interchain distance in the PP-42C14, which may reduce the interchain hopping of the excitons which cause the 520 nm band. The PPV-60C20 (Fig. IV-16) gave one band at 530 nm. The 505 nm band which appeared in the PPV spectrum was not observed. This can be explained by the absorption spectrum of PPV-60C20 (Fig. IV-20a), which had a broad absorption band around 500 nm. While the absorption spectra of other samples do not show any absorption peak around 500 nm. (Fig. IV-19, 20b) Therefore, the emission band at 505 nm for PPV-60C20 might be self-absorbed. However, the PPV and 42C14 blend (Fig. IV-17) showed only a broad peak centered at 520 nm which indicates that the interchain distance between the PPV backbone is not increased. The other reason can cause the intensity change is the film thickness. Since these films do not have the same thickness, the intensity change might result from the thickness difference. Different carbonyl content in these films may gave different peak intensity as well.

### 3. EXPERIMENTAL

The starting materials were bought from Aldrich Chemical Co. and used with no further purification. The tetrahydrothiophene was bought from Eastman Chemical Co. and used without further purification. Proton and carbon NMR spectra, reported in ppm, were obtained on a Bruker W-270 and Varian Unit at 270 MHz and 400 MHz, respectively, using a chloroform solution with tetramethylsilane as an internal standard. Quantitative  $^{13}\text{C}$  NMR was obtained on a Bruker MLS-300. Thermogravimetric analysis was performed on a Perkin-Elmer. UV-vis data were obtained with Perkin-Elmer Lambda 4B from PPV precursor and PPV rotaxane precursor aqueous solutions. Photoluminescence data were obtained with a Perkin-Elmer luminescence spectrometer LS-50 from PPV and PPV rotaxane precursors in aqueous solutions. The dynamic light scattering measurements were made with a Brookhaven BI-2030 AT digital correlator equipped with 130 channels at a  $90^\circ$  scattering angle. Conductivity measurements were performed on Keithly 617 programmable electrometer.

#### 1. Synthesis of p-Xylylene Bis(tetrahydrothiophenium) Chloride (122)

$\alpha,\alpha'$ -Dichloroxylylene (20.00 g, 114 mmol) was mixed with tetrahydrothiophene (60.44 g, 685 mmol) in 400 mL fresh HPLC methanol in a 1L 3 neck flask equipped with  $\text{N}_2$  purge and condenser. The reaction was started by warming the solution to  $50^\circ\text{C}$  in an oil bath. The solution was stirred at this temperature for 20 hours, cooled to room temperature and concentrated to about 100 mL. The concentrated solution was precipitated into 600 mL dry acetone at  $0^\circ\text{C}$ . (The acetone was dried by distillation of fresh HPLC acetone in the presence of Drierite.) The white precipitate was filtered and dried *in vacuo* at room temperature. The compound was dissolved in 80 mL of fresh methanol and reprecipitated into 600 mL dry acetone at  $0^\circ\text{C}$ . The reprecipitation afforded 26.19 g (77%) of white powder.  $^1\text{H}$  NMR  $\delta$ : (270 MHz,  $\text{D}_2\text{O}$ ) 2.31 (8H, m,

SCH<sub>2</sub>), 3.47 (8H, m, SCH<sub>2</sub>), 4.57 (4H, s, benzylic CH<sub>2</sub>), 4.79 (s, HOD), 7.63 (4H, s, ArH).

## **2. Synthesis of Poly(1,4-phenylenevinylene) (124)**

p-Xylylene bis(tetrahydrothiophenium) chloride (3 g, 9 mmol) was dissolved in 21.3 mL distilled deionized water and cooled to 0 °C in an ice bath. Aqueous NaOH solution (21.3 mL, 0.4 M, 9 mmol) was added to the monomer solution dropwise. Gelation was observed in 5 minutes after the addition of NaOH solution. The reaction was run for 1 hour. The solution was titrated against an aqueous potassium hydrogen terephthalate solution (0.1 M) after the reaction. The monomer conversion was 37%. The reaction solution was dialyzed against deionized water for 3 days. The precursor solution was cast into a film after dialysis. The film was dried by vaporizing the solvent under continuous N<sub>2</sub> flow at room temperature for 2 days. IR 3375, 3023, 2997, 2937, 1516, 1423, 965, 832. The PPV precursor film was converted to PPV by heating it in a drying pistol at the reflux temperature of diethylene glycol (bp 245 °C) for 24 hours in vacuum. IR 3568, 3023, 2950, 1689, 1596, 1516, 1423, 965, 839.

## **3. Molecular weight measurement of Poly(1,4-phenylenevinylene) precursor 123**

The Rayleigh factor  $R(\theta)$  was measured using the KMX-6. The refractive index differences were measured by a differential refractometer at 5 different concentrations. The molecular weight of the poly(1,4-phenylenevinylene) precursor was found to be 557 kg/mole and 530 kg/mole assuming no elimination and 10% elimination, respectively. (Fig. IV-6)

## **4. Synthesis of Poly(1,4-phenylenevinylene) precursor in the presence of 18-crown-6**

p-Xylylene bis(tetrahydrothiophenium) chloride (1.5 g, 4.3 mmol) was dissolved in 10.7 mL distilled deionized water and cooled to 0 °C in an ice bath. 18-Crown-6 was dissolved in 10 mL of deionized water and mixed with aqueous NaOH solution (10.7 mL,

0.4 M, 4.3 mmol). The mixed solution was dropped into the monomer solution. No gelation was observed during the reaction. After 3 hours of reaction, the solution was dialyzed against deionized water for 3 days. The reaction solution was cast into film after dialysis. The film was dried by vaporizing the solvent under continuous N<sub>2</sub> flow at room temperature for 2 days. IR 3375, 3023, 2944, 2864, 1609, 1516, 1423, 965, 832.

### **5. Synthesis of poly[(1,4-phenylenevinylene)-rotaxa-(42-crown-14)] (167) with prethreading**

p-Xylylene bis(tetrahydrothiophenium) chloride (4.00 g, 11.4 mmol) and 42-crown-14 (7.01 g, 11.4 mmol) were dissolved in 22.1 mL distilled deionized water and cooled to 0 °C in an ice bath. The solution was stirred at that temperature for 4 hours. Aqueous NaOH solution (27.5 mL, 0.4 M, 11.4 mmol) was added to the light yellow prethreaded solution dropwise. No gelation was observed during the reaction time. After 1 hour of reaction, the solution was neutralized by standard aqueous HCl solution (0.1M). The solution was dialyzed against deionized water for 3 days. The solvent was removed and the residue was heated in a drying pistol at the reflux temperature of ethylene glycol (bp 198 °C) under vacuum for 24 hours. The obtained polyrotaxane mixture was extracted in a Soxhlet for 10 days with hot methanol to remove the free crown ether. Quantitative solid state <sup>13</sup>C NMR δ: 70.93 (28 C per ring, integr. 189.7), 136.72, 128.14 (6 arom and 2 aliph C per repeating unit, integr. 748.9), 34% of crown ether by mass (n/x=11.8).

The sample for conductivity measurement was prepared by casting the PPV rotaxane precursor solution onto glass; it was thermally converted to PPV rotaxane by heating in a drying pistol at reflux temperature of ethylene glycol (bp 198°C) in vacuum. The conductivity was measured by a conventional four-probe method; The measurement was done as follows: An in-line four-point probe is placed on a film which was cast on glass the substrate. A direct current is passed through the film between the outer probes and the resulting potential difference is measured between inner probes. (Fig. 18) The resistivity is calculated from the current and potential value:

$$\rho = 2\pi S(V/I)$$

$\rho$  = Resistivity,

V = Potential difference

I = Current

S = Probe spacing (S =  $10^{-1}$  cm for Keithly 617 model)

The conductivity was calculated as reciprocal of the resistivity:

$$\sigma = 1/\rho$$

The conductivity was  $8.5 \times 10^{-11}$  S/cm for undoped polyrotaxane and  $1.06 \times 10^{-5}$  S/cm for polyrotaxane doped with concentrated sulfuric acid. The doping was carried out by immersing the polyrotaxane film in concentrated  $H_2SO_4$  solution for 1 hour. The doped film was dipped into deionized water several times and dried under vacuum at room temperature over night.

## 6. Synthesis of poly[(1,4-phenylenevinylene)-rotaxa-(60-crown-20)] (168)

60-Crown-20 (4.89 g, 5.56 mmole) and p-xylylene bis(tetrahydrothiophenium) chloride (4.89 g, 0.0139 mole) were dissolved in 30 mL of deionized water and charged into a 200 mL 3 neck flask equipped with an addition funnel and nitrogen inlet. Aqueous NaOH solution (33.1 mL, 0.42 M, 0.0139 mole) was added into the flask very slowly. A white precipitate formed upon the addition of NaOH solution. The reaction solution was stirred at 0 °C for 1 hour and at room temperature for 1 day. The precipitate was dissolved upon the addition of water and stirring. The greenish-yellow solution was dialyzed in a membrane (MWCO=6,000) for 3 days. The PPV rotaxane precursor was then converted to PPV rotaxane by thermal elimination at 200 °C under vacuum. The PPV rotaxane solid obtained was extracted by methanol to remove the free crown ethers. Quantitative solid state  $^{13}C$  NMR  $\delta$ : 71.09 (40 C per ring,  $CH_2$ , integr. 101.2), 136.63, 128.27 (6 arom and 2 aliph. C per repeating unit, integr. 124.9), crown ether content was 58% by mass ( $n/x=6.15$ ).

The sample for conductivity measurement was prepared by casting the PPV rotaxane precursor solution onto glass and thermally converting it to PPV rotaxane in a drying pistol at reflux temperature of ethylene glycol(bp 198 °C) in vacuum. The conductivity was measured by a conventional four-probe method, following the procedure described above. Conductivity  $2.0 \times 10^{-11}$  S/cm (undoped),  $2.7 \times 10^{-9}$  S/cm (doped with concentrated  $H_2SO_4$ ). The doping was carried out by immersing the polyrotaxane film in concentrated  $H_2SO_4$  solution for 1 hour. The doped film was dipped into deionized water several times and dried under vacuum at room temperature over night.

## **7. Photoluminescence measurement of PPV and PPV rotaxanes**

The PPV film was obtained by casting the aqueous PPV precursor solution on a glass slide and thermally converting to PPV at the reflux temperature of ethylene glycol (bp 198 °C) in vacuum. The films of PPV-42C14 and PPV-60C20 rotaxanes were obtained by casting aqueous solution of **163** and **164** on glass slides and converting to PPV rotaxanes under the same conditions as the PPV film. The PPV and 42C14 blend was made by dissolving the 42C14 (10 mg) in PPV precursor aqueous solution (5.1 g) and a film was cast from this solution. The film was converted to PPV and 42C14 blend under the same conditions as the PPV film. Photoluminescence spectra of these films were obtained with 320 nm wavelength of excitation light.

## REFERENCES

1. R. W. Lenz, C. C. Han, J. S. Smith, F. E. Karasz, *J. Polym. Sci.: Part A: Polym. Chem.*, **1988**, *26*, 3241; R. Garay, R. W. Lenz, *Macromol. Chem., Suppl.*, **1989**, *15*, 1-7; F. R. Denton III, P. M. Lahti, F. E. Karasz, *J. Polym. Sci.: Part A: Polym. Chem.*, **1992**, *30*, 2223
2. C. C. Han, R. L. Elsenbaumer, *Mol. Cryst. Liq. Cryst.*, **1990**, *189*, 183
3. S. Shi, F. Wudl, *Macromolecules*, **1990**, *23*, 2119
4. W. B. Liang, D. M. Rice, F. E. Karasz, F. R. Denton III, P. M. Lahti, *Polymer*, **1992**, *33*, 1780
5. R. O. Garay, U. Baier, C. Bubeck, K. Mullen, *Adv. Mater.*, **1993**, *5*, 561
6. I. Murase, T. Ohnishi, T. Noguchi, M. Hirooka, *Polym. Commun.*, **1984**, *25*, 327
7. S. Tokito, T. Momii, H. Murata, T. Tsutsui, S. Saito, *Polymer*, **1990**, *31*, 1139
8. P. L. Burn, A. B. Holmes, A. Kraft, D. D. C. Bradley, A. R. Brown, R. H. Friend, R. W. Gymer, *Nature*, **1992**, *356*, 47
9. I. D. W. Samuel, B. Crystall, G. Rumbles, P. L. Burn, A. B. Holmes, R. H. Friend, *Synthetic Metals*, **1993**, *54*, 281
10. D. A. Halliday, P. L. Burn, D. D. C. Bradley, R. H. Friend, O.M. Gelsen, A. B. Holmes, A. Kraft, J. H. F. Martens, K. Pichler, *Adv. Mater.*, **1993**, *5*, 40
11. G. Montaudo, D. Vitalini, R. W. Lenz, *Polymer*, **1987**, *28*, 837
12. F. E. Karasz, J. D. Capistran, D. R. Gagnon, R. W. Lenz, *Mol. Cryst. Liq. Cryst.*, **1985**, *118*, 327
13. J. M. Machado, F. R. Denton III, J. B. Schlenoff, F. E. Karasz, P. M. Lahti, *J. Polym. Sci.: Part B: Polym. Phys.*, **1989**, *27*, 199
14. D. R. Gagnon, J. D. Capistran, F. E. Karasz, R. W. Lenz, S. Antoun, *Polymer*, **1987**, *28*, 567
15. G. Holzworth, L. Soni, D. N. Schulz, *Macromolecules*, **1986**, *19*, 422
16. J. H. Simpson, N. Egger, M. A. Masse, D. M. Rice, F. E. Karasz, *J. Polym. Sci.: Part B: Polym. Phys.*, **1990**, *28*, 1859
17. S. H. Askari, S. D. Rughooputh, F. Wudl, *Proc. ACS Div. Polym. Mat. Sci. Eng.* **1988**, *59*, 1068
18. I. Murase, T. Ohnishi, T. Noguchi, M. Hirooka, *Synthetic Metals*, **1987**, *17*, 639
19. G. E. Wnek, J. C. W. Chien, F. E. Karasz, C. P. Lillya, *Polymer*, **1979**, *20*, 1441; J. C. W. Chien, R. D. Gooding, F. E. Karasz, C. P. Lillya, G. E. Wnek, K. Yao, *Org. Coat. Plast. Chem.*, **1980**, *43*, 886

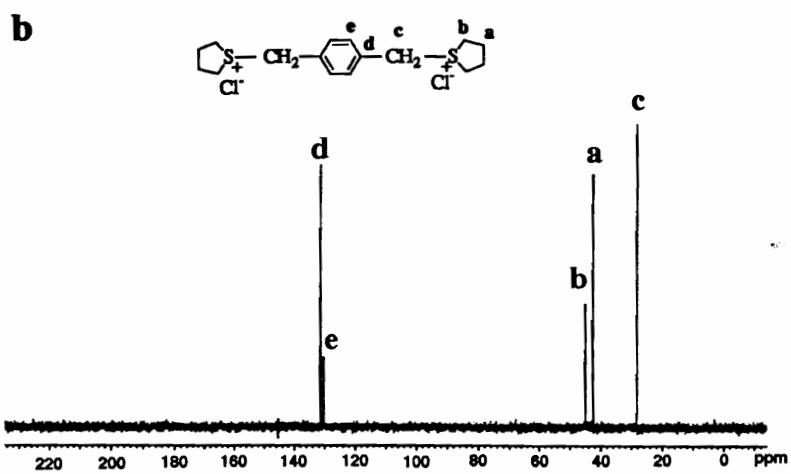
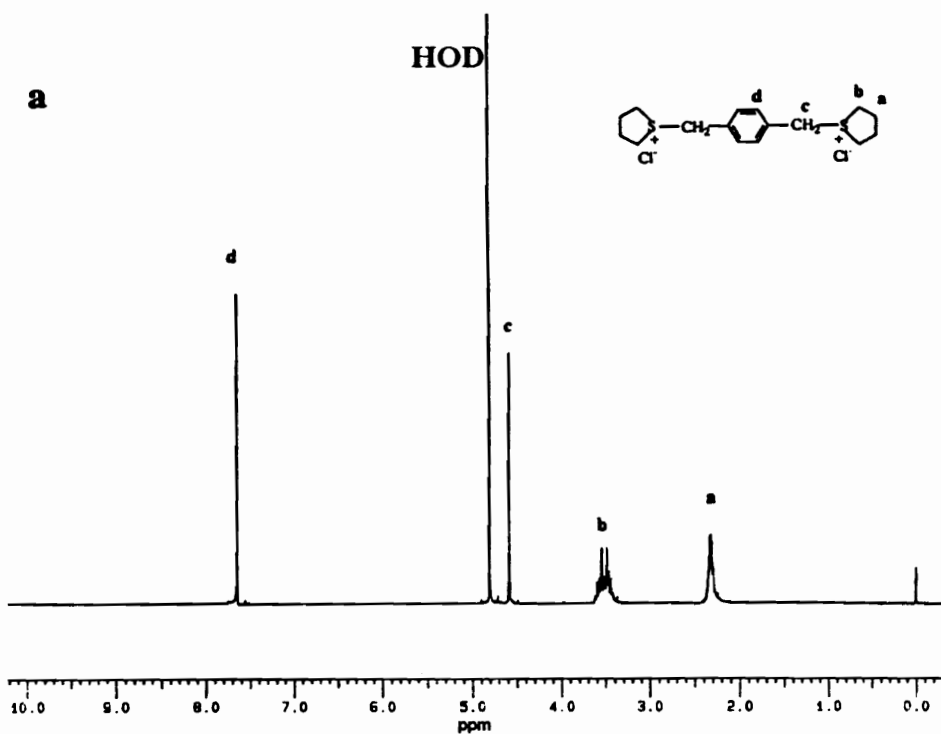


**Figure IV-1. a) 270 MHz  $^1\text{H}$  NMR; b) 100 MHz  $^{13}\text{C}$  NMR spectra of p-xylylene bis(tetrahydrothiophenium) chloride in  $\text{D}_2\text{O}$ .**

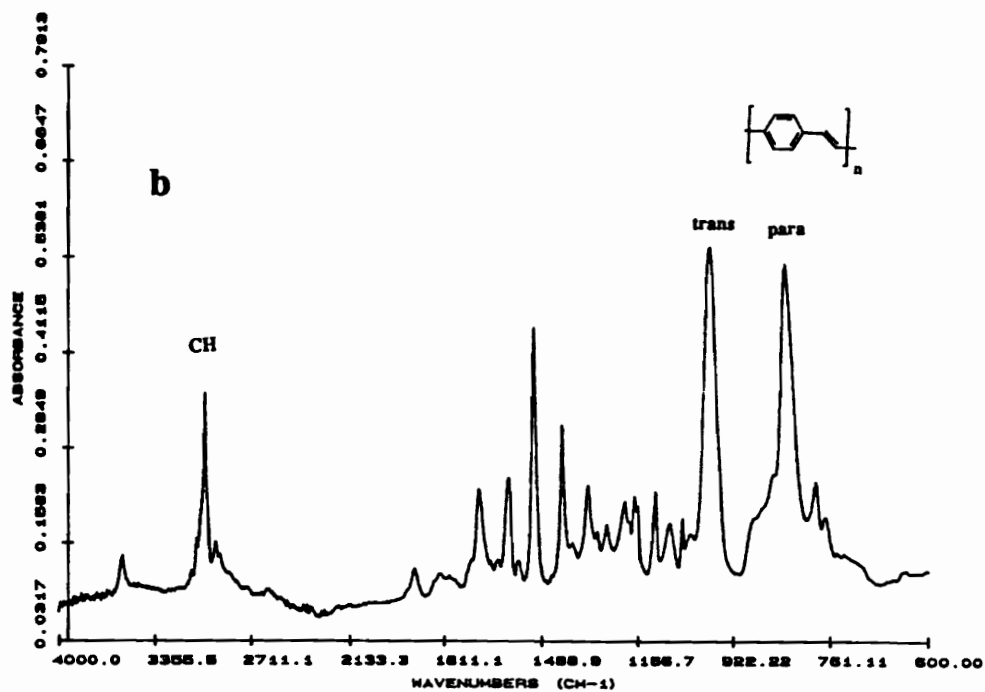
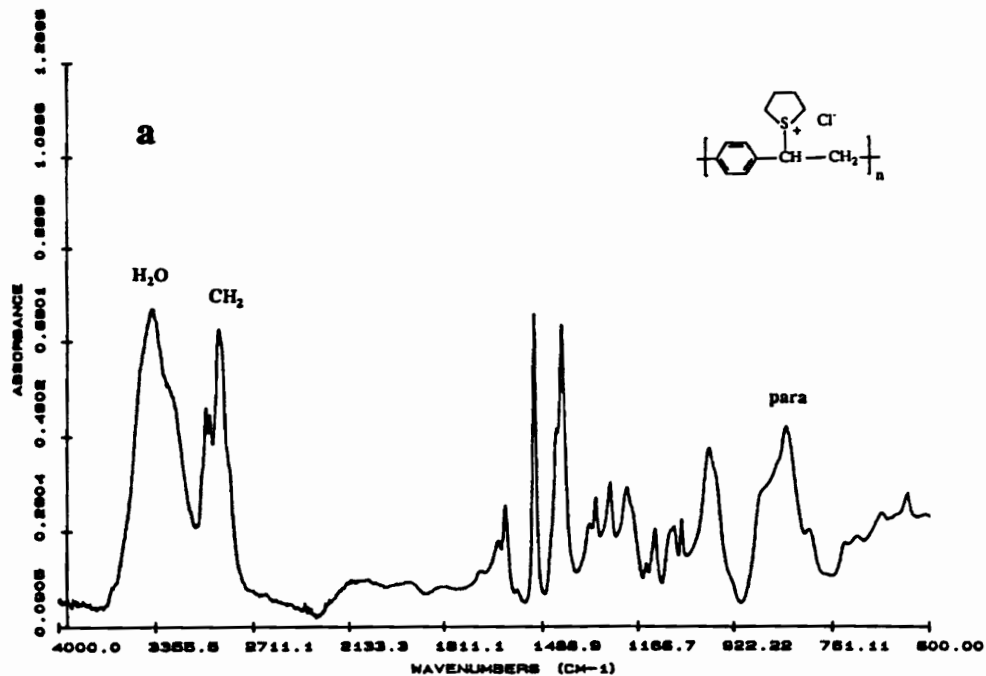


**Figure IV-2. FTIR spectra of a) poly(1,4-phenylenevinylene) precursor; b) poly(1,4-phenylenevinylene) measured as free standing films.**

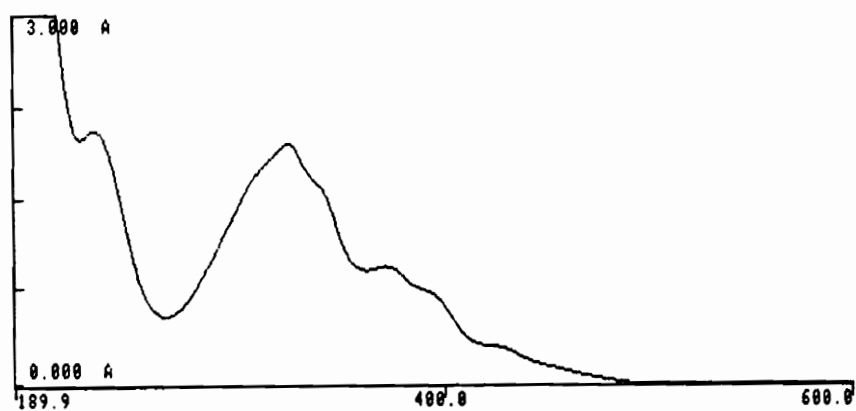
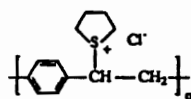


**Figure IV-3. UV-vis spectrum of poly(1,4-phenylenevinylene) precursor measured in deionized water.**

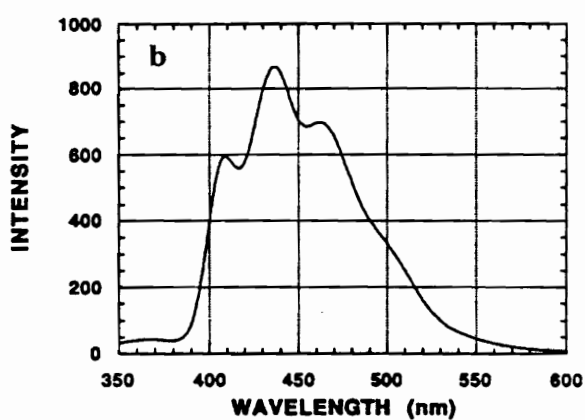
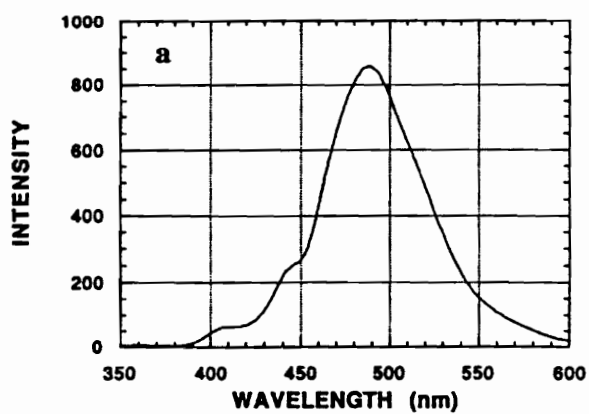


**Figure IV-4. Photoluminescence spectra of poly(1,4-phenylenevinylene) precursor measured in deionized water a) exposed to light; b) kept away from light. excitation wavelength: 320 nm**

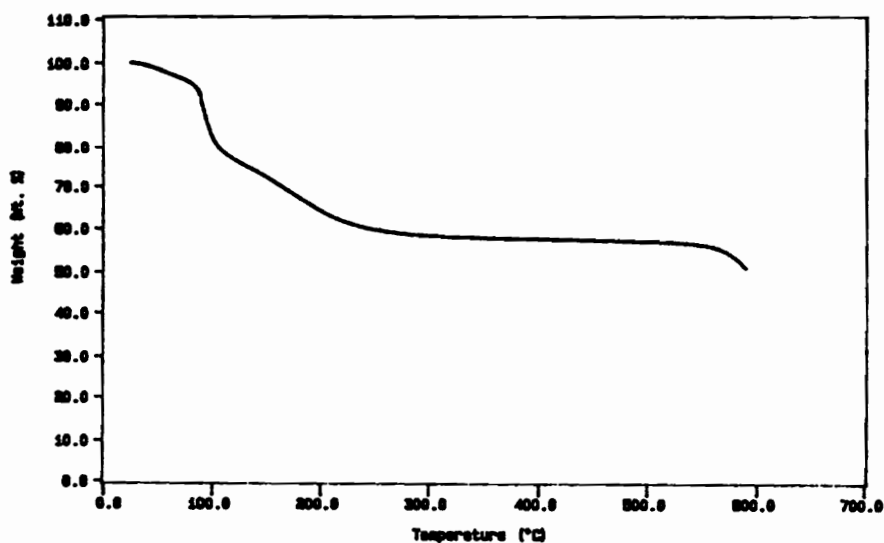


**Figure IV-5. Thermogravimetric analysis of poly(1,4-phenylenevinylene) precursor in N<sub>2</sub>.  
scan rate: 10 °C/min**

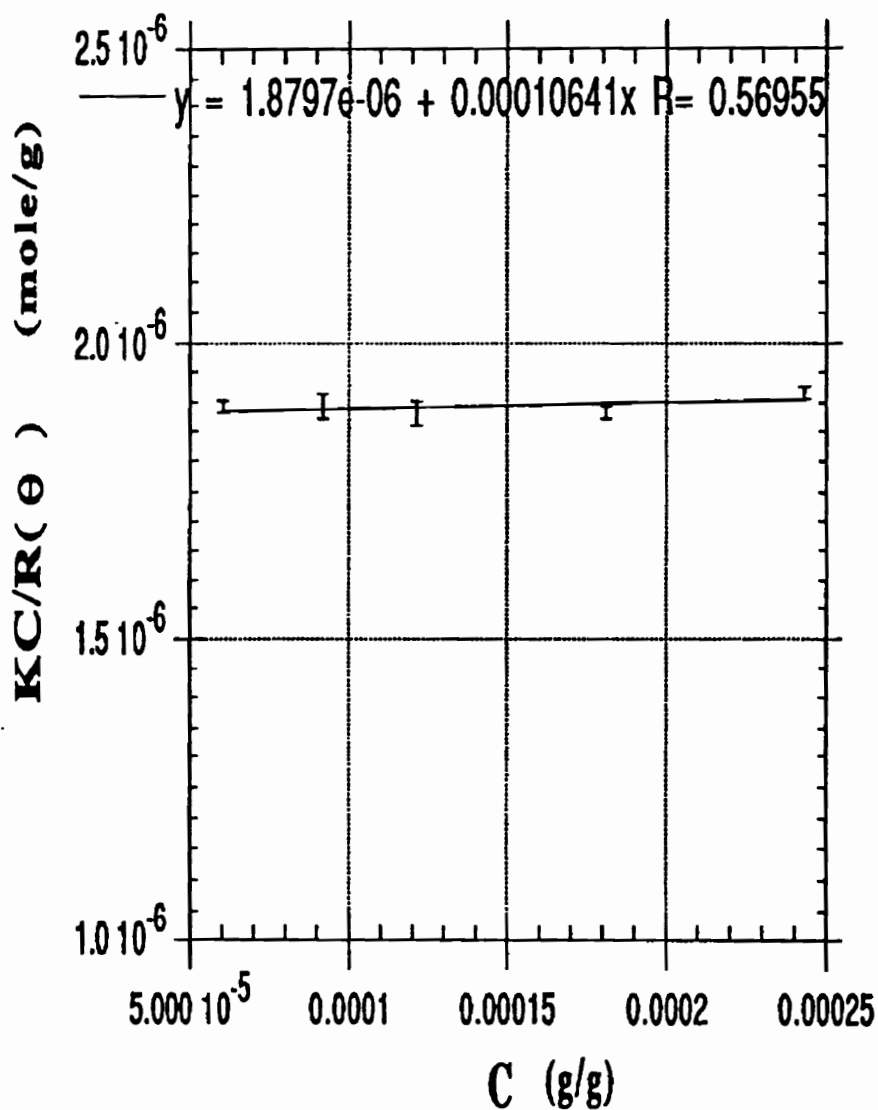


**Figure IV-6. Molecular weight measurement of the poly(1,4-phenylenevinylene) precursor in deionized water by the low angle laser light scattering :  $Kc/R(\theta)$  vs  $c$  .**

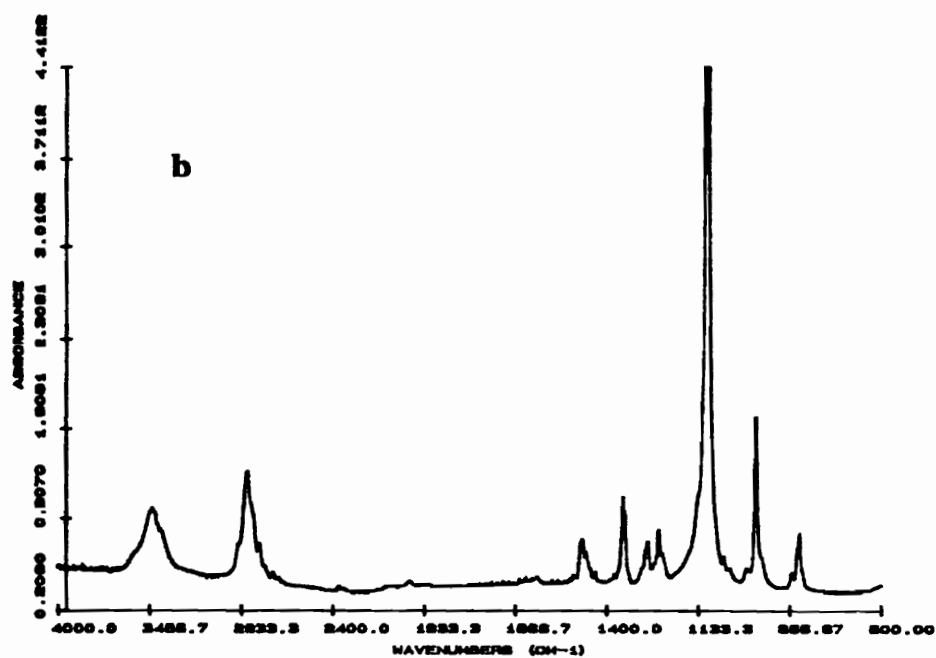
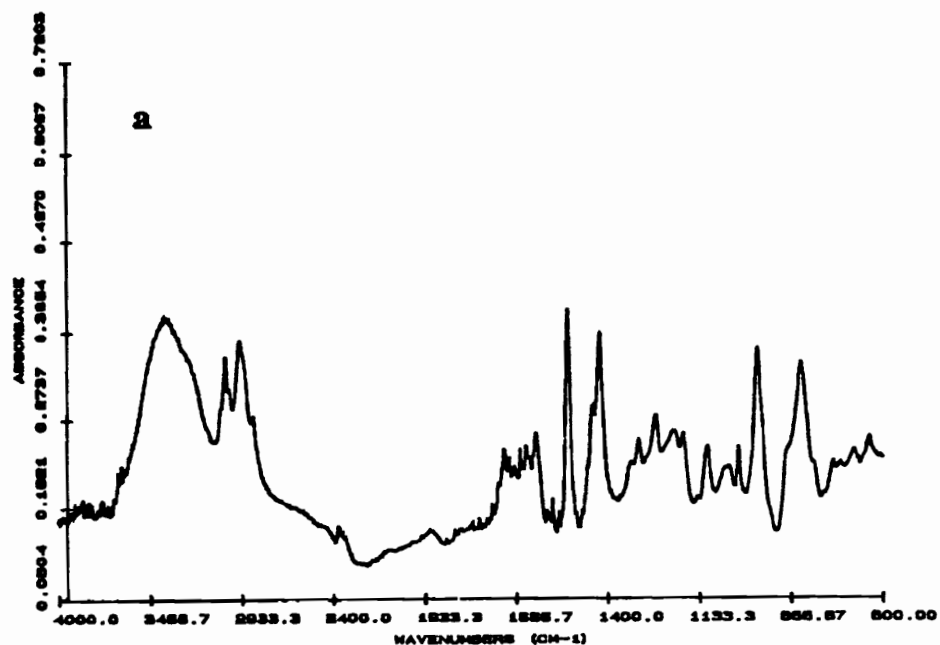
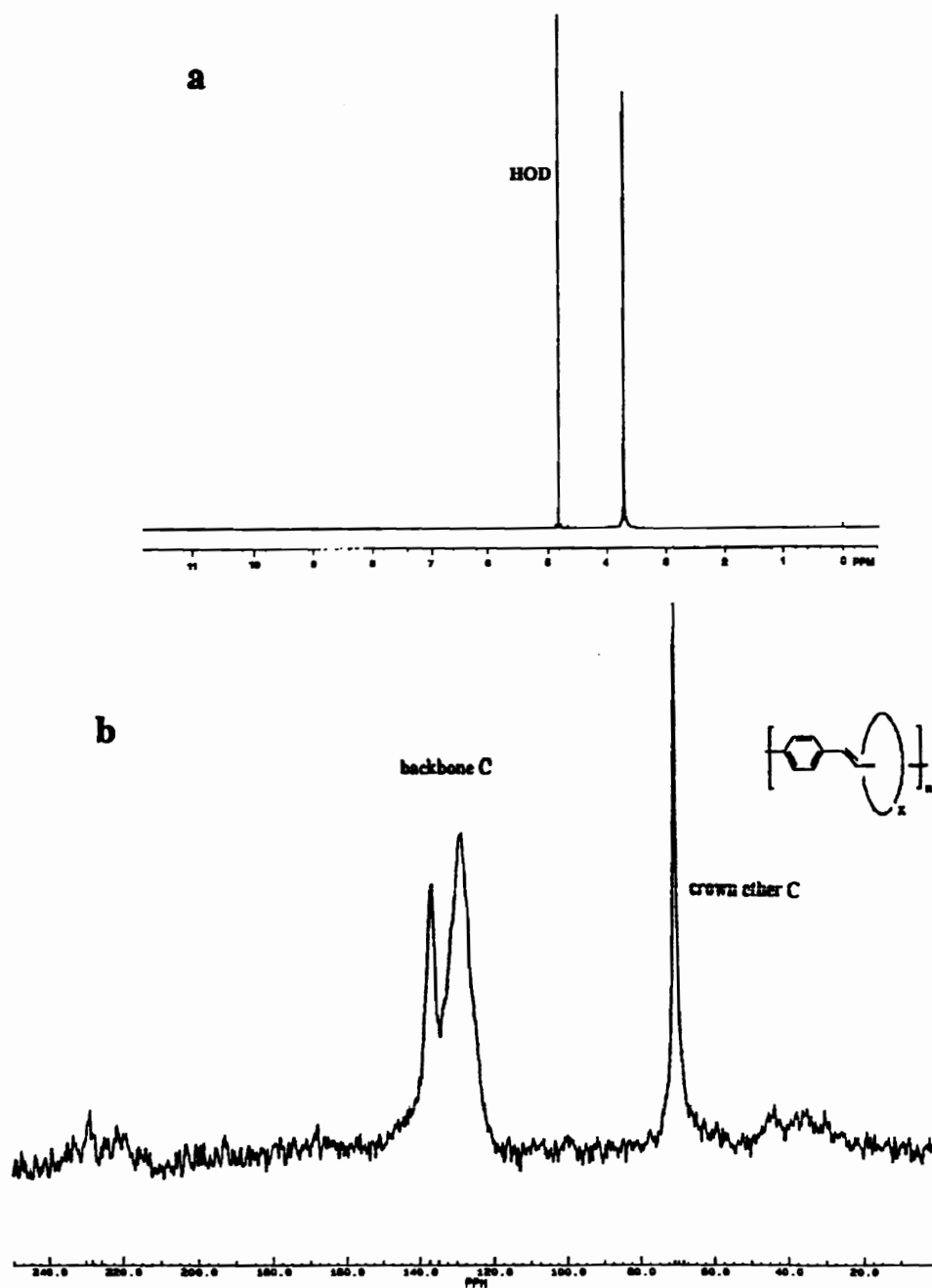
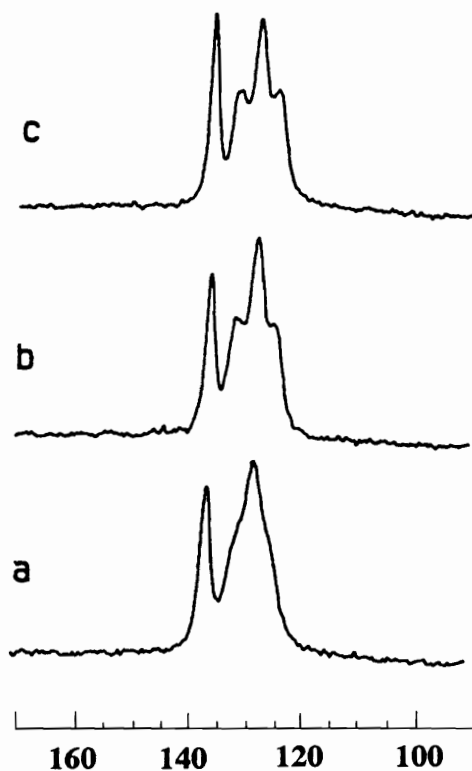


Figure IV-7. FTIR spectra of a) poly(1,4-phenylenevinylene) precursor synthesized in the presence of 18-crown-6 measured as a free standing film; b) 18-crown-6 measured in a KBr pellet.



**Figure IV-8. a) 400 MHz  $^1\text{H}$  NMR spectrum of the extract from poly[(1,4-phenylenevinylene)-rotaxa-(42-crown-14)] in  $\text{D}_2\text{O}$ ; b) Quantitative  $^{13}\text{C}$  solid state 75 MHz NMR of poly[(1,4-phenylenevinylene)-rotaxa-(42-crown-14)].**



**Figure IV-9.** 75 MHz  $^{13}\text{C}$  solid state cross-polarization magic-angle spinning (CPMAS) NMR spectra of unstretched poly(1,4-phenylenevinylene) films which had been annealed at: a) 200; b) 250; c) 300 °C (ref. 28).

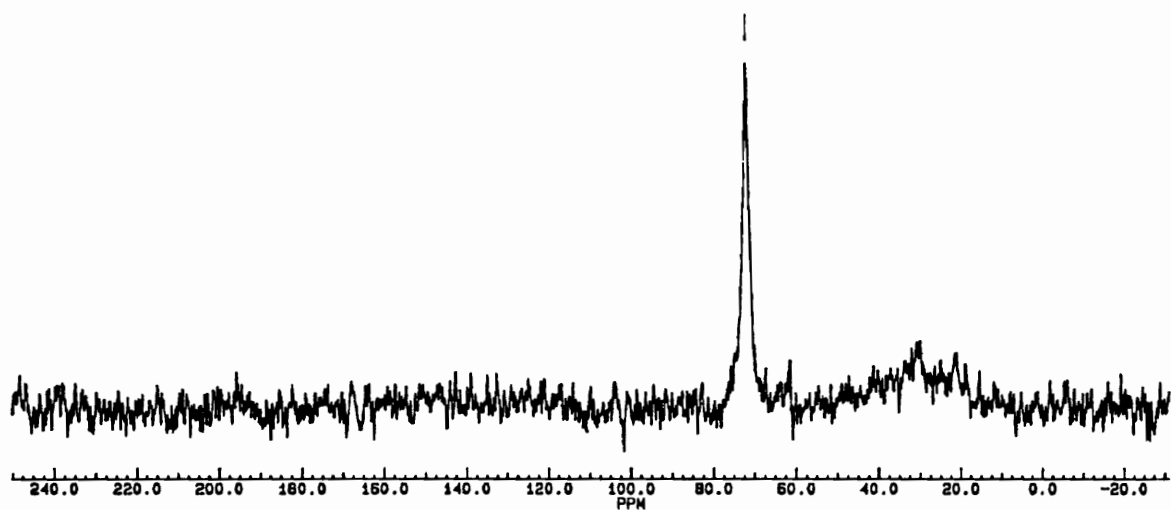


**Figure IV-10. 75 Mhz  $^{13}\text{C}$  solid stateNMR spectrum of 42-crown-14.**

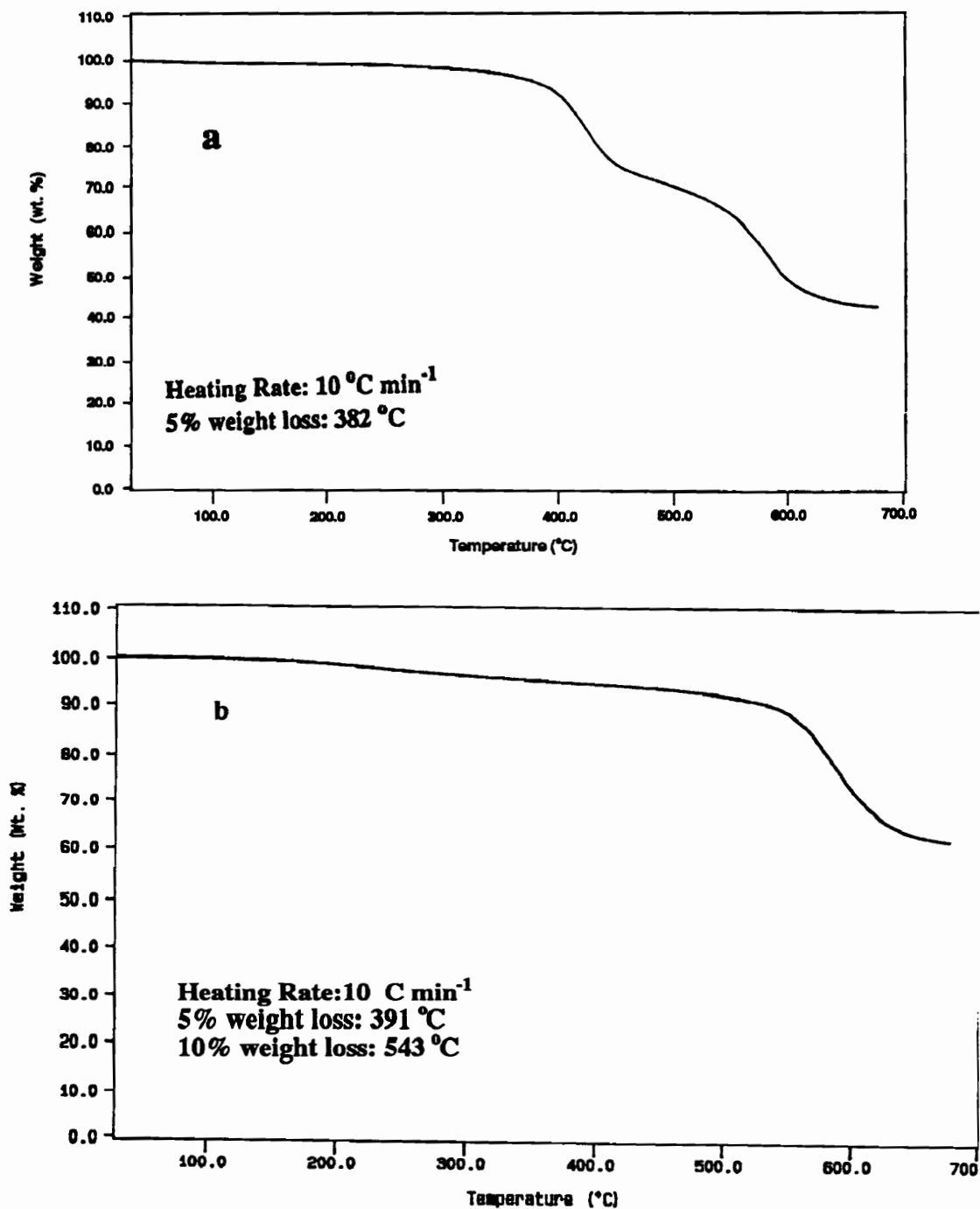


Figure IV-11. Thermogravimetric analysis of a) poly[(1, 4-phenylenevinylene)-rotaxa-(42-crown-14)] in N<sub>2</sub>; b) poly(1,4-phenylenevinylene) in N<sub>2</sub>.

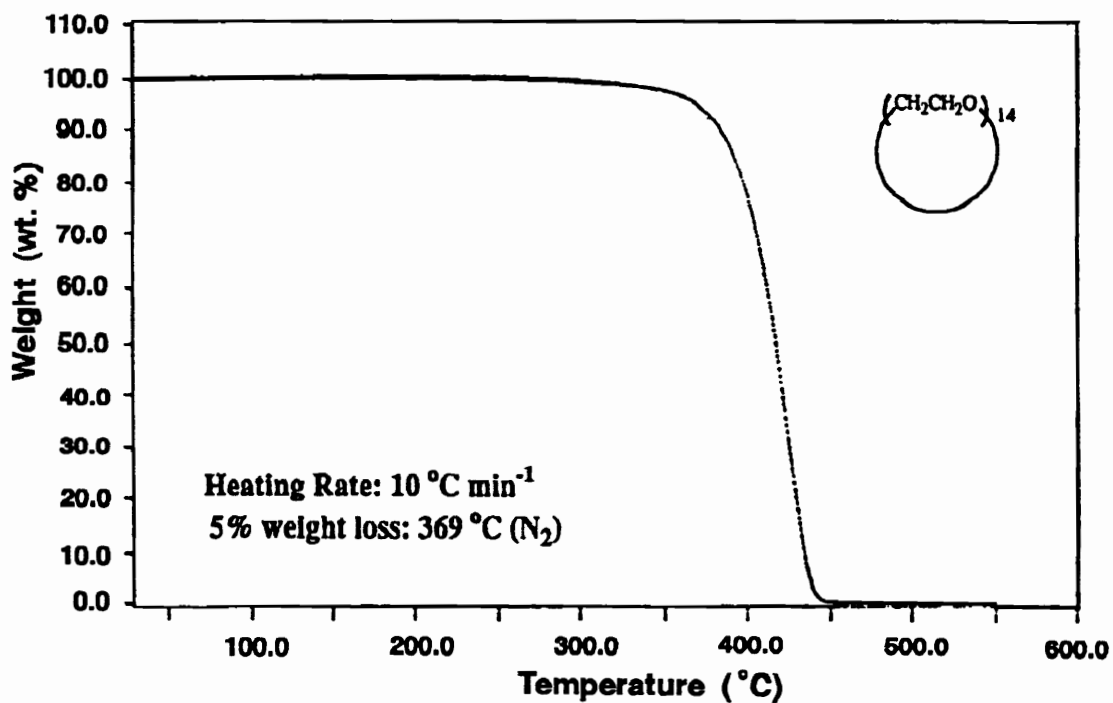
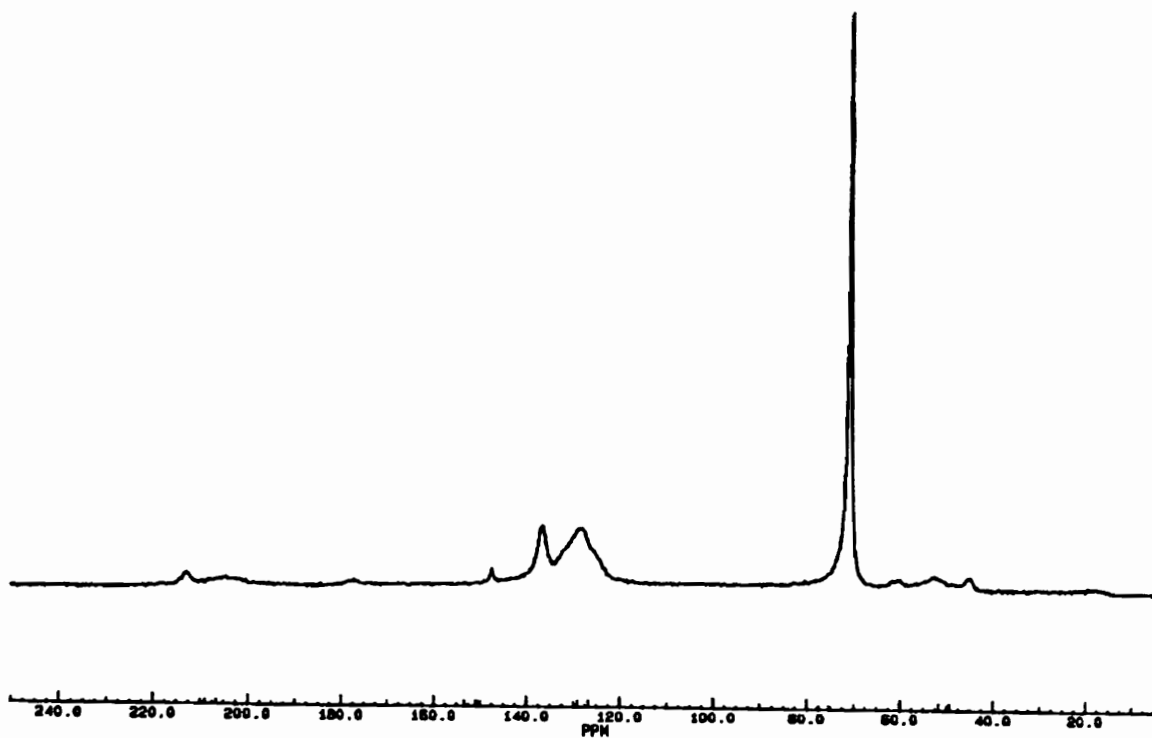
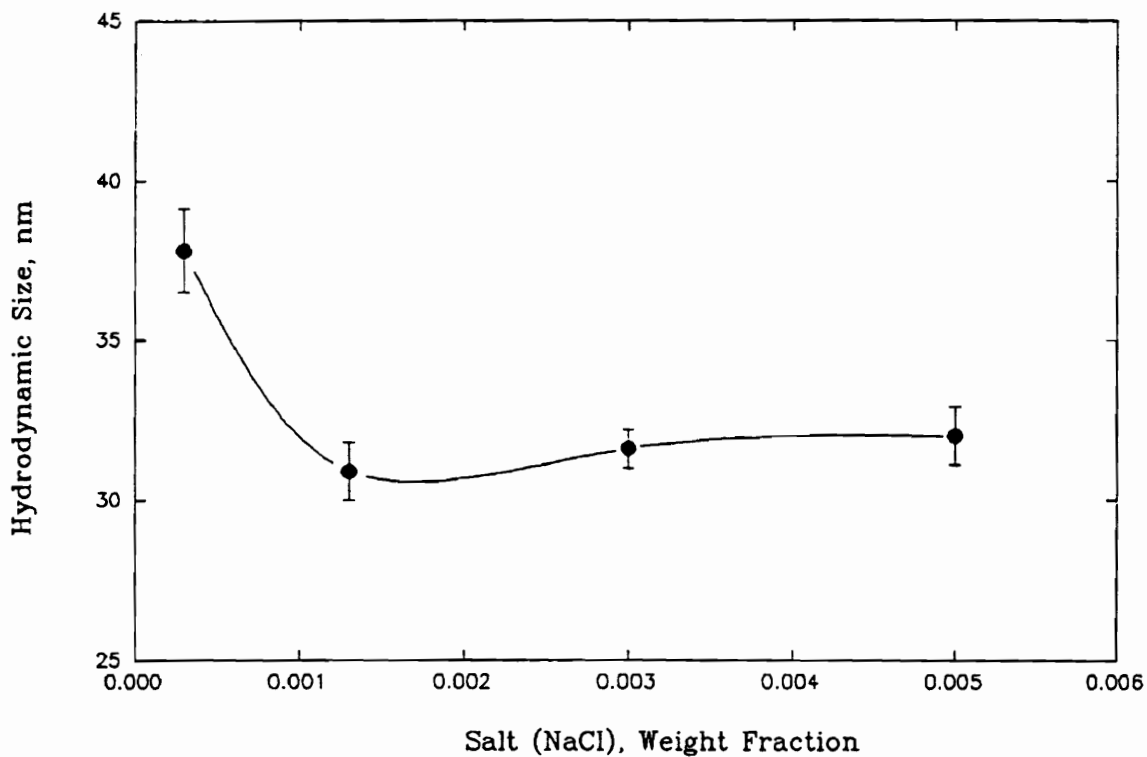


Figure IV-11. c) Thermogravimetric analysis of 42-crown-14 in N<sub>2</sub>.



**Figure IV-12. Quantitative 75 Mhz  $^{13}\text{C}$  solid state NMR of poly[(1,4-phenylenevinylene)-rotaxa-(60-crown-20)].**



**Figure IV-13. Hydrodynamic size of poly(1,4-phenylenevinylene) precursor measured in deionized water at different salt (NaCl) concentrations.**

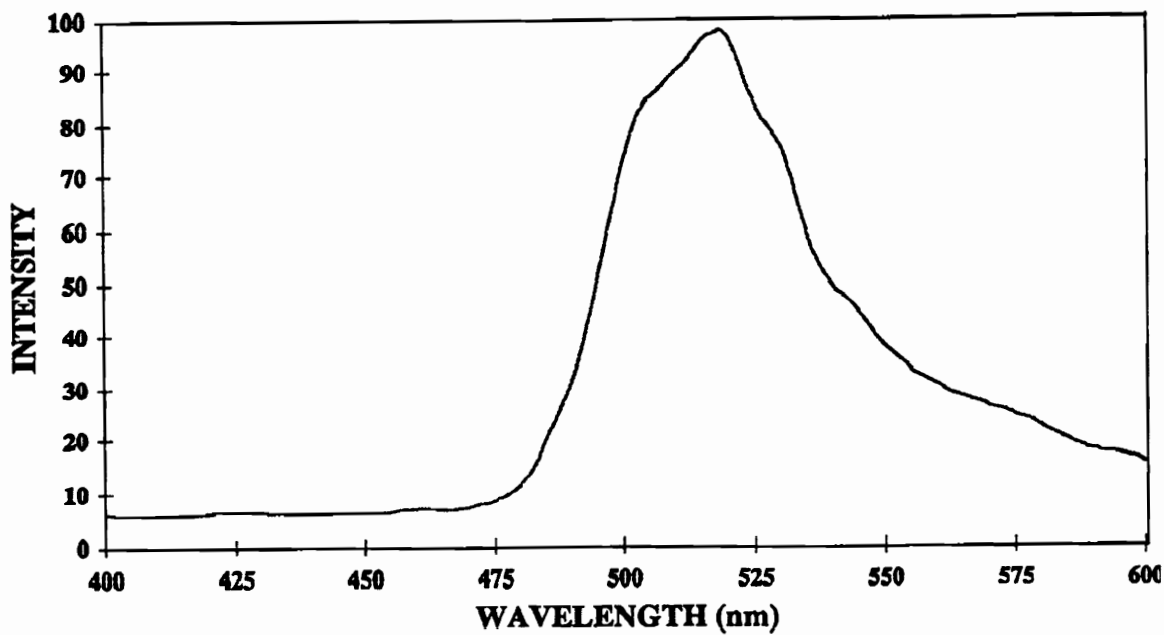


**Figure IV-14. Photoluminescence spectrum of poly(1,4-phenylenevinylene) film measured with 320 nm incident light. film thickness:  $40.3 \pm 19.6 \mu\text{m}$**

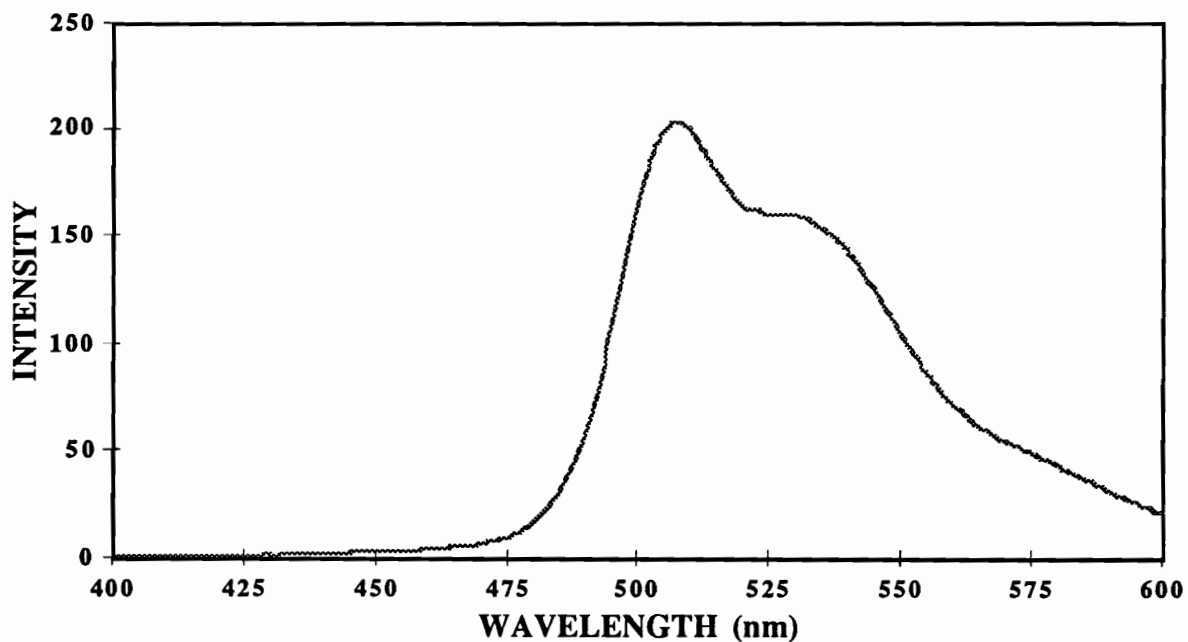


**Figure IV-15. Photoluminescence spectrum of poly[(1,4-phenylenevinylene)-rotaxa-(42-crown-14)] film measured with 320 nm incident light. film thickness:  $73.4 \pm 33.8 \mu\text{m}$**

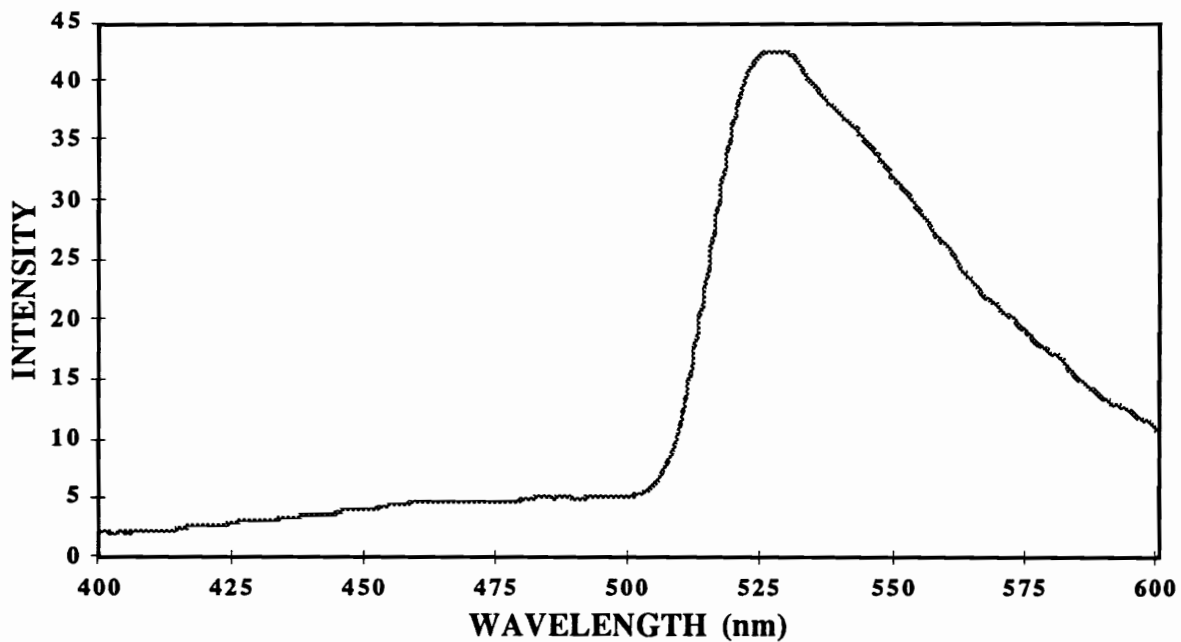


**Figure IV-16** Photoluminescence spectrum of poly[(1,4-phenylenevinylene)-rotaxa-(60-crown-20)] film measured with 320 nm incident light. film thickness:  $57.0 \pm 9.0 \mu\text{m}$

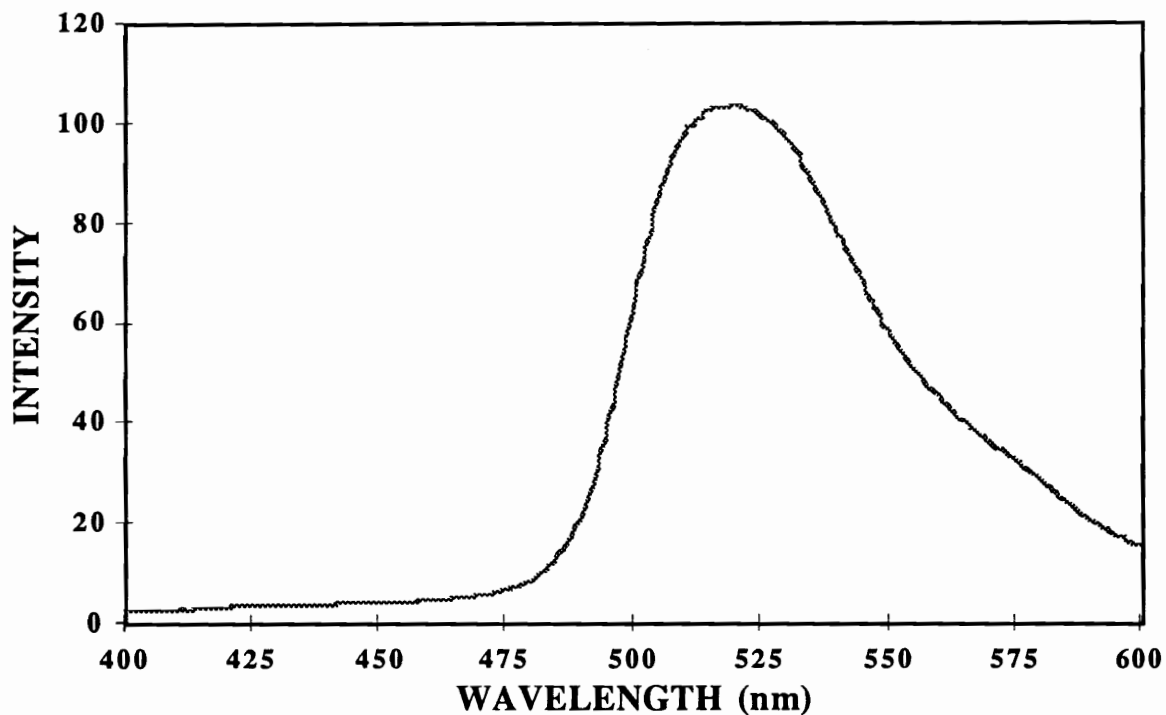


**Figure IV-17. Photoluminescence spectrum of poly(1,4-phenylenevinylene) and 42-crown-14 blend (1.9:1 wt ratio) film measured with 320 nm incident light. film thickness:  $91.6 \pm 14.1 \mu\text{m}$**

# FOUR-PROBE METHOD

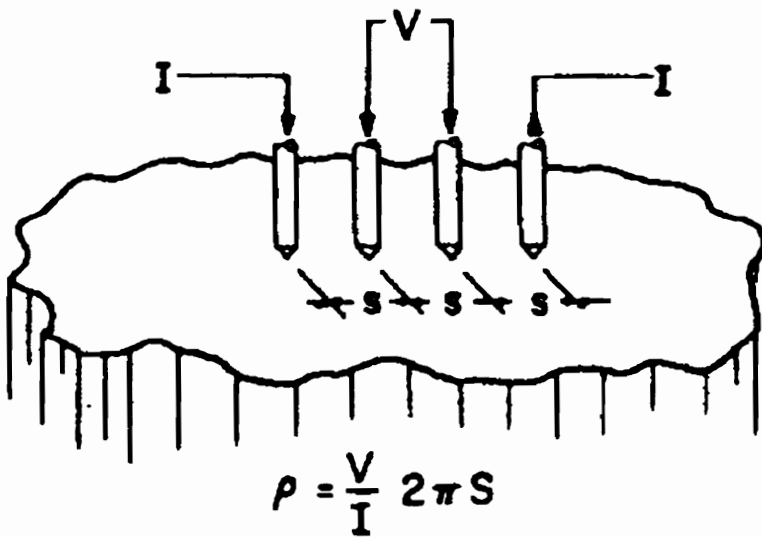
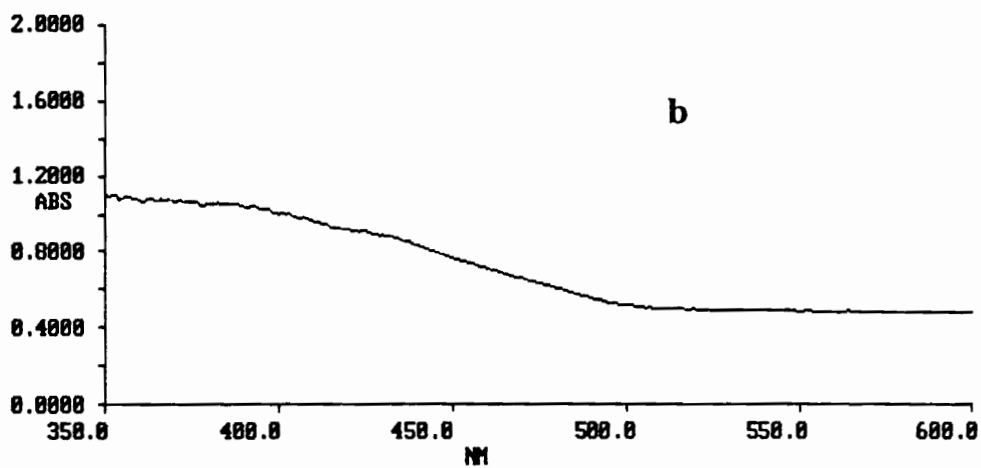
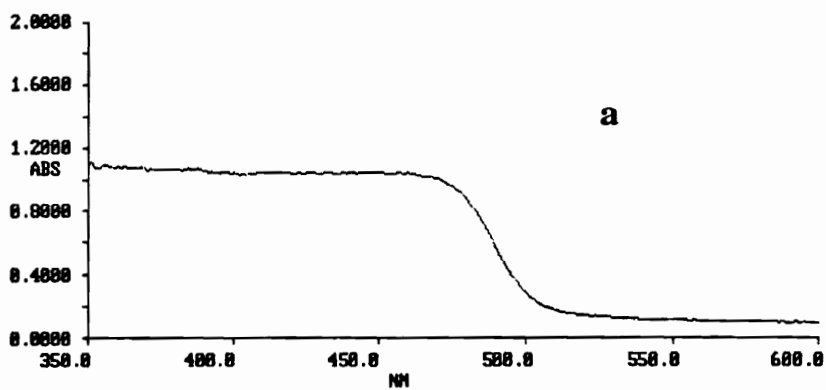
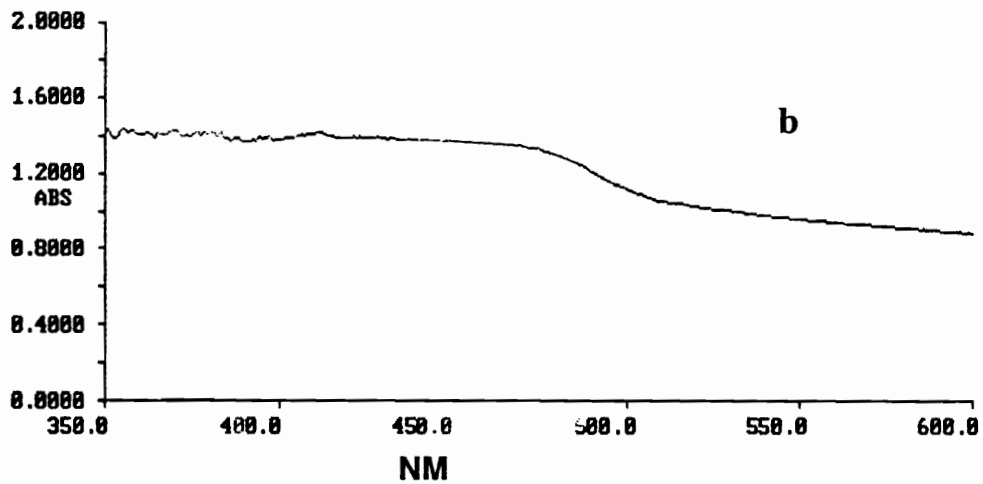
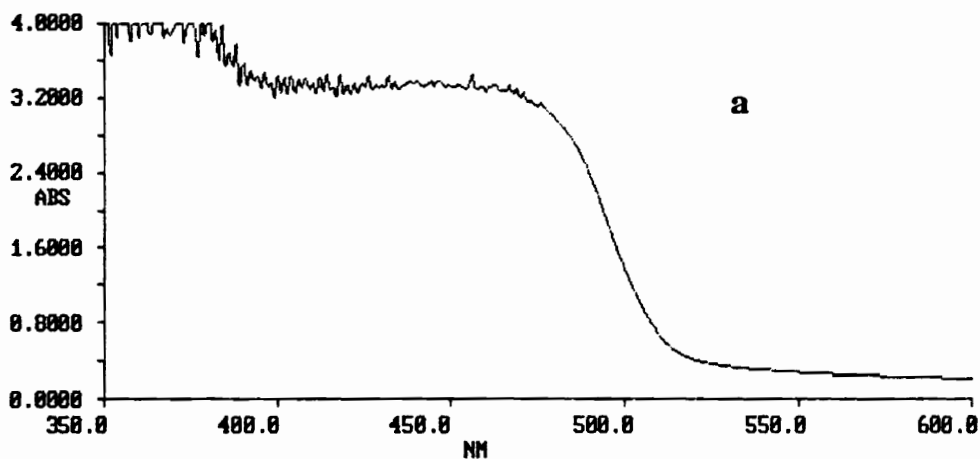


Figure IV-18. Diagram of conductivity measurement via a four-probe method.



**Figure IV-19. Absorption spectra of: a) poly(1,4-phenylenevinylene); b) poly[(1,4-phenylenevinylene)-rotaxa-(42-crown-14)] films.**



**Figure IV-20. Absorption spectra of: a) poly[(1,4-phenylenevinylene)-rotaxa-60-crown-20]; b) Physical blend of poly(1,4-phenylenevinylene) and 42-crown-14 films.**

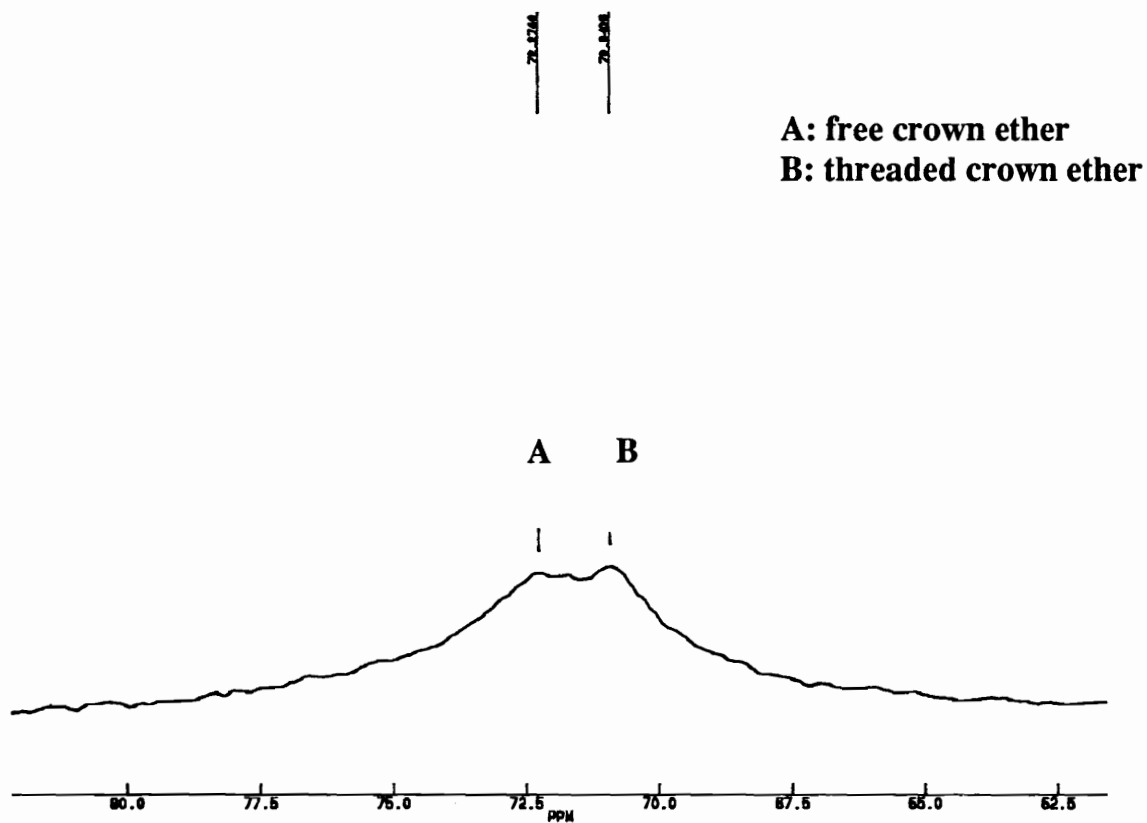


**Figure IV-21 75 MHz  $^{13}\text{C}$ CPMAS spectrum of crown ether and PPV42C14 rotaxane mixture**

## **Vita**

Feng Wang was born in Shanghai, China on September 21, 1969. When he was six, he moved to Chongqing, a southwestern city in China. He spent the next fifteen years in Chongqing and obtained his Bachelor of Engineering in Metallurgy and Material engineering from Chongqing University. He began his graduate career at Virginia Polytechnic and State University in the fall of 1991. After he joined Dr. Harry W. Gibson's group, he was involved in the synthesis of conductive polyrotaxane research.